Stellingen

1. Stotteraars vallen vaak in herhaling

   — Th.J.L. Schoenaker en E.H Versteegh-Vermeij *Stotterjijofstotterik: Instructies voor stotteraar en luisteraar*, 2e druk, Bohn Scheltema & Holkema, Utrecht, 1985, p. 14,43

2. Een goede Nederlandse term voor *surfactant* is opacs

3. Het is nogal rechtlijnig gedacht dat een lijn altijd recht moet zijn

4. Hoewel formeel correcter, is de door Boruvka en Neumann voorgestelde definitie van de oppervlaktespanning voor gekromde grensvlakken niet handelbaar

   — Hoofdstuk 2 dit proefschrift

5. De door Mareschal *et al.* berekende normaaldruk voldoet niet aan het door hen gestelde evenwichtscriterium

   — J. Chem. Phys., **106** (1997), 645

6. De door Szleifer *et al.* gebruikte overschotsdruk is fysisch irreëel

   — J. Chem. Phys., **92** (1990), 6800

7. Het roostermodel van Scheutjens en Fleer is uitermate geschikt voor de beschrijving van het fasegedrag van surfactantsystemen

   — Hoofstuk 3 en 5 dit proefschrift

8. In de wetenschap kan wat recht is, krom gepraat worden

   — Hoofdstuk 4 en 5 dit proefschrift

9. Wanneer het intellectuele eigendom van een proefschrift rust bij de universiteit, zou het college voor promoties het proefschrift moeten kunnen verdedigen tegenover de promovendus

10. Het beschikbaar stellen van geld aan AIO's en postdocs voor symposiabezoek is een effectieve bezuiniging op wachtgeld

11. Het houden van 'Engelse' voordrachten voor een Nederlandse werkgemeenschap leidt tot het ontwikkelen van een eigen dialect van het Engels en een verarming van de Nederlandse taal

12. De titel 'Bachelor of Science' (BSc) doet vermoeden dat MSc staat voor 'Married to Science'

13. Het verplicht voeren van bedrijfsreclame op lease-auto's verhoogt de verkeersveiligheid

14. De oplossing van de fileproblematiek moet in de statistische fysica moeten worden gezocht

15. Als milieu-evenwichten zo gevoelig liggen als met het erkennen van het versterkte broeikaseffect wordt beweerd, kunnen alternatieve energiebronnen als zonne- en windenergie mileubedreigend zijn

Stellingen behorende bij het proefschrift 'Thermodynamic and Mechanical Properties of Curved Interfaces: A discussion of models', S.M. Oversteegen, Wageningen, 18 januari 2000.

Thermodynamic and Mechanical Properties of Curved Interfaces

A discussion of models

promotor: dr. J. Lyklema,
emeritus hoogleraar in de fysische chemie, met bijzondere aandacht voor de grensvlak- en kolloïdchemie

co-promotoren: dr. ir. F.A.M. Leermakers,
universitair docent bij de Leerstoelgroep Fysische Chemie en Kolloïdkunde

dr. ir. P.A. Barneveld,
universitair docent bij de Leerstoelgroep Fysische Chemie en Kolloïdkunde

Thermodynamic and Mechanical Properties of Curved Interfaces

A discussion of models

Martijn Oversteegen

Proefschrift

ter verkrijging van de graad van doctor

op gezag van de rector magnificus

van Wageningen Universiteit,

dr. C.M. Karssen,

in het openbaar te verdedigen

op dinsdag 18 januari 2000

des namiddags te vier uur in de Aula.

Nederlandse titel: Thermodynamische en Mechanische Eigenschappen van Gekromde Grensvlakken; een bespreking van modellen

ISBN 90-5808-178-8
Subject headings: interfacial thermodynamics/curved interfaces/capillarity.

Omslagontwerp: Angelique Asbreuk

Dit proefschrift is tot stand gekomen met steun van Chemische Wetenschappen met een subsidie van de Nederlandse Organisatie voor Wetenschappelijk Onderzoek (CW-NWO).

Voorwoord

Na vier jaar broeden, is mijn geesteskind uit de dop gekomen. Zoals bij alle nakomelingen, is de rol van de vader essentieel. Ik wil dan ook op de eerste plaats de 'peetvaders' Peter Barneveld en Frans Leermakers bedanken. Als ik een vraagstelling beantwoord dacht te hebben, wist Peter me vaak te prikkelen tot het uitzoeken van een onderliggend, fundamenteler probleem. De resultanten van ons gezamenlijk denkwerk zijn in heel dit proefschrift terug te vinden. Als wij niet tot een oplossing konden komen, stond de deur van Frans, ondanks zijn overvolle agenda, altijd open. De vele discussies die dan ontstonden hebben eveneens de inhoud van dit proefschrift sterk beïnvloed. De bijdragen die Jan van Male en Henk Huinink aan deze besprekingen hebben geleverd, zijn impliciet terug te vinden in deze dissertatie. Zonder de numerieke constateringen van Jan waren de hier gepresenteerde resultaten ongetwijfeld minder vernieuwend geweest. De gedachtevorming omtrent de thermodynamica van gekromde systemen is door de inbreng van Henk versneld. Ook hun ben ik dus dank verschuldigd. Hans Lyklema wist mij in de schrijffases te behoeden voor onduidelijkheden in de uiteindelijke formuleringen; dankzij hem heeft het werk een passend 'jasje' gekregen.

Om goed te kunnen broeden, is een warm nest een belangrijke voorwaarde. Mede door het volleyballen, de proffenavonden, de wandelweekeinden, de labuitjes en de fietstochten ben ik altijd met veel plezier naar Fysko gegaan. Omdat de werksfeer van de leerstoelgroep niet wordt bepaald door enkele personen in het bijzonder, wil ik iedereen hartelijk bedanken die daar in de loop van de afgelopen vier jaar is gekomen, gegaan of gebleven. Met name Marcel Giesbers wil ik bedanken voor zijn luisterend oor en adviezen. Maarten van der Wielen, Desiree Barten, Joost Maas, Marcel van Eijk en Remco Fokkink bewezen eveneens dat een (verre) buur een goede vriend kan zijn. Mijn trouwste symposiummaatjes, Edwin Currie en Bert Torn, maakten uitstapjes altijd extra plezierig.

Ook buiten het wetenschappelijke wereldje heb ik de afgelopen jaren veel steun in de rug gekregen. Karin, Christel en Nicole hebben me diverse keren opgebeurd door me met hun vrouwelijke nuchterheid met beide benen op de grond te houden. Van de 'Blote Konten', die voor het mannelijk tegenwicht zorgden, wil ik met name Bob bedanken; hij heeft zich zo'n beetje ontpopt als mijn persoonlijk therapeut via onze vele e-mails.

Wanneer ik mij zo nu en dan weer in Twente meldde, was er altijd 'De Groep' voor een avondje film of kroeg. Ik bedank hen allemaal dat ze er altijd voor me waren.

Met het afronden van mijn proefschrift komt er formeel een einde aan mijn opleiding. Hoewel mijn ouders tegen het eind van het VWO al niet meer precies wisten waar ik mij mee bezig hield, hebben ze me toch altijd onvoorwaardelijk gesteund. Dit blindelings vertrouwen heeft mij gemaakt tot wat ik nu ben. Hopelijk geef ik hun daarmee voldoende trots om mijn dank duidelijk te maken.

Tenslotte bedank ik mij Sandra. Zij heeft de afgelopen jaren de grillige ontwikkeling van mijn (wetenschappelijke) persoonlijkheid het dichtst bij meegemaakt. Zij is altijd in mij blijven geloven en me blijven nemen zoals ik ben. Ik zal haar nog heel wat jaartjes knuffelen om daarvoor te danken!

Contents

CHAPTER 1

Introduction

ABSTRACT

Curved interfaces are a result of the cooperative behaviour of molecules, which is demonstrated by means of a simple packing model for surfactant molecules. Several more sophisticated ways to model interfaces are brought up. It is outlined how these models will be discussed in this thesis.

1.1. INTERFACIAL GEOMETRY

Curved interfaces are ubiquitous in everyday life [1]. Often they result from the cooperative behaviour of surfactant molecules, which have a wide variety of applications as, e.g., detergents (cleaning), soaps (personal care), emulsifiers (proteins in food science), and phospholipids (biological membranes). Their chemical structures determine the interfacial geometry and by that the physics of a surfactant system to a large extent. As a first approximation, the formation of different interfacial geometries can be demonstrated qualitatively from packing constraints using a simple schematic representation of surfactant molecules, as shown in table 1.1. The closest packing is determined by the effective size or excluded volume of the surfactant molecule. Besides the chemical structure, the effective size of a surfactant molecule also depends on variables such as the temperature and ionic strength. Suppose the headgroup of a surfactant molecule has in a given physical chemical environment an effective area a, whereas the surfactant as a whole has an effective length l and a volume v, as shown in figure 1.1. The surfactant may be considered as a cylinder in the case that the area times the length equals the volume

$$\frac{v}{al} = 1$$

If adsorbed, such surfactants can only be packed parallel to each other and therefore form planar interfaces. A typical example of such a surfactant is DODAB, where the ratio v/l of the tails is (approximately) the same as the area a of the headgroup (*cf.* table 1.1).

Suppose now that the surfactants aggregate to a spherical micelle of radius R. Assuming that the headgroups with effective area a are all on the surface of the sphere, the number of surfactants in the aggregate, N, can be found from the area of the sphere, $N = 4\pi R^2/a$. Alternatively, the number of surfactants can also be determined from

the volume of the sphere, $N = \frac{4}{3}\pi R^3/v$. The two numbers N are only consistent if $R = 3v/a$. Since the effective length of the surfactants cannot exceed the radius of the spherical micelle, $R > l$, the condition to have spherical aggregates is given by

$$\frac{v}{al} < \frac{1}{3}$$

A typical example of a surfactant that forms spherical aggregates is SDS at not too high concentrations. A part of the spherical micelle is shown schematically in figure 1.1.

Analogously, the radius of a cylindrical aggregate is given by $R = 2v/a > l$. Consequently, surfactants form cylindrical interfaces when

$$\frac{v}{al} < \frac{1}{2}$$

Indeed, for $\frac{1}{3} < v/al < \frac{1}{2}$ cylindrical structures are found, for which $C_{12}E_5$ is a typical example. Due to the difference in dispersion interactions, the headgroup area of the ethylene oxide units is larger than the area of the hydrocarbon tail.

Apparently, the *surfactant parameter*, v/al, is a convenient first order approximation to demonstrate the existence of various interfacial geometries [2]. For values of the surfactant parameter greater than unity the headgroup area is relatively small and inverse micelles are preferred, which is typically found for AOT. The values of the surfactant parameter and the consequent interfacial geometry are summarised schematically in figure 1.1.

The above analysis can be generalized to the cases that surfactants are adsorbed at an interface between two adjacent phases in microemulsions or vesicles [3]. The geometry of surfactant interfaces can be understood in terms of the effective surfactant area, a, length, l, and volume, v. For saturated hydrocarbon chains the effective length and volume can be estimated empirically [2, 4]. However, the headgroup area for ionic surfactants is determined by electrostatic repulsions, rather than excluded volume alone. The addition of much extra salt screens the charges of the headgroups, resulting into a smaller effective headgroup area which promotes more planar surfactant layers. As mentioned before, the temperature and the solvent may for instance also influence the surfactant parameter.

Despite its restrictions, the packing model provides some basic features on what might influence the interfacial geometry and hence the physics of a solution containing surfactant aggregates. Using this knowledge, one can play around with the surfactant's architecture in order to obtain a desired interfacial geometry. An example is linking surfactants chemically such that a 'gemini' surfactant is created, which indeed effects the phase behaviour drastically [5]. Another type of amphiphilic molecules are block

TABLE 1.1. Examples of some common surfactants, *viz.* the anionic surfactants sodium dodecylsulphate (SDS) and sodium bis(2-ethylhexyl) sulfosuccinate (AOT), the non-ionic surfactant dodecyl penta(ethylene oxide) $C_{12}E_5$, and the cationic surfactant di-octadecyldimethylammonium bromide (DODAB)

Surfactant	Chemical structure and its schematic representation
SDS	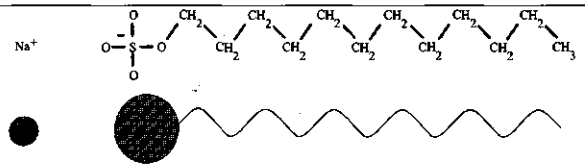
$C_{12}E_5$	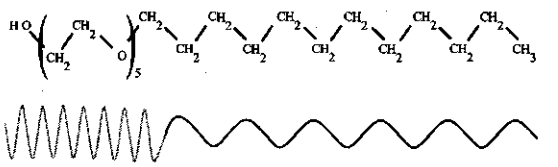
DODAB	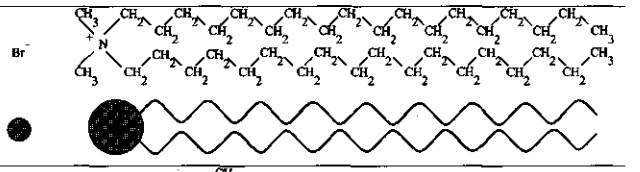
AOT	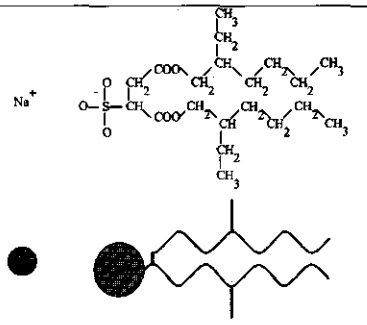

copolymers that consist of chemically linked lyophilic and lyophobic blocks. Of the many types of water-soluble polymer moieties that can act as a hydrophilic groups [6], the poly(ethylene oxide), E_n (*cf.* table 1.1), is most frequently used. When an E_n group is chemically bound to either side of a poly(propylene oxide) block, P_m, the resulting molecule, $E_nP_mE_n$, is of the type of widely used commercially available surfactants known as *pluronics*. The values of n and m are typically of the order of magnitude of $10^1 - 10^2$. These types of surfactants are particularly powerful in adjusting the

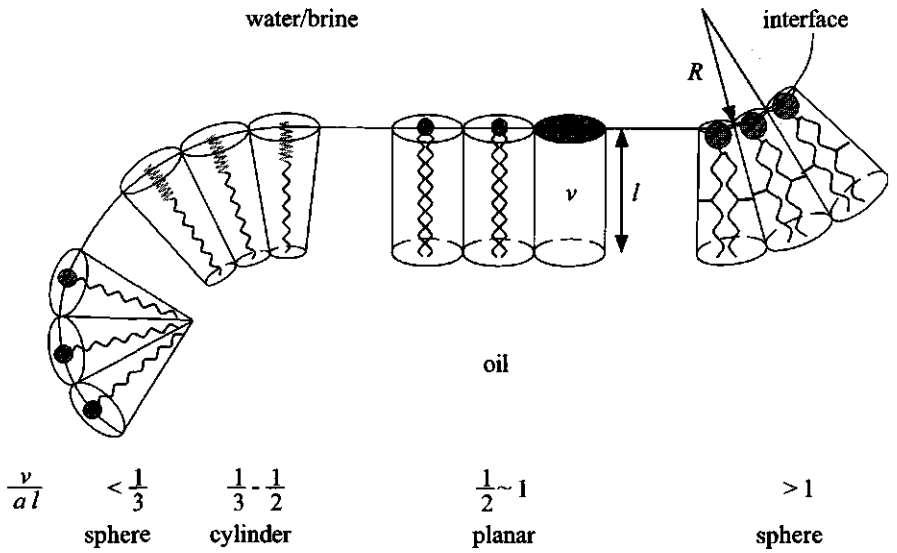

FIGURE 1.1. The surfactant parameter, v/al, demonstrates qualitatively the existence of various interfacial geometries based on packing constraints only

interfacial geometry of aggregates and solid interfaces [7]. The interfacial geometry can be tuned by choosing the proper kind of oil-phase, ionic strength, and playing around with the $n : m$ ratio [8].

1.2. MODELLING CURVED INTERFACES

The interfacial geometry depends in part on the chemical structure of the molecules, as illustrated in the previous section for surfactant molecules. However, the above packing model is only a first approximation for which the molecular parameters can only be obtained empirically. To gain a more profound insight into the geometry of interfaces, other models must be used. Models are generally only attempts to describe what has been observed experimentally. These descriptions are not necessarily unique; it is possible that different models with different assumptions or approximations might still describe the same physical behaviour.

Although models are used to describe experimental observations, they can sometimes also be useful to predict physical properties that are not yet observed. This makes them valuable to understand processes. A few of the different ways of modelling are briefly discussed below.

1.2.1. Simulations

One class of modelling techniques is formed by simulations. Three kinds of simulations can be distinguished, all with their own advantages and drawbacks if applied to interfacial phenomena [9, 10].

Molecular Dynamics. Molecular dynamics simulations provides a method to determine dynamic properties of a system. Molecules are seen as a (branched) chain of units, which are constantly moving due to mutual forces. Solving Newton's laws, all momenta and positions, the so-called *phase space*, can be evaluated as a function of time using brute force algorithms [11]. In this way molecular dynamics can be used to evaluate dynamic properties like diffusion coefficients and the viscosity. Owing to the huge computer times needed using brute force algorithms to evaluate Newton's laws, only a relatively short time period – typically in the order of picoseconds – can be observed. This does not guarantee equilibrium values of the observed parameters.

Brownian Dynamics. Brownian dynamics simulations are typically used for larger particles in a medium, for instance colloids. The large particles obtain a net momentum due to interactions and random forces of the small solvent particles. Solving Newton's laws with a stochastic friction term, again dynamic properties of the system can be obtained [12].

Monte Carlo. Monte Carlo simulations sample the phase space randomly. The randomly chosen points of the phase space are averaged with a proper weight, determined by the probability of that event [13]. Since the phase space is not sampled as a function of time, dynamic properties cannot be derived straightforwardly. However, since a much larger part of the phase space can be sampled, equilibrium can be guaranteed.

1.2.2. Dimensional scaling

Another class to describe the physics of a system is scaling. Starting from dimensional analysis, physical properties can be related to each other [14]. A simple example of scaling has already been given in section 1.1 where the interfacial geometry of a surfactant layer was derived qualitatively from the volume of a surfactant molecule relative to the effective headgroup area and tail length.

A similar, more complicated, example of scaling is in predicting the aggregation structure in a melt of diblock copolymers in the so-called strong segregation limit [15]. In such systems the polymers consist of a block of length n of type X that is chemically linked to a block of length m of type Y. In the strong segregation limit the block types are indifferent to themselves, but X and Y strongly repel each other. The fraction f of

X in the system is given by

$$f \equiv \frac{n}{n+m}$$

As a usual step in scaling models, the total block length is defined to be unity, i.e. $n + m \equiv 1$. If the system tends to aggregate in a planar bilayer, the thickness of a layer consisting of X must be equal to f. Considering unit length and width of the aggregates, the volume equals f whilst the total interfacial area is given by $a_f = 2$.

Consider the same volume but now for a cylindrical phase of unit length, i.e. $f = \pi R_c^2$. The radius of such a cylinder is given by $R_c = \sqrt{f/\pi}$. Hence, the interfacial area is $a_c = 2\pi R_c = 2\sqrt{\pi f}$. By analogy, from the radius of a spherical aggregate of the same volume, $R_s = \sqrt[3]{\frac{3f}{4\pi}}$, the interfacial area is $a_s = 4\pi R_s^2 = \sqrt[3]{36\pi f^2}$.

Since a system tends to minimise the interfacial area [16], a cylindrical aggregate is more favourable than a spherical in case $a_c < a_s$

$$2\sqrt{\pi f_{s\to c}} < \sqrt[3]{36\pi f_{s\to c}^2} \Rightarrow f_{s\to c} > \frac{4\pi}{81} \approx 0.16$$

Moreover, a planar interfaces is more favourable than a cylinder in case $a_f < a_c$

$$2 < 2\sqrt{\pi f_{c\to f}} \Rightarrow f_{c\to f} > \frac{1}{\pi} \approx 0.32$$

For symmetrical diblock copolymers, i.e. $f = 0.50$, the system tends to form planar aggregates since there is no preference to curve in another way. For $f > 0.5$, the above analysis can be applied for the block consisting of Y. That is, for $f > 0.68$ one expects inverted cylindrical aggregates, whereas for $f > 0.84$ one expects inverted spherical aggregates. Despite the approximation of the strong segregation limit, the predicted 'phase transitions' at the different values for f are found experimentally [17].

As also found for the packing model, the above scaling model can be extended to, for instance, microemulsions [18]. The drawback of scaling that it can only predict certain trends rather than giving quantitative results. For instance, in the above examples scaling was unable to predict the phase behaviour but had to be put in rather than that it followed from the scaling itself.

1.2.3. Density functional theory

In density functional theories, state variables are expressed as an integral of the corresponding state variable density. In particular, it is assumed that the state variable density consists of a homogeneous bulk contribution with an additional term to account for the inhomogeneous parts as found in the interfacial region [19]. The contributions are typically expressed in terms of the molecular density profile, which makes the state variable a functional of the density. Consequently, such a functional considers the

average contribution of the molecules to the interactions, i.e. it considers a so-called mean-field rather than the individual contributions of the molecules [20]. By optimizing the state variable, the molecular density profile can be obtained from which the physics of a system can be described phenomenologically.

1.2.4. Mean-Field lattice theory

Another example of modelling (polymeric) surfactants is found in the mean-field lattice theory [21, 22]. Molecules are build from segments that are placed onto the lattice. Each segment is placed next to the previous segment of the same molecule, performing a weighted random walk on the lattice. These segments feel the averaged interactions of all other segments, i.e. they encounter a mean-field of all the molecules instead of a sum of the single contributions. Since each segment contributes to the field of the other segments, it also contributes to its own interactions. So, a field must be found that is self-consistent.

Since no individual interactions are taken into account explicitly, fluctuations are averaged out. Consequently, a relatively short computing time compared to molecular dynamics and Monte Carlo simulations is needed to obtain equilibrium quantities. This makes the mean-field lattice theory a useful alternative to obtain equilibrium information for molecular dynamics simulations, whereas molecular dynamics can provide information on the interactions in the mean-field approximation [23]. Since Monte Carlo simulations are able to include fluctuations, they give better qualitative information than the mean-field approaches both for aggregation structures [24, 25] and at interfaces [26, 27].

In the case of polymers, the mean-field lattice calculations can for good solvents be recovered by an analytical model [28, 29]. Moreover, this lattice theory also showed that certain behaviour, predicted to be universal by dimensional scaling, only holds for infinitely long chains. On the other hand, scaling theories point to a few features where the mean-field approximation fails [30]. For instance, the phase transition for diblock copolymers predicted by the lattice theory [31] differs from the scaling results as derived in the previous paragraph, of which the latter are in agreement with experiments.

1.3. OUTLINE OF THE THESIS

The aim of this thesis is to give a consistent thermodynamic and mechanical description of the physics of curved interfaces. It has been shown here that simple models may give some insight into the existence of different interfacial geometries. However, more sophisticated models are needed to give a profound understanding of curved interfaces

in general. Several models as known in the literature are elaborated, discussed and compared to the above-mentioned mean-field lattice theory.

In chapter 2 the mathematical foundation for the description of the curvature of interfaces is given. Subsequently, a thermodynamic framework is set up in order to predict the stability of (curved) interfaces. This leads, next to the well-known interfacial tension, to two other characteristics needed to describe curved interfaces. The difference between the thermodynamic approaches as proposed by Gibbs [32] and more recently elaborated by Neumann *et al.* [33], are discussed. It will be shown that the interfacial characteristics can be related to the pressure profile in the system. However, these so-called mechanical expressions derived here from a thermodynamic route, differ essentially from the ones in the literature found by mechanical procedures [33]. The thermodynamic consistency of the methods is investigated by deriving the generalized Laplace equation of capillarity.

Since the (local) pressure is strongly related to the interfacial properties, the thermodynamic and mechanical meaning of the pressure is scrutinized in chapter 3 both for homogeneous and inhomogeneous systems. The virial equation of state and its properties is among others illustrated by means of molecular dynamics simulations. A statistical thermodynamic pressure is found from a lattice gas model. The characteristics of this pressure is compared to the properties of the virial pressure, the van der Waals equation of state and a Landau density functional theory.

The dependence of the interfacial characteristics on the curvature will be considered phenomenologically in chapter 4. A first order curvature correction has been proposed by Tolman [34]. However, for some applications a correction up to second order in the curvature, as first proposed by Helfrich [35], may be more appropriate. The mechanical expressions found for these phenomenological descriptions are discussed and evaluated with the lattice gas model. The results are related to the ones found from an analytical description and a van der Waals model as elaborated by Blokhuis *et al.* [36].

The lattice model is extended to chain molecules, in order to model surfactant bilayer membranes in chapter 5. The thermodynamic and mechanical description of the preceding chapters give consistent physics of a $C_{12}E_5$ bilayer. Interpretation of the phenomenological description yields the generic phase behaviour as also observed experimentally [37, 38].

REFERENCES

[1] S. Hyde, S. Andersson, K. Larsson, Z. Blum, T. Landh, S. Lidin, and B.W. Ninham. *The Language of Shape: the role of curvature in condensed matter physics, chemistry and biology.* Elsevier, 1997.

[2] J. Israelachvili. *Intermolecular and Surface Forces.* Academic Press, 2nd edition, 1991.

[3] D.J. Mitchell and B.W. Ninham. *J. Chem. Soc. Faraday Trans. 2*, 77:601, 1981.

[4] D.F. Evans and H. Wennerström. *The Colloidal Domain: where physics, chemistry, biology and technology meet.* VCH Publishers, 1994.

[5] R. Zana. *Current Opinion in Colloid Interface Sci.*, 1:566, 1996.

[6] P. Alexandridis. *Current Opinion in Colloid Interface Sci.*, 1:490, 1996.

[7] P. Alexandridis and T.A. Hatton. *Colloids and Surfaces A: Physicochem. Eng. Aspects*, 96:1, 1995.

[8] P. Holmqvist, P. Alexandridis, and B. Lindman. *J. Phys. Chem. B*, 102:1149, 1998.

[9] D. Frenkel and B. Smit. *Understanding Molecular Simulation: from algorithms to applications.* Academic Press, 1996.

[10] M.P. Allen and D.J. Tildesley. *Computer Simulations of Liquids.* Oxford University Press, 1986.

[11] D.C. Rapaport. *The Art of Molecular Dynamics simulation.* Cambridge University Press, 1995.

[12] M.T.A. Bos and J.H.J. van Opheusden. *Phys. Rev. E*, 53:5044, 1996.

[13] D. Frenkel. Advanced monte carlo techniques. In M.P. Allen and D.J. Tildesley, editors, *Computer Simulations in Chemical Physics*, volume 1, pages 93–152. Kluwer Academic Publishers, 1993.

[14] P.G. de Gennes. *Scaling Concepts in Polymer Physics.* Cornell University Press, 1979.

[15] A.N. Semenov. Theory of microphase separation in block copolymers in strong segregation limit. Lecture Notes RPK course on Polymer Physics, 1995.

[16] J. Lyklema. *Fundamentals of Interface and Colloid Science*, volume I. Academic Press, 1991.

[17] F.S. Bates, M.F. Schulz, A.K. Khandpur, S. Förster, J.H. Rosedale, K. Almdal, and K. Mortensen. *Faraday Discuss.*, 98:7, 1994.

[18] N. Dan and M. Tirell. *Macromolecules*, 26:637, 1993.

[19] S.A. Safran. Statistical thermodynamics of surfaces, interfaces, and membranes. In D. Pines, editor, *Frontiers in Physics*, volume 90. Addison-Wesley, 1994.

[20] P.M. Chaikin and T.C. Lubensky. *Principles of Condensed Matter Physics.* Cambridge University Press, 1995.

[21] F.A.M. Leermakers, P.P.A.M. van der Schoot, J.M.H.M. Scheutjens, and J. Lyklema. The equilibrium structure of micelles. In K.L. Mittal, editor, *Surfactants in Solution*, volume 7, page 43. Plenum Press, 1989.

[22] P.N. Hurter, J.M.H.M. Scheutjens, and T.A. Hatton. *Macromolecules*, 26:5592, 1993.

[23] N.M. van Os, L.A.M. Rupert, B. Smit, K. Esselink, M.R. Böhmer, and L.K. Koopal. *Colloids Surfaces A: Physicochem. Eng. Aspects*, 81:217, 1993.

[24] C.M. Wijmans and P. Linse. *Langmuir*, 11:3748, 1995.

[25] A.D. Mackie, A.Z. Panagiotopoulos, and I. Szleifer. *Langmuir*, 13:5022, 1997.

[26] Y. Wang and W.L. Mattice. *Langmuir*, 10:2281, 1994.

[27] F. Schmid and M. Müller. *Macromolecules*, 28:8639, 1995.

[28] G.J. Fleer, J. van Male, and A. Johner. *Macromolecules*, 32:825, 1999.

[29] G.J. Fleer, J. van Male, and A. Johner. *Macromolecules*, 32:845, 1999.

[30] C.C. van der Linden. *Polymer Adsorption Theory: universal aspects and intricacies.* PhD thesis, Wageningen Agricultural University, 1994.

[31] M.W. Matsen and F.S. Bates. *Macromolecules*, 29:7641, 1996.

[32] J.W. Gibbs. *The Scientific Papers*, volume 1. OxBow Press, 1993.

[33] J. Gaydos, L. Boruvka, Y. Rotenberg, P. Chen, and A.W. Neumann. Generalized theory of capillarity. In A.W. Neumann and J.K. Spelt, editors, *Applied Surface Thermodynamics*. Marcel Dekker, 1996.

[34] R.C. Tolman. *J. Chem. Phys.*, 17:333, 1949.

[35] W. Helfrich. *Z. Naturforsch*, 28c:693, 1973.

[36] E.M. Blokhuis and D. Bedeaux. *Mol. Phys.*, 80:705, 1993.

[37] R. Strey, R. Schomäcker, D. Roux, F. Nallet, and U. Olsson. *J. Chem. Soc. Faraday Trans.*, 86:2253, 1990.

[38] D.J. Mitchell, G.J.T. Tiddy, L. Waring, T. Bostock, and M.P. McDonald. *J. Chem. Soc. Faraday Trans. 1*, 79:975, 1983.

CHAPTER 2

Thermodynamics of Curved Interfaces

ABSTRACT

The boundary between two adjacent phases is often not sharp. Consequently, one has to choose a particular position of the interface in order to assign interfacial thermodynamic characteristics. The chosen interface is first described mathematically to arrive at expressions that account for the curvature of the interface. Subsequently, the thermodynamic parameters of the interfacial zone are considered as a function of the position of the interface. Some thermodynamic quantities are related to the pressure profile through the system. Unlike the usual approach in the literature, these mechanic expressions are derived from their thermodynamic definition. Although these expressions differ from the ones given in the literature, it is shown that these lead to the same generalized Laplace equation of capillarity. Finally, thermodynamics of small systems is introduced in order to describe an open system with many interfaces.

2.1. MATHEMATICAL DESCRIPTION OF AN INTERFACE

The boundary between two adjacent bulk phases at equilibrium is often not of the size of individual molecules. That is, the local concentration of each component going from one phase to the other is not a step function but changes gradually. The interfacial region is that part of the system where the local concentrations deviate from both bulk concentrations. Following the Guggenheim convention, one can split up the system into three subsystems, i.e. two bulk phases and the interfacial region [1–3]. In the more customary Gibbs convention, the two-phase system is split up into two bulk phases separated by an infinitesimally thin, i.e. mathematical, interface. The bulk values of quantities, e.g. the concentration, are extrapolated up to the dividing plane and all the deviations from the actual values, i.e. the excess amounts, are assigned to the interface. In this section a closer look is taken at the curvature of that interface as a basis to describe the interface thermodynamically in subsequent sections.

2.1.1. Definition of curvature

Let the height z of an interface in Cartesian coordinates be given by a certain function $h(x, y)$. At each point P of the interface one can define a vector $\hat{n}$ of unit length that is perpendicular to the interface at that particular point. From figure 2.1 it can be seen that the direction of this so-called normal vector is approximately proportional to

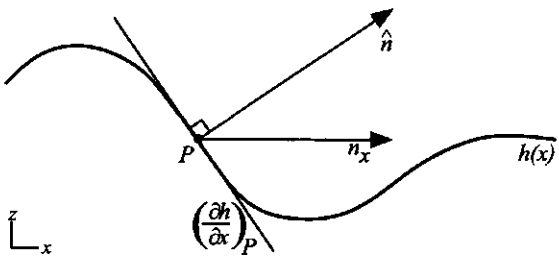

FIGURE 2.1. The normal of a curve given by $z = h(x)$ is proportional to the gradient in each point P.

the gradient along the interface in the point P. This is exact if the z-axis of the local coordinate system is parallel to the normal vector

$$\hat{n} = \frac{\nabla h}{|\nabla h|}$$

Now an infinitesimal step $d\vec{r}$ is taken along the interface. The normal changes as

$$\frac{d\hat{n}}{d\vec{r}} = \frac{1}{|\nabla h|}\frac{d\nabla h}{d\vec{r}} + \nabla h \frac{d1/|\nabla h|}{d\vec{r}} = \frac{1}{|\nabla h|}\left\{\frac{d\nabla h}{d\vec{r}} - \frac{\nabla h}{|\nabla h|}\frac{d|\nabla h|}{d\vec{r}}\right\} \equiv \mathbf{Q}$$

The tensor $\mathbf{Q}$ completely determines the curvature of the interface and is called the *curvature tensor*. In Cartesian coordinates the elements of the curvature tensor are given by

$$Q_{ij} = \frac{1}{|\nabla h|}\left\{\frac{\partial^2 h}{\partial i \partial j} - \frac{1}{|\nabla h|}\frac{\partial h}{\partial i}\frac{\partial |\nabla h|}{\partial j}\right\}$$

where $i, j = x, y, z$ respectively. Using $|\nabla h| = \sqrt{\left(\frac{\partial h}{\partial x}\right)^2 + \left(\frac{\partial h}{\partial y}\right)^2 + 1}$, this expression reduces to

$$Q_{ij} = \frac{1}{|\nabla h|^3}\left\{\frac{\partial^2 h}{\partial i \partial j}|\nabla h|^2 - \frac{\partial h}{\partial i}\left(\frac{\partial h}{\partial x}\frac{\partial^2 h}{\partial x \partial j} + \frac{\partial h}{\partial y}\frac{\partial^2 h}{\partial y \partial j}\right)\right\} \tag{2.1}$$

where use has been made of the property $\frac{\partial^2 h}{\partial i \partial j} = \frac{\partial^2 h}{\partial j \partial i}$, which holds if the second derivatives of h are continuous functions. Since tensors are independent of the choice of the coordinate system, its characteristic polynomial Λ is invariant under transformation of the coordinate system. Consequently, the roots of Λ, the eigenvalues λ, are also invariant under rotation. The eigenvalues of the curvature tensor are thus uniquely related to the curvature of the interface. From this point of view, it makes sense to determine the eigenvalues and use them in further analysis to determine interfacial properties.

The characteristic polynomial of a 3×3 matrix contains three coefficients: *viz.* the determinant $|\mathbf{Q}|$, the sum of the principal minors M_i and the trace Q_{ii}

$$\Lambda(\lambda) = |\mathbf{Q}| - \lambda \sum_{i=1}^{3} M_i + \lambda^2 \sum_{i=1}^{3} Q_{ii} - \lambda^3 \tag{2.2}$$

From eqn (2.1) it can easily be seen that $Q_{zi} = Q_{iz} = 0$, where $i = x, y, z$. Straightforward expansion shows that the determinant of the curvature tensor vanishes. Making the sum of the principal minors explicit yields

$$\sum_{i=1}^{3} M_i = \frac{\frac{\partial^2 h}{\partial x^2}\frac{\partial^2 h}{\partial y^2} - \left(\frac{\partial^2 h}{\partial x \partial y}\right)^2}{\left(\left(\frac{\partial h}{\partial x}\right)^2 + \left(\frac{\partial h}{\partial y}\right)^2 + 1\right)^2}$$

Since the z-axis is implicitly chosen parallel to the normal vector on the interface, the local coordinate system is such that in the origin $\frac{\partial h}{\partial x} = \frac{\partial h}{\partial y} = 0$. Moreover, in the origin the differential $\frac{\partial^2 h}{\partial x \partial y}$ vanishes [4]. Hence

$$\sum_{i=1}^{3} M_i \equiv K = \frac{\partial^2 h}{\partial x^2}\frac{\partial^2 h}{\partial y^2} \tag{2.3}$$

Writing the trace explicitly gives

$$\sum_{i=1}^{3} Q_{ii} = \frac{\frac{\partial^2 h}{\partial x^2}\left(\left(\frac{\partial h}{\partial y}\right)^2 + 1\right) + \frac{\partial^2 h}{\partial y^2}\left(\left(\frac{\partial h}{\partial x}\right)^2 + 1\right) - 2\frac{\partial h}{\partial x}\frac{\partial h}{\partial y}\frac{\partial^2 h}{\partial x \partial y}}{\left(\left(\frac{\partial h}{\partial x}\right)^2 + \left(\frac{\partial h}{\partial y}\right)^2 + 1\right)^3}$$

Evaluated in the origin of the local coordinate system this reduces to

$$\sum_{i=1}^{3} Q_{ii} \equiv J = \frac{\partial^2 h}{\partial x^2} + \frac{\partial^2 h}{\partial y^2} \tag{2.4}$$

The characteristic polynomial as given in eqn (2.2) evaluated in the origin of the local coordinate system, i.e. at a certain point P at the interface, using eqn (2.3) and eqn (2.4), reduces to

$$\begin{aligned}\Lambda(\lambda) &= -\lambda\left(\frac{\partial^2 h}{\partial x^2}\frac{\partial^2 h}{\partial y^2}\right) + \lambda^2\left(\frac{\partial^2 h}{\partial x^2} + \frac{\partial^2 h}{\partial y^2}\right) - \lambda^3 \\ &= -\lambda\left(\lambda^2 - J\lambda + K\right)\end{aligned} \tag{2.5}$$

The eigenvalues of the curvature tensor are the roots of the characteristic polynomial. Obviously, one of the eigenvalues equals zero. Assuming that there are two other eigenvalues c_1 and c_2, the characteristic polynomial can be written as

$$\Lambda(\lambda) = -\lambda\left((\lambda - c_1)(\lambda - c_2)\right) = -\lambda\left(\lambda^2 - (c_1 + c_2)\lambda + c_1 c_2\right)$$

Comparison with eqn (2.5) yields alternative expressions for the sum of the principal minors and the trace in terms of the eigenvalues, respectively

$$J = c_1 + c_2 = \frac{\partial^2 h}{\partial x^2} + \frac{\partial^2 h}{\partial y^2} \tag{2.6}$$

$$K = c_1 c_2 = \frac{\partial^2 h}{\partial x^2}\frac{\partial^2 h}{\partial y^2} \tag{2.7}$$

The eigenvalues of the curvature tensor c_1 and c_2 are called *the principal curvatures.* The sum of both principal curvatures, J, is called *the total curvature.* The product of the principal curvatures, K, is called *the Gaussian curvature.* Note that these local quantities completely determine the curvature at each point of an interface. However, if the interface is (relatively) flat, i.e. $\left|\frac{\partial h}{\partial x}\right| \ll 1$ and $\left|\frac{\partial h}{\partial y}\right| \ll 1$, the values of J and K apply to the entire interface.

Henceforth, the set of J and K will be used to describe the curvature instead of the principal curvatures. This implies a coordinate transformation. The Jacobian of this transformation

$$\begin{vmatrix} \frac{\partial J}{\partial c_1} & \frac{\partial J}{\partial c_2} \\ \frac{\partial K}{\partial c_1} & \frac{\partial K}{\partial c_2} \end{vmatrix} = \begin{vmatrix} 1 & 1 \\ c_2 & c_1 \end{vmatrix} = c_1 - c_2 \tag{2.8}$$

shows that J and K are independent variables if $c_1 \neq c_2$ [5].

Several textbooks use the *mean curvature* H instead of the total curvature J. The mean curvature is defined as the average of both principal curvatures: $H \equiv \frac{1}{2}(c_1 + c_2)$. Another frequently used magnitude is the deviatoric curvature D, which is half the difference of the principal curvatures: $D = \frac{1}{2}(c_1 - c_2)$. Note that this parameter is not symmetrical in c_1 and c_2.

2.1.2. Derivation of expressions for J and K

Consider a two-dimensional interface given by $z = h(x, y)$. The origin of the local coordinate system is placed at the point P with the z-axis parallel to the normal at that point. The unit vector in the direction of the tangent at point P' at a distance $-\frac{1}{2}\Delta x$ from P is denoted as $\hat{h}_x(-\frac{1}{2}\Delta x)$. Similarly, $\hat{h}_x(\frac{1}{2}\Delta x)$ denotes the unit vector in the direction of the tangent at point P'' at a distance $\frac{1}{2}\Delta x$ from P. The angle between the two unit vectors is given by α, as shown in figure 2.2.

A circle is placed at the convex side of the interface. The radius R_x of this circle is chosen such that its circumference fits the arc $P'P''$ best. The sector of the circle between P' and P'' has an angle β, as also shown in figure 2.2.

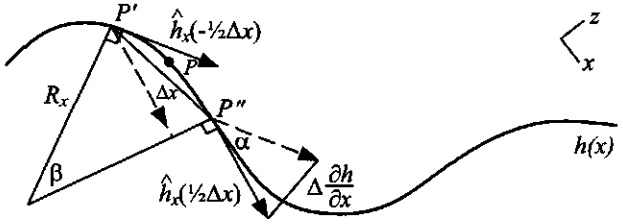

FIGURE 2.2. The change of the gradient along the interface, $\Delta\frac{\partial h}{\partial x}$, can be related to a sector of a circle of radius R_x in order to determine the principal curvature in point P.

From elementary geometrics it can be seen that the angles α and β are equal. Consequently, from the similarity of the triangles it follows

$$\frac{\Delta x}{R_x} = \frac{\Delta\frac{\partial h}{\partial x}}{\left|\hat{h}_x\right|}$$

The length of a unit vector is unity by definition. Therefore the limit $\Delta x \to 0$ in point P yields

$$\frac{\partial}{\partial x}\frac{\partial h}{\partial x} = \frac{1}{R_x}$$

Similarly, it can be derived that $\frac{\partial^2 h}{\partial y^2} = \frac{1}{R_y}$. Using their definitions, eqn (2.6) and eqn (2.7), the following expressions are derived for the local total and Gaussian curvature

$$J = \frac{1}{R_x} + \frac{1}{R_y},\ K = \frac{1}{R_x R_y} \tag{2.9}$$

In the above analysis the radii are defined positive relative to the concave side of the interface. A planar interface has infinite radii in both directions, so $J_{flat} = K_{flat} = 0$. A cylindrical interface has a finite radius R in one direction and infinite in the other, therefore $J_{cyl} = \frac{1}{R}$, $K_{cyl} = 0$. A spherical interface has radii R in both directions, so $J_{sph} = \frac{2}{R}$, $K_{sph} = \frac{1}{R^2}$. From the Jacobian, eqn (2.8), it followed that J and K are independent unless $c_1 = c_2$ or, alternatively, $\frac{1}{R_x} = \frac{1}{R_y}$. As seen, this is only the case for planar and spherical interfaces.

Note that for all aforementioned interfaces the curvatures are uniform over the entire interface. However, this is not generally the case. An example is a saddle plane. In the saddle point of a regular saddle plane there are two identical local radii R. However, in one direction the interface has a convex curvature ($R > 0$), whereas in the other it is curved concavely and R has to be taken negative. Therefore, $J_{sad} = 0$ and $K_{sad} = \frac{-1}{R^2}$ locally in the saddle point of a regular saddle plane. In other points of the regular

saddle plane the local curvatures have to be derived from eqn (2.6) and eqn (2.7), where $h(x,y) = \frac{1}{2R}(x^2 - y^2)$ with respect to a global coordinate system of which the origin is located in the saddle point. It is also possible to define an average curvature of the interface [6].

In the above section the curvatures were defined by the change of the normal vector along the mathematical interface. From a molecular point of view, the curvature might in particular systems also be defined in terms of the change of the director, i.e. the normalized orientation, of the molecules. Both definitions are equivalent provided that all molecules are at the interface. However, since the interface is usually not infinitely sharp, as stated before, the application of the latter definition of the curvature is restricted to a system-average. Owing to the thermal motion of the molecules, the system-average change of the directors gives a smaller curvature than an interface-average change of the normal vector of a mathematical interface [7]. A curvature defined in terms of the change of the director can therefore serve as an order parameter for the geometry of the system [8]. However, since the Gibbs convention is more generally applicable, the first-mentioned definition will be used in the subsequent sections.

2.2. GENERALIZED LAPLACE EQUATION OF CAPILLARITY

In this section a two-phase system is considered that consists of a phase α and a phase β separated by a curved interface. Thermodynamic equations can be derived for the two phases and the interface. By varying the position of the dividing plane between the two phases, the volumes of both phases are changed and so are the extensive properties of each phase. However, the intensive quantities of the total system, such as the temperature and the Laplace pressure difference between both phases, are not affected. So, generally valid thermodynamic equations must be invariant with respect to the position of the interface.

Gibbs counted the two principal curvatures c_1 and c_2 separately in the change of the internal energy of the interface [9]

$$dU^s = TdS^s + \sum_i \mu_i dn_i^s + \gamma_G dA + A\mathbb{C}_x dc_1 + A\mathbb{C}_y dc_2 \tag{2.10}$$

where U is the internal energy, T the temperature, S the entropy, μ_i the chemical potential of molecules of type i and n_i the number of molecules of type i. The superscripts s denote interfacial excess quantities. Moreover, γ_G represents the interfacial tension and A the interfacial area at the dividing plane located at R_s (see figure 2.3). $\mathbb{C}_x$ and $\mathbb{C}_y$ are the curvature coefficients.

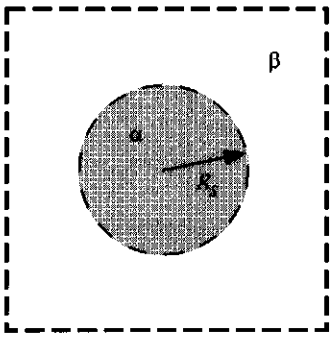

FIGURE 2.3. Schematic representation of a system consisting of two phases, α and β, respectively, separated by an infinitesimal thin (curved) interface at R_s to which the excesses are assigned.

Combining the curvature terms, eqn (2.10) can be rewritten as

$$dU^s = TdS^s + \sum_i \mu_i dn_i^s + \gamma_G dA + \frac{1}{2}A\left(\mathbb{C}_x + \mathbb{C}_y\right) d(c_1 + c_2) + \frac{1}{2}A\left(\mathbb{C}_x - \mathbb{C}_y\right) d(c_1 - c_2)$$

Gibbs considered spherical interfaces, i.e. $c_1 = c_2$, so the last term in the previous equation vanishes. This is also thought to be a good approximation for moderately curved interfaces, i.e. $c_1 \approx c_2$. He also assumed a position of the arbitrary interface, the so-called surface of tension [10, 11], where $\mathbb{C}_x + \mathbb{C}_y$ vanishes [9]. Consequently, only the first three terms on the right hand side remain. This is the well-known expression for the internal energy of interfaces [1]. Using the principle of minimum energy yields the well-known Laplace equation of capillarity [1, 9]

$$\Delta p = \gamma_G J \tag{2.11}$$

This equation effectively states that the volume work against the Laplace pressure difference Δp balances the interfacial work [10, 12]. However, the position of the surface of tension is sometimes hard to locate [3, 13, 14], as will be illustrated in section 2.6.2. Therefore a more rigorous formalism may be required, as will be put forward in the subsequent sections.

In terms of the total and Gaussian curvatures, J and K, the change in internal energy U^s of the interface becomes

$$dU^s = TdS^s + \sum_i \mu_i dn_i^s + \gamma_G dA + A\mathbb{C}_1 dJ + A\mathbb{C}_2 dK \tag{2.12}$$

The coefficients $\mathbb{C}_1$ and $\mathbb{C}_2$ are the so-called bending stress and torsion stress, respectively [11]. Note that compared to eqn (2.10) the definition of the interfacial tension

has formally been changed. In eqn (2.10) the interfacial tension is the derivative of the energy with respect to the interfacial area at constant entropy, number of molecules and principal curvatures c_1 and c_2. In eqn (2.12) the interfacial tension is the derivative of the energy with respect to the interfacial area at constant entropy, number of molecules and curvatures J and K. Since J and K are constant as c_1 and c_2 are constant, the formal difference between the interfacial tensions γ_G is irrelevant [15].

Integration of eqn (2.12) yields

$$U^s = TS^s + \sum_i \mu_i n_i^s + \gamma_G A \tag{2.13}$$

where Euler's theorem for homogeneous functions has been used. From that theorem it follows that the 'intensive' variables J and K do not contribute to the integration [2, 16]. Varying the interfacial area A at constant curvatures J and K is possible using radial integration [3, 12]. Physically, this means that the internal energy of the total system is obtained by adding infinitesimal conical subsystems.

2.2.1. The grand potential

In order to arrive at a more general applicable Laplace equation than eqn (2.11), only the mechanical work is of current interest. To that end, a Legendre transformation is performed that yields the so-called grand potential Ω

$$\Omega \equiv U - TS - \sum_i \mu_i n_i \tag{2.14}$$

Gibbs derived for the change in internal energy U^b of either bulk phase [1]

$$dU^b = TdS^b - p^b dV^b + \sum_i \mu_i dn_i^b \tag{2.15}$$

where p^b is the bulk pressure of phase $b = \alpha$ or β with volume V^b. Integration yields

$$U^b = TS^b - p^b V^b + \sum_i \mu_i n_i^b$$

For the grand potential of either bulk phase it therefore follows

$$\Omega^b = -p^b V^b \tag{2.16}$$

The grand potential of the interface follows from eqn (2.13)

$$\Omega^s = \gamma_G A \tag{2.17}$$

Hence, using eqn (2.16) and eqn (2.17), the grand potential Ω of the two-phase system is written as

$$\Omega = \Omega^\alpha + \Omega^\beta + \Omega^s = -p^\alpha V^\alpha - p^\beta V^\beta + \gamma_G A \tag{2.18}$$

Since the total volume of the system is given by $V = V^\alpha + V^\beta$, eqn (2.18) can be rewritten as

$$\Omega = \gamma_G A - \Delta p V^\alpha - p^\beta V \tag{2.19}$$

where $\Delta p \equiv p^\alpha - p^\beta$ is the Laplace pressure difference between the two phases α and β.

2.2.2. Arbitrary dividing plane

The grand potential Ω is a measurable property of the considered system and can therefore not be a function of the choice of the position of the dividing plane. Neither can this be the case for the pressures of the bulk phases and, consequently, the Laplace pressure difference. If the position of the dividing plane is shifted notionally, i.e. if the position of the interface is changed without affecting the system physically, the grand potential of the equilibrium state should not change. Therefore, corresponding to the principle of minimum free energy [17, 18], the derivative of eqn (2.18) with respect to the arbitrary dividing plane R_s yields

$$\left[\frac{d\Omega}{dR_s}\right] = -p^\alpha \left[\frac{dV^\alpha}{dR_s}\right] - p^\beta \left[\frac{dV^\beta}{dR_s}\right] + A \left[\frac{d\gamma_G}{dR_s}\right] + \gamma_G \left[\frac{dA}{dR_s}\right] = 0 \tag{2.20}$$

where the square brackets denote the notional shift of the dividing plane [12]. As the total volume V does not change by the choice of a dividing plane either, it is seen that $dV^\alpha = -dV^\beta$. Now, eqn (2.20) can be rewritten as

$$\Delta p = p^\alpha - p^\beta = A \left[\frac{d\gamma_G}{dR_s}\right] \left[\frac{dR_s}{dV^\alpha}\right] + \gamma_G \left[\frac{dA}{dR_s}\right] \left[\frac{dR_s}{dV^\alpha}\right] \tag{2.21}$$

The change of the grand potential of the interface can be derived from eqn (2.17)

$$d\Omega^s = \gamma_G dA + A d\gamma_G \tag{2.22}$$

On the other hand, from eqn (2.12) and the definition of Ω, eqn (2.14), it can also be derived that

$$\begin{aligned} d\Omega^s =& dU^s - TdS^s - S^s dT - \sum_i \mu_i dn_i^s - \sum_i n_i^s d\mu_i \\ =& - S^s dT + \gamma_G dA + A\mathbb{C}_1 dJ + A\mathbb{C}_2 dK - \sum_i n_i^s d\mu_i \end{aligned} \tag{2.23}$$

Because only a notional displacement is studied, the intensive variables T and μ_i's are unaffected by shifting the dividing plane. Thus, the following Gibbs-Duhem relation is derived from eqn (2.22) and eqn (2.23)

$$[d\gamma_G] = \mathbb{C}_1 [dJ] + \mathbb{C}_2 [dK] \tag{2.24}$$

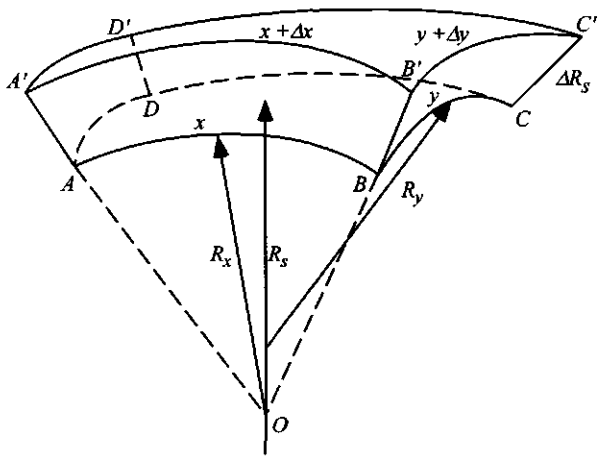

FIGURE 2.4. Section of the interface at R_s with local radii of curvature R_x and R_y.

Using eqn (2.24) differentiated with respect to R_s, eqn (2.21) can be rewritten as

$$\Delta p = A\left[\frac{dR_s}{dV^\alpha}\right]\left(\mathbb{C}_1\left[\frac{dJ}{dR_s}\right]+\mathbb{C}_2\left[\frac{dK}{dR_s}\right]\right)+\gamma_G\left[\frac{dA}{dV^\alpha}\right] \tag{2.25}$$

Finally, expressions for the remaining derivatives in eqn (2.25) can be derived from geometrical considerations in order to arrive at the generalized Laplace equation. This will be done now.

The interface is chosen to be at R_s taken positive relative to the concave side of the interface, i.e. from the inside of bulk phase α, as shown in figure 2.3. A segment of the interface $ABCD$ of size $x \times y$ is considered. The local radius in the x-direction is assumed to be R_x and in the y-direction R_y, as shown in figure 2.4. Now, a step ΔR_s is taken in the direction of R_s. The section of the interface $A'B'C'D'$ at $R_s + \Delta R_s$ is parallel to $ABCD$ and has an area $(x + \Delta x) \times (y + \Delta y)$. If an infinitesimal step is taken, $\Delta R_s \to dR_s$, the volume between the parallel section of the interface $ABCD$ and $A'B'C'D'$ is given by $dV^\alpha = xydR_s = AdR_s$. Therefore

$$\left[\frac{dV^\alpha}{dR_s}\right] = A \tag{2.26}$$

Substitution into eqn (2.25) gives

$$\Delta p = \mathbb{C}_1\left[\frac{dJ}{dR_s}\right]+\mathbb{C}_2\left[\frac{dK}{dR_s}\right]+\gamma_G\left[\frac{dA}{dV^\alpha}\right] \tag{2.27}$$

The triangles OAB and $OA'B'$ are similar, so [17, 19]

$$\frac{x}{x+\Delta x} = \frac{R_x}{R_x+\Delta R_s} \Leftrightarrow \Delta x = \frac{1}{R_x}x\Delta R_s$$

Similarly, it can be derived that

$$\frac{y}{y+\Delta y} = \frac{R_y}{R_y + \Delta R_s} \Leftrightarrow \Delta y = \frac{1}{R_y} y \Delta R_s$$

Using these expressions as well as the ones for J and K, eqn (2.9), the interfacial area at $R_s + \Delta R_s$ is given by [15]

$$\begin{aligned} A(R_s + \Delta R_s) = &(x + \Delta x)(y + \Delta y) = xy + x\Delta y + y\Delta x + \Delta x \Delta y \\ =&xy + xy\frac{1}{R_x}\Delta R_s + xy\frac{1}{R_y}\Delta R_s + xy\frac{1}{R_x}\frac{1}{R_y}(\Delta R_s)^2 \\ =&A\left\{1 + J\Delta R_s + K(\Delta R_s)^2\right\} \end{aligned} \tag{2.28}$$

For an infinitesimal step $(\Delta R_s)^2$ is negligible. So, in the limit $\Delta R_s \to dR_s$, using eqn (2.26) and $dA = A(R_s + dR_s) - A$, it follows that

$$\left[\frac{dA}{dV^\alpha}\right] = \left[\frac{dA}{dR_s}\right]\left[\frac{dR_s}{dV^\alpha}\right] = J \tag{2.29}$$

Substitution into eqn (2.27) gives

$$\Delta p = \gamma_G J + \mathbb{C}_1 \left[\frac{dJ}{dR_s}\right] + \mathbb{C}_2 \left[\frac{dK}{dR_s}\right] \tag{2.30}$$

Since the interfaces are taken to be parallel, R_x and R_y are both linear functions of R_s [20]. Using the definition of the curvatures, eqn (2.9), the derivatives of the curvatures with respect to the position of the dividing plane yield [15]

$$\begin{aligned} \left[\frac{dJ}{dR_s}\right] &= \left[\frac{d\left(\frac{1}{R_x} + \frac{1}{R_y}\right)}{dR_s}\right] \\ &= -\frac{1}{R_x^2} - \frac{1}{R_y^2} = -\left(\frac{1}{R_x} + \frac{1}{R_y}\right)^2 + 2\frac{1}{R_x}\frac{1}{R_y} = -J^2 + 2K \end{aligned} \tag{2.31}$$

$$\left[\frac{dK}{dR_s}\right] = \left[\frac{d\left(\frac{1}{R_x}\frac{1}{R_y}\right)}{dR_s}\right] = -\frac{1}{R_x^2}\frac{1}{R_y} - \frac{1}{R_x}\frac{1}{R_y^2} = -\left(\frac{1}{R_x} + \frac{1}{R_y}\right)\frac{1}{R_x}\frac{1}{R_y} = -JK \tag{2.32}$$

Substitution of eqn (2.31) and eqn (2.32) into eqn (2.30) yields

$$\Delta p = \gamma_G J - \mathbb{C}_1\left(J^2 - 2K\right) - \mathbb{C}_2 JK \tag{2.33}$$

This is the so-called *generalized Laplace equation of capillarity*, with the interfacial tension according to Gibbs as introduced in eqn (2.10) or, analogously, in eqn (2.12) [15].

Using eqn (2.6) and eqn (2.7) for J and K, eqn (2.12) can be rewritten in the form of eqn (2.10)

$$dU^s = TdS^s + \sum_i \mu_i dn_i^s + \gamma_G dA + A\left(\mathbb{C}_1 + \mathbb{C}_2 c_2\right) dc_1 + A\left(\mathbb{C}_1 + \mathbb{C}_2 c_1\right) dc_2 \tag{2.34}$$

From the identity of eqn (2.10) and eqn (2.34) the relation between the bending and torsion stress, $\mathbb{C}_1$ and $\mathbb{C}_2$, and the curvature coefficients, $\mathbb{C}_x$ and $\mathbb{C}_y$, follows immediately. Substitution of these relations in the generalized Laplace equation, eqn (2.33), yields this equation in terms of curvature coefficients

$$\Delta p = \gamma_G J - \mathbb{C}_x c_1^2 - \mathbb{C}_y c_2^2 \tag{2.35}$$

For spherical interfaces the last two terms can be merged. At the surface of tension the sum of the curvature coefficients vanishes by definition, so the last two terms of eqn (2.35) vanish at that interface. In this way the classical Laplace equation, eqn (2.11), is recovered. From eqn (2.21), using eqn (2.26) and eqn (2.29), it is found that the generalized Laplace equation can also be given as

$$\Delta p = \gamma_G J + \left[\frac{d\gamma_G}{dR_s}\right] \tag{2.36}$$

So, the last two terms of eqn (2.35) are equal to the derivative of the interfacial tension with respect to the arbitrary dividing plane which must vanish at the surface of tension. Therefore, the condition $[d\gamma_G/dR_s] = 0$ is more often used to define the surface of tension than the original definition by Gibbs. However, it has been shown that these definitions are equivalent for spherical and moderately curved interfaces.

2.3. INTERFACIAL TENSION ACCORDING TO BORUVKA AND NEUMANN

The first law of thermodynamics states that the internal energy of U of a system can only change due to heat flow q and work w done on the system

$$dU = đq + đw$$

where the strokes refer to the fact that q and w are not state variables. The second law of thermodynamics provides an expression for the heat flow for reversible processes

$$đq_{\text{rev}} = TdS$$

The work terms for the energy are the 'generalized forces', f_i, acting on the system over certain 'generalized distances', dX_i [21]

$$đw = \sum_i f_i dX_i$$

Therefore, the change of the internal energy should strictly be of the form [20]

$$dU = \sum \text{intensive variables } d\,(\text{extensive variables}) \tag{2.37}$$

According to Euler's theorem, only a total differential of this form can be integrated. If a change in a desired state variable also contains terms of the form

$$\sum \text{extensive variables } d\,(\text{intensive variables})$$

one should perform a Legendre transformation in order to arrive at a total differential of the form eqn (2.37) of an other state variable. That state variable can be integrated and the inverse Legendre transformation gives the desired state variable. It is then seen that Euler's theorem effectively states that changes in intensive variables drop out after integration [2, 16]. This also can be seen in a more physical way. Intensive properties are independent of the system's size, whereas extensive variables are proportional to it. So, when the characteristic function of the total system is obtained by adding infinitesimal subsystems, the intensive variables do not contribute.

In order to arrive at the internal energy of an interface as given by eqn (2.13) from its change eqn (2.12), the curvatures were explicitly taken to be intensive variables. However, this is not strictly the case [2] because, unlike e.g. the temperature, they might change upon changing the system's size. Moreover, the curvatures were assumed to be uniform over the interface. These deficiencies are overcome by introducing the extensive curvatures [19]

$$\mathcal{J} = \int J dA,\ \mathcal{K} = \int K dA \tag{2.38}$$

Where J and K are the local curvatures, as given by eqn (2.6) and eqn (2.7). In terms of the extensive curvatures $\mathcal{J}$ and $\mathcal{K}$ the change of the internal energy of the interface can be written as

$$dU^s = TdS^s + \sum_i \mu_i dn_i^s + \gamma_{BN} dA + \mathbb{C}_1 d\mathcal{J} + \mathbb{C}_2 d\mathcal{K} \tag{2.39}$$

Here, γ_{BN} is the interfacial tension proposed by Boruvka and Neumann, i.e. defined such that the curvatures are taken to be extensive. From eqn (2.12) it is seen that the interfacial tension according to Gibbs is the change of the energy with respect to a change in the interfacial area at constant curvatures, whereas it follows from eqn (2.39) that the interfacial tension according to Boruvka and Neumann is the change of the energy with respect to a change in the interfacial area at constant product of area and curvature. That means that the interfacial tension according to Gibbs represents pure stretching whereas the interfacial tension according to Boruvka and Neumann incorporates bending work [18]. Since it is difficult to realize a constant product of

interfacial area and curvature, the latter interfacial tension is of little relevance for conducting experiments. Integration of eqn (2.39) using Euler's theorem yields [19]

$$U^s = TS^s + \sum_i \mu_i n_i^s + \gamma_{BN} A + \mathbb{C}_1 \mathcal{J} + \mathbb{C}_2 \mathcal{K} \tag{2.40}$$

If the interface is uniformly curved, i.e. J and K are independent of the position on the chosen interface, eqn (2.38) can be written as [15, 20]

$$\mathcal{J} = JA, \ \mathcal{K} = KA \tag{2.41}$$

Substitution in eqn (2.40) yields

$$\begin{aligned} U^s =& TS^s + \sum_i \mu_i n_i^s + \gamma_{BN} A + \mathbb{C}_1 JA + \mathbb{C}_2 KA \\ =& TS^s + \sum_i \mu_i n_i^s + (\gamma_{BN} + \mathbb{C}_1 J + \mathbb{C}_2 K) A \end{aligned} \tag{2.42}$$

Comparison with eqn (2.13) yields the relation between γ_G and γ_{BN} for uniformly curved interfaces [15]

$$\gamma_G = \gamma_{BN} + \mathbb{C}_1 J + \mathbb{C}_2 K \tag{2.43}$$

Substitution in eqn (2.33) yields the generalized Laplace equation according to Boruvka and Neumann [17]

$$\Delta p = \gamma_{BN} J + 2\mathbb{C}_1 K \tag{2.44}$$

It has been shown that this expression remains valid for non-uniformly curved interfaces and in the absence of an external field [17]. This expression for the Laplace pressure is formally more correct although it has been proven that for uniformly, moderately curved interfaces it can also be written as eqn (2.33), which, in turn, reduces to the classical Laplace equation at the surface of tension.

2.4. INTERFACIAL PROPERTIES FROM PRESSURE PROFILES

Consider different infinitesimal elements of a two-phase system at equilibrium, e.g. as shown in figure 2.3. Obviously, in either bulk phase the forces on all faces of this element must be equal. However, for an element in the interfacial region the forces parallel to the faces of the element may differ from those perpendicular to it [22]. These deviations give rise to extra stress in the interfacial region: the interfacial tension. From this point of view it is customary to relate the prevailing local pressure profile $p_T(\vec{r})$ to the grand potential [23]

$$\Omega = -\int p_T(\vec{r}) d\vec{r} \tag{2.45}$$

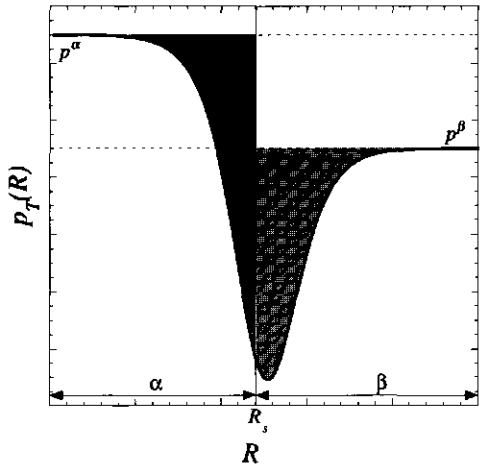

FIGURE 2.5. An example of a pressure profile p_T going in radial direction R from phase α to phase β.

This is the so-called mechanical expression of the grand potential, i.e. based on the pressure profile.

The grand potential of a bulk phase Ω^b as given by eqn (2.16) can be written as a volume integral

$$\Omega^b = -p^b V^b = -\int_{V^b} p^b d\vec{r} \tag{2.46}$$

If there were no interfacial contributions in the two-phase system, the grand potential would simply be the sum of the grand potentials of both phases. However, as stated, in the interfacial region the actual pressure p_T lateral to the interface differs from the bulk pressures. An example of a pressure profile is given in figure 2.5. If only the bulk phases were accounted for, the grey area would be algebraically counted as an excess for phase α and the same applies for the hatched area for phase β. Upon comparison of the thermodynamic expression, eqn (2.18), and the mechanical expression, eqn (2.45), for the total grand potential with the bulk grand potential as given by eqn (2.46), it is found that the excess amounts indeed constitute the grand potential of the interface

$$\Omega^s = \gamma_G A = \int_{V^\alpha} (p^\alpha - p_T(\vec{r}))d\vec{r} + \int_{V^\beta} (p^\beta - p_T(\vec{r}))d\vec{r} \tag{2.47}$$

It is now convenient to define $p^{\alpha\beta}$, which equals p^α in phase α and p^β in phase β, thus

$$\Omega^s = \int (p^{\alpha\beta} - p_T(\vec{r}))d\vec{r} \tag{2.48}$$

Using the principle of parallel interfaces [11, 19] the volume integral can be replaced by an integral over a one dimensional coordinate through the whole system relative to the centre of the inner phase α by applying eqn (2.26) as well as eqn (2.28) with $R = R_s + \Delta R_s$

$$\begin{aligned}\Omega^s &= \int \left(p^{\alpha\beta} - p_T(R)\right) A(R) dR \\ &= A \int \left[1 + (R - R_s)J + (R - R_s)^2 K\right] \left(p^{\alpha\beta} - p_T(R)\right) dR\end{aligned}$$

Using the grand potential of the interface, eqn (2.17), the interfacial tension γ_G according to Gibbs is given by [15]

$$\gamma_G = \mathbb{P}_0 + \mathbb{P}_1 J + \mathbb{P}_2 K \tag{2.49}$$

where the zeroth, first, and second bending moments are introduced, defined as

$$\mathbb{P}_0 \equiv \int (p^{\alpha\beta} - p_T(R)) dR \tag{2.50a}$$

$$\mathbb{P}_1 \equiv \int (R - R_s)(p^{\alpha\beta} - p_T(R)) dR \tag{2.50b}$$

$$\mathbb{P}_2 \equiv \int (R - R_s)^2 (p^{\alpha\beta} - p_T(R)) dR \tag{2.50c}$$

It is tempting to match eqn (2.49) term-wise to eqn (2.43). Indeed, since J and K are generally independent, in the literature it is sometimes found that corresponding terms of eqn (2.49) and eqn (2.43) are matched in order to obtain integral expressions for the bending stress, torsion stress, and interfacial tension according to Boruvka and Neumann in terms of the pressure profile [19, 20]. That is, the interfacial tension according to Boruvka and Neumann, the bending stress and torsion stress are equated as the zeroth, first, and second bending moments respectively, *viz.* $\gamma_{BN} = \mathbb{P}_0$, $\mathbb{C}_1 = \mathbb{P}_1$, and $\mathbb{C}_2 = \mathbb{P}_2$. Others actually *define* the bending stress, torsion stress, and interfacial tension this way [11, 24]. However, it is in principle possible that other combinations of moments of the pressure profile also lead to the same thermodynamically consistent state variable γ_G since $\mathbb{P}_0$, $\mathbb{P}_1$, and $\mathbb{P}_2$ are functions of J and K themselves. The molecules will generally redistribute upon bending which affects the (excess) pressure profile and hence the various bending moments, as can be seen from eqn (2.50). From this point of view the matching procedure and, by that, the validity of the mechanical expressions for the bending stress and torsion stress is questionable. Progress can be made when expressions for $\mathbb{C}_1$ and $\mathbb{C}_2$ are found from their thermodynamic definitions.

2.5. MECHANICAL EXPRESSIONS FOR BENDING AND TORSION STRESS

The Gibbs-Duhem relation derived from comparison of eqn (2.22) and eqn (2.23) reads

$$d\gamma_G = -s^s dT + \mathbb{C}_1 dJ + \mathbb{C}_2 dK - \sum_i \Gamma_i d\mu_i \tag{2.51}$$

where s^s is the excess entropy per unit area and $\Gamma_i \equiv n_i^s/A$ the excess number of molecules of type i per unit area or the *adsorbed amount* or *surface concentration.* This is the most general version of the well-known Gibbs adsorption equation. Bending an interface may force molecules to adsorb at or desorb from the interface. This changes in general the composition of the adjacent bulk phases and hence the chemical potential of the components, as also can be seen from the Maxwell relations $\left(\frac{\partial \mu_i}{\partial J}\right)_{T,A,K,\{n_i^s\}} = \left(\frac{\partial A\mathbb{C}_1}{\partial n_i^s}\right)_{T,A,J,K,\{n^s_{i\neq j}\}}$ and $\left(\frac{\partial \mu_i}{\partial K}\right)_{T,A,J,\{n_i^s\}} = \left(\frac{\partial A\mathbb{C}_2}{\partial n_i^s}\right)_{T,A,J,K,\{n^s_{i\neq j}\}}$. Consequently, the set of variables that determine the interfacial tension, T, J, K, and μ_i's, is in those specific cases redundant. This makes the chemical potentials curvature-dependent

$$(d\mu_i)_T = \left(\frac{\partial \mu_i}{\partial J}\right)_{T,K} dJ + \left(\frac{\partial \mu_i}{\partial K}\right)_{T,J} dK$$

Substitution in the Gibbs adsorption equation, eqn (2.51), gives

$$d\gamma_G = -s^s dT + \left(\mathbb{C}_1 - \sum_i \Gamma_i \left(\frac{\partial \mu_i}{\partial J}\right)_{T,K}\right) dJ + \left(\mathbb{C}_2 - \sum_i \Gamma_i \left(\frac{\partial \mu_i}{\partial K}\right)_{T,J}\right) dK \tag{2.52}$$

From this total differential it follows that the bending stress is thermodynamically found as

$$\mathbb{C}_1 = \left(\frac{\partial \gamma_G}{\partial J}\right)_{T,K} + \sum_i \Gamma_i \left(\frac{\partial \mu_i}{\partial J}\right)_{T,K} \tag{2.53}$$

and the torsion stress as

$$\mathbb{C}_2 = \left(\frac{\partial \gamma_G}{\partial K}\right)_{T,J} + \sum_i \Gamma_i \left(\frac{\partial \mu_i}{\partial K}\right)_{T,J} \tag{2.54}$$

Obviously, in the case that the chemical potentials are constant upon bending, the terms containing μ_i vanish. Using the mechanical expression for γ_G, eqn (2.49), eqn (2.53) is written as

$$\mathbb{C}_1 = \mathbb{P}_1 + \left(\frac{\partial \mathbb{P}_0}{\partial J}\right)_{T,K} + J\left(\frac{\partial \mathbb{P}_1}{\partial J}\right)_{T,K} + K\left(\frac{\partial \mathbb{P}_2}{\partial J}\right)_{T,K} + \sum_i \Gamma_i \left(\frac{\partial \mu_i}{\partial J}\right)_{T,K} \tag{2.55}$$

and, by the same token,

$$\mathbb{C}_2 = \mathbb{P}_2 + \left(\frac{\partial \mathbb{P}_0}{\partial K}\right)_{T,J} + J\left(\frac{\partial \mathbb{P}_1}{\partial K}\right)_{T,J} + K\left(\frac{\partial \mathbb{P}_2}{\partial K}\right)_{T,J} + \sum_i \Gamma_i \left(\frac{\partial \mu_i}{\partial K}\right)_{T,J} \tag{2.56}$$

where J and K are generally independent state-variables.

It is crucial to distinguish notional from actual bending of the interface. In the former case one changes the position of the dividing plane mathematically and by that the curvature without affecting the system physically. As will be shown in section 2.5.1, the derivatives of the moments of the pressure profiles can be determined explicitly if the curvature is changed notionally. The derivatives of the moments of the pressure profiles, the generalized Laplace equation of capillarity, and the thermodynamic expression for the interfacial tension, eqn (2.43), can be substituted into eqn (2.55) and eqn (2.56). It is then found that all derivatives with respect to the curvatures in eqn (2.55) and eqn (2.56) cancel. Hence, in the case of notional bending the bending and torsion stress are identified as the first and second bending moment, respectively. Consequently, from eqn (2.43) and eqn (2.49) it follows straightforwardly that the interfacial tension according to Boruvka and Neumann equals the zeroth bending moment for the case that the interface is bend only notionally.

However, according to the actual definition of bending and torsion stress, one has to do real work. That is, for a given choice of the position of the dividing plane the curvature of the interface is changed physically. Since bending generally leads to a redistribution of the molecules, as stated before, one needs a molecular model to evaluate the derivatives of the pressure profile with respect to the curvature in eqn (2.55) and eqn (2.56). This implies that eqn (2.55) and eqn (2.56) are the most general expressions for the bending and torsion stress, respectively, in terms of the pressure profile. Inserting these into eqn (2.43) yields, after comparison with eqn (2.49), for the interfacial tension according to Boruvka and Neumann,

$$\begin{aligned}\gamma_{BN} = \mathbb{P}_0 - \left(\frac{\partial \mathbb{P}_0}{\partial J}\right)_{T,K} J - \left(\frac{\partial \mathbb{P}_1}{\partial J}\right)_{T,K} J^2 - \left(\frac{\partial \mathbb{P}_0}{\partial K}\right)_{T,J} K \\ - \left\{\left(\frac{\partial \mathbb{P}_2}{\partial J}\right)_{T,K} + \left(\frac{\partial \mathbb{P}_1}{\partial K}\right)_{T,J}\right\} JK - \left(\frac{\partial \mathbb{P}_2}{\partial K}\right)_{T,J} K^2 \\ - \sum_i \Gamma_i \left\{\left(\frac{\partial \mu_i}{\partial J}\right)_{T,K} J + \left(\frac{\partial \mu_i}{\partial K}\right)_{T,J} K\right\}\end{aligned} \tag{2.57}$$

Although this interfacial tension is formally more correct because it considers the curvatures as extensive variables, it is also of little relevance in simulations since detailed knowledge of the pressure profile as a function of curvature is required. Indeed, for a planar interface ($J = K = 0$), both eqn (2.49) and eqn (2.57) reduce to the Kirkwood-Buff expression for the interfacial tension [25].

The mechanical expressions for the interfacial tension according to Boruvka and Neumann, eqn (2.57), the bending stress, eqn (2.55), and the torsion stress, eqn (2.56), differ significantly from those suggested in the literature [15, 20]. Consequently, it has been proven mathematically that matching the terms of eqn (2.43) and eqn (2.49) is disputable.

2.5.1. Mechanical derivation of the generalized Laplace equation

A thorough analysis both in thermodynamic and mechanic terms gives a result that differs essentially from the result that is found with the matching procedure in the literature. The thermodynamic consistency of the above expressions is illustrated by deriving the generalized Laplace equation of capillarity from the mechanical expressions. To that end, it is again of interest how the interfacial tension depends on the choice of the position of the interface, without affecting the system physically. When eqn (2.43) is used for the derivative of γ_G with respect to the position of the arbitrary interface, it is found that

$$\left[\frac{d\gamma_G}{dR_s}\right] = \left[\frac{d\gamma_{BN}}{dR_s}\right] + J\left[\frac{d\mathbb{C}_1}{dR_s}\right] + K\left[\frac{d\mathbb{C}_2}{dR_s}\right] + \mathbb{C}_1\left[\frac{dJ}{dR_s}\right] + \mathbb{C}_2\left[\frac{dK}{dR_s}\right] \tag{2.58}$$

As before, the square brackets denote the notional change of the position of the interface [12]. Substitution of the Gibbs-Duhem relation eqn (2.24) differentiated with respect to R_s into eqn (2.58) yields

$$\left[\frac{d\gamma_{BN}}{dR_s}\right] + J\left[\frac{d\mathbb{C}_1}{dR_s}\right] + K\left[\frac{d\mathbb{C}_2}{dR_s}\right] = 0 \tag{2.59}$$

Using the mechanical expressions for the interfacial tension according to Boruvka and Neumann, eqn (2.57), the bending stress, eqn (2.55), and the torsion stress, eqn (2.56), it turns out that all the derivatives of the bending moments and chemical potentials differentiated with respect to the position of the arbitrary dividing plane cancel. Consequently, eqn (2.59) can be rewritten as

$$\begin{aligned}
&\left[\frac{d\mathbb{P}_0}{dR_s}\right] + J\left[\frac{d\mathbb{P}_1}{dR_s}\right] + K\left[\frac{d\mathbb{P}_2}{dR_s}\right] \\
&\quad = \left\{\left(\frac{\partial\mathbb{P}_0}{\partial J}\right)_{T,K} + J\left(\frac{\partial\mathbb{P}_1}{\partial J}\right)_{T,K} + K\left(\frac{\partial\mathbb{P}_2}{\partial J}\right)_{T,K} + \sum_i \Gamma_i\left(\frac{\partial\mu_i}{\partial J}\right)_{T,K}\right\}\left[\frac{dJ}{dR_s}\right] \\
&\quad + \left\{\left(\frac{\partial\mathbb{P}_0}{\partial K}\right)_{T,J} + J\left(\frac{\partial\mathbb{P}_1}{\partial K}\right)_{T,J} + K\left(\frac{\partial\mathbb{P}_2}{\partial K}\right)_{T,J} + \sum_i \Gamma_i\left(\frac{\partial\mu_i}{\partial K}\right)_{T,J}\right\}\left[\frac{dK}{dR_s}\right]
\end{aligned} \tag{2.60}$$

Now the derivatives of the bending moments with respect to the position of the arbitrary dividing plane, as found on the left-hand side of eqn (2.60), are evaluated. To

that end, the excess pressure profile is written as

$$p^{\alpha\beta} - p_T(R) = p^{\alpha}\left(1 - \theta(R - R_s)\right) + p^{\beta}\theta(R - R_s) - p_T(R) \tag{2.61}$$

where $\theta(R - R_s)$ is the Heaviside step function

$$\theta(R - R_s) = \begin{cases} 0 & R < R_s \\ 1 & R \geq R_s \end{cases}$$

The grand potential is a state variable and therefore not a function of the position of the arbitrary dividing plane. It therefore follows from eqn (2.45) that p_T can neither be a function of R_s. Hence, the derivative of the excess pressure profile with respect to R_s becomes

$$\left[\frac{\partial\left(p^{\alpha\beta} - p_T(R)\right)}{\partial R_s}\right] = p^{\alpha}\delta(R - R_s) - p^{\beta}\delta(R - R_s) = \Delta p\delta(R - R_s)$$

where $\delta(R - R_s)$ is the Dirac delta function and $\Delta p \equiv p^{\alpha} - p^{\beta}$ is again the Laplace pressure difference. Changing the order of differentiation and integration yields for $\mathbb{P}_0$

$$\left[\frac{\partial \int p^{\alpha\beta} - p_T(R)dR}{\partial R_s}\right] = \int\left[\frac{\partial p^{\alpha\beta} - p_T(R)}{\partial R_s}\right]dR = \int \Delta p\delta(R - R_s)dR = \Delta p \tag{2.62}$$

By way of illustration, consider again the pressure profile p_T as in figure 2.5. The arbitrary dividing plane was chosen at R_s, so the integral over the excess pressure profile can be determined, indicated with both the dark grey and hatched area in figure 2.5. Now, the plane is shifted over a distance dR_s and again the integral over the excess pressure profile can be determined. This is the grey and hatched area in figure 2.6. The difference between the two integrals equals exactly the light grey area with the size of $\Delta p dR_s$, recovering eqn (2.62) graphically [20].

This equivalence can also be shown mathematically by splitting the integral into a part up to and one beyond R_s, i.e. one integral over phase α and one over phase β

$$\begin{aligned}
\frac{\partial \int p^{\alpha\beta} - p_T(R)dR}{\partial R_s} &= \frac{\partial}{\partial R_s}\int_0^{R_s}(p^{\alpha} - p_T)dR + \frac{\partial}{\partial R_s}\int_{R_s}^{R_\infty}(p^{\beta} - p_T)dR \\
&= \frac{\partial}{\partial R_s}\int_0^{R_s} p^{\alpha}dR + \frac{\partial}{\partial R_s}\int_{R_s}^{R_\infty} p^{\beta}dR - \frac{\partial}{\partial R_s}\int_0^{R_\infty} p_T(R)dR \\
&= \frac{\partial}{\partial R_s}\left(p^{\alpha}R_s - 0\right) + \frac{\partial}{\partial R_s}\left(p^{\alpha}R_\infty - p^{\beta}R_s\right) = p^{\alpha} - p^{\beta}
\end{aligned}$$

where R_∞ is the system's radius and use has been made of the fact that the integral over p_T does not depend on the position of R_s. Once again, only the Laplace pressure difference remains. Although the integration limits depend on R_s, the identity of

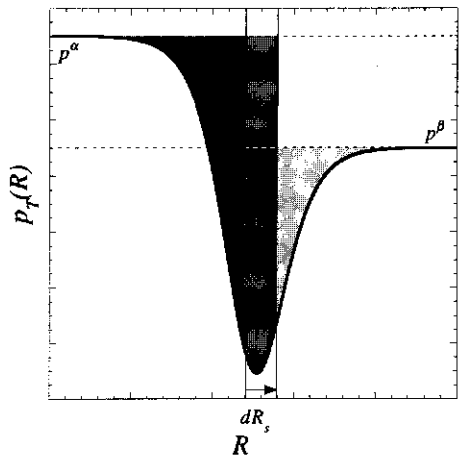

FIGURE 2.6. The shift of the dividing plane by dR_s in the example pressure profile p_T gives a total change of $\left(p^\alpha - p^\beta\right) dR_s$ for the excess pressure.

the results of both methods proves that exchange of differentiation and integration in eqn (2.62) is allowed.

The derivative of the first bending moment, $\mathbb{P}_1$, can now also be determined

$$\begin{aligned}\left[\frac{\partial \mathbb{P}_1}{\partial R_s}\right] &= \left[\frac{\partial \int (R - R_s)\left(p^{\alpha\beta} - p_T(R)\right) dR}{\partial R_s}\right] \\ &= -\int p^{\alpha\beta} - p_T(R) dR + \int (R - R_s)\Delta p \delta(R - R_s) dR \\ &= -\int p^{\alpha\beta} - p_T(R) dR = -\mathbb{P}_0\end{aligned}$$

In a similar way it is found that the derivative of the second moment is given by

$$\begin{aligned}\left[\frac{\partial \mathbb{P}_2}{\partial R_s}\right] &= \left[\frac{\partial \int (R - R_s)^2\left(p^{\alpha\beta} - p_T(R)\right) dR}{\partial R_s}\right] \\ &= -2\int (R - R_s)\left(p^{\alpha\beta} - p_T(R)\right) dR = -2\mathbb{P}_1\end{aligned}$$

Substitution of the derivatives of the respective bending moments into eqn (2.60) gives

$$\begin{aligned}\Delta p =& \mathbb{P}_0 J + 2\mathbb{P}_1 K \\ &+ \left\{ \left(\frac{\partial \mathbb{P}_0}{\partial J}\right)_{T,K} + J\left(\frac{\partial \mathbb{P}_1}{\partial J}\right)_{T,K} + K\left(\frac{\partial \mathbb{P}_2}{\partial J}\right)_{T,K} + \sum_i \Gamma_i \left(\frac{\partial \mu_i}{\partial J}\right)_{T,K} \right\} \left(2K - J^2\right) \\ &- \left\{ \left(\frac{\partial \mathbb{P}_0}{\partial K}\right)_{T,J} + J\left(\frac{\partial \mathbb{P}_1}{\partial K}\right)_{T,J} + K\left(\frac{\partial \mathbb{P}_2}{\partial K}\right)_{T,J} + \sum_i \Gamma_i \left(\frac{\partial \mu_i}{\partial K}\right)_{T,J} \right\} JK \end{aligned} \tag{2.63}$$

where use has been made of eqn (2.31) and eqn (2.32) for the derivatives of the curvatures with respect to the position of the dividing plane. If $\mathbb{P}_0$ is expressed in terms of γ_{BN}, using eqn (2.57), and $\mathbb{P}_1$ in terms of $\mathbb{C}_1$, using eqn (2.55), all derivatives of the bending moments and chemical potentials cancel and it is obtained that

$$\Delta p = \gamma_{BN} J + 2\mathbb{C}_1 K$$

This recovers the generalized Laplace equation according to Boruvka and Neumann, eqn (2.44). This equivalence shows the consistency of the mechanical expressions for the thermodynamic interfacial variables. Ironically, all derivatives of the bending moments that were extra for the mechanical expressions for γ_{BN}, $\mathbb{C}_1$, and $\mathbb{C}_2$ compared to the results known in the literature cancel in eqn (2.63). Consequently, the results found by matching eqn (2.43) and eqn (2.49), i.e. $\gamma_{BN} = \mathbb{P}_0$, $\mathbb{C}_1 = \mathbb{P}_1$, and $\mathbb{C}_2 = \mathbb{P}_2$, give the same generalized Laplace equations of capillarity which in turn seems to support the consistency of the matching procedure [17, 20].

In order to determine the interfacial tension, bending stress, and torsion stress from the mechanical expressions for a particular system, one has to introduce a molecular model for the (local) pressure. It will be shown in section 3.2.6 that for the case of a simple lattice model the above mechanical expressions yield unambiguous results, unlike those reported in the literature.

The method of Boruvka and Neumann, as elaborated in section 2.3, to treat the curvatures as extensive parameters formally yields more correct, generally applicable interfacial parameters. However, since the curvature and interfacial area can no longer be separated in this approach, the practical relevance is limited. It turns out that for uniformly curved interfaces the thermodynamic approach as first elaborated by Gibbs can be identified with the approach by Boruvka and Neumann. It has been shown in section 2.4 that from a quasi-thermodynamic analysis the classical interfacial tension according to Gibbs can be obtained from the bending moments of a given system.

However, as shown in section 2.5, the interfacial tension according to Boruvka and Neumann also requires derivatives with respect to the curvature thereof. This makes the approach by Boruvka and Neumann neither practically nor theoretically easily applicable.

2.6. SYSTEMS WITH MANY INTERFACES

In previous sections, systems with only one interface have been considered. However, there is a wide variety of systems with many interfaces, for instance oil/water emulsions. Since standard thermodynamics strictly only considers macroscopic systems, systems with many interfaces can only be described macroscopically. Although this is satisfactory for many purposes, it might also be of interest to consider one subsystem from such an 'ensemble' of small systems. Hill derived a complete framework of thermodynamic expressions to describe such small, open systems on a mesoscopic level allowing fluctuations [26, 27]. This thermodynamics of small systems has been applied successfully to the formation of micelles [28, 29] and microemulsions [13] and will be reviewed briefly here.

2.6.1. Thermodynamics of small systems

The macroscopic system is divided into $\mathcal{N}$ identical, non-interacting small systems in such a way that each small system contains exactly one object, e.g. a micelle or a microemulsion droplet. Since all small systems are identical, the system is assumed to be monodisperse. Although this is a very crude approximation for many systems, polydispersity can be accounted for by a weighted ensemble average over monodisperse systems [27, 30]. The change of the macroscopic internal energy U_t of a system that consists of a set of $\mathcal{N}$ small systems is written as

$$dU_t = TdS_t - p^\beta dV_t + \sum_i \mu_i dn_{ti} + \varepsilon d\mathcal{N} \tag{2.64}$$

where the subscript t denotes a property of the total, macroscopic, system. The outer phase β is here taken to be the continuous phase. The new element is that the 'subdivision work' $\varepsilon d\mathcal{N}$ has been introduced. Conjugated to the number of small systems, $\mathcal{N}$, is the so-called subdivision potential, ε, which represents the energy that is required to subdivide the system at constant total entropy, volume and number of molecules. This resembles the 'insertion work' $\mu_i dn_{ti}$ in which the chemical potential, μ_i, conjugated to the number of molecules, n_{ti}, represents the required energy to change the number of molecules of type i at constant entropy, volume, and other molecules $j \neq i$.

For further elaboration, it is not convenient to relate the subdivision potential to a characteristic function at constant total entropy. A more useful definition follows from the Gibbs energy, found from the Legendre transformation $G_t \equiv U_t - TS_t + p^\beta V_t$. Its change follows from the definition and eqn (2.64)

$$dG_t = -S_t dT + V_t dp^\beta + \sum_i \mu_i dn_{ti} + \varepsilon d\mathcal{N} \tag{2.65}$$

In this way, ε can be related to a characteristic function at constant temperature, external pressure and number of molecules. Since this is a linear homogeneous function, integration yields

$$G_t = \sum_i \mu_i n_{ti} + \varepsilon \mathcal{N} \tag{2.66}$$

The Gibbs energy G per small system containing n_i molecules of type i is

$$G = \sum_i \mu_i n_i + \varepsilon \tag{2.67}$$

For a closed set of $\mathcal{N}$ mutually open systems at equilibrium, the Gibbs energy must be minimised

$$(dG_t)_{T,p^\beta,n_{ti}} = 0 \tag{2.68}$$

From eqn (2.65) it is then found

$$\left(\frac{\partial G_t}{\partial \mathcal{N}}\right)_{T,p^\beta,n_{ti}} = \varepsilon = 0 \tag{2.69}$$

This equilibrium condition for the formation of small objects in a system, found from eqn (2.68), resembles the equilibrium condition for a chemical reaction, $\sum_i \nu_i \mu_i = 0$. In the general chemical reaction $\sum_i \nu_i A_i = 0$ the stoichiometric coefficients ν_i of the substances A_i have to be taken negative for the reactants and positive for the products. As the reaction progresses along the reaction coordinate ξ, the number of molecules of species i changes by an amount of $dn_i = \nu_i d\xi$. Consequently, the Gibbs energy changes as $dG = (\sum_i \nu_i \mu_i)\, d\xi$. From the equilibrium condition, eqn (2.68), the stated equilibrium condition is found straightforwardly [2, 16]. Physically this means that the system changes the number of molecules until the (weighted) chemical potentials are balanced. The total system of small objects changes the number of subdivisions completely analogously until, as will be shown in section 2.6.2, the total mechanical work for the formation of another object is zero. If the system cannot further decrease the number of objects, i.e. $\mathcal{N} = 1$, the limit of the thermodynamics of small systems has been reached. Although this system is an equilibrium state and the Gibbs energy is minimal, it does not satisfy eqn (2.69) since ε must then be equal to the 'regular'

interfacial terms, as indeed will be demonstrated in section 2.6.2. Therefore, $\varepsilon = 0$ is *not* the general equilibrium condition if the system does not subdivide spontaneously, e.g. a single oil drop at equilibrium with its saturated vapour. This is the analogue of a chemical reaction that goes to completion.

Note that the above analysis is phenomenological: no assumptions had to be made about the size, shape, or nature of the small system. Therefore, the small system can for instance also be a polymer in a solvent. In that case eqn (2.67) must reduce to the 'regular' equilibrium expression for the Gibbs energy of bulk systems, i.e. $\varepsilon = 0$.

2.6.2. Expression for the subdivision potential

A closer look is taken at the thermodynamics of the small system itself. Here, the small system consists of an inner bulk phase α and a continuous phase β, as shown in figure 2.3. The subdivision is chosen such that the object is located in the centre of the small system. From eqn (2.15) and eqn (2.12) the change in internal energy U of a homogeneously curved small system is given by

$$\begin{aligned} dU =& TdS - p^{\alpha}dV^{\alpha} - p^{\beta}dV^{\beta} + \sum_i \mu_i dn_i + \gamma_G dA + \mathbb{C}_1 AdJ + \mathbb{C}_2 AdK \\ =& TdS - \Delta p dV^{\alpha} - p^{\beta}dV + \sum_i \mu_i dn_i + \gamma_G dA + \mathbb{C}_1 AdJ + \mathbb{C}_2 AdK \end{aligned}$$

The corresponding change in Gibbs energy is

$$dG = -SdT - \Delta p dV^{\alpha} + V dp^{\beta} + \sum_i \mu_i dn_i + \gamma_G dA + \mathbb{C}_1 AdJ + \mathbb{C}_2 AdK \tag{2.70}$$

Owing to the nature of thermodynamics of small systems, this is not a linear homogeneous function [26, 28]. This is due to the fact that if the small system is $\mathcal{N}$ times enlarged, the system will break up spontaneously into $\mathcal{N}$ new small systems and has to do $\varepsilon\mathcal{N}$ work extra. However, since the object is located in the centre of the system, one can integrate over an angle in the system, as has also been done in section 2.2.1 to integrate over the interfacial area A at constant curvatures [3, 12]. Radial integration of eqn (2.70) gives

$$G = -\Delta p V^{\alpha} + \sum_i \mu_i n_i + \gamma_G A \tag{2.71}$$

Comparison of eqn (2.67) with eqn (2.71) yields for the subdivision potential

$$\varepsilon = \gamma_G A - \Delta p V^{\alpha} \tag{2.72}$$

It follows from eqn (2.69) and eqn (2.72) that at equilibrium the interfacial work equals the volume work against the outer pressure p^{β}, i.e. the total mechanical work in the small system is balanced.

Alternatively, the subdivision potential can be related to the grand potential, which was introduced in section 2.2.1, using eqn (2.67)

$$\varepsilon = G - \sum_i \mu_i n_i = U + p^\beta V - TS - \sum_i \mu_i n_i = \Omega + p^\beta V \tag{2.73}$$

As stated, in the limit of only one subsystem ($\mathcal{N} = 1$) the result must equal the expression for the grand potential if only one interface is present. Indeed, substitution of eqn (2.72) into eqn (2.73) yields eqn (2.19). This shows the consistency of the thermodynamics of small systems as derived by Hill and the thermodynamics of curved interfaces as derived in the previous sections [27].

The expression for the subdivision potential, eqn (2.72), gives for the Laplace pressure difference of each droplet

$$\Delta p = \frac{\gamma_G A}{V^\alpha} - \frac{\varepsilon}{V^\alpha} \tag{2.74}$$

The derivative of the interfacial tension with respect to the location of the dividing plane then reads, recalling that this choice should not affect the equilibrium state variables Δp and $\varepsilon = 0$

$$\left[\frac{d\gamma_G}{dR_s}\right] = \Delta p \left(\frac{1}{A}\left[\frac{dV^\alpha}{dR_s}\right] - \frac{V^\alpha}{A^2}\left[\frac{dA}{dR_s}\right]\right)$$

Applying the geometrical expressions eqn (2.26) and eqn (2.29), this recovers the generalized Laplace equation as given by eqn (2.36). So, as stated before, using the fact that the grand potential is independent of the notional position dividing plane, eqn (2.20), corresponds to the principle of minimum Gibbs energy.

If many objects have been formed at equilibrium, i.e. $\mathcal{N} > 1$, $\varepsilon = 0$, the Laplace equation eqn (2.74) is given by

$$\Delta p = \frac{\gamma_G A}{V^\alpha}$$

For spherical objects this reduces to

$$\Delta p = \frac{3\gamma_G}{R}$$

for any choice of the arbitrary dividing plane. On the other hand, the corresponding generalized Laplace equation reads according to eqn (2.36)

$$\Delta p = \frac{2\gamma_G}{R} + \left[\frac{d\gamma_G}{dR}\right]$$

Apparently, for a system with many spherical droplets must apply

$$\left[\frac{d\gamma_G}{dR}\right] = \frac{\gamma_G}{R}$$

As mentioned in section 2.2.2, the surface of tension is found where $[d\gamma_G/dR]$ vanishes. Apparently, this is either where $\gamma_G = 0$ or where $R \to \infty$. This implies that $\Delta p = 0$ for both cases, which is physically unacceptable. Consequently, for a system of many spherical droplets ($\mathcal{N} > 1$) at equilibrium ($\varepsilon = 0$) the surface of tension cannot be located from this analysis [13, 14].

The preceding analysis leading to eqn (2.72) ignored the translational entropy of the small system. In very dilute systems, i.e. no interactions between the objects in the total system, this can be corrected by adding the ideal entropy of mixing, i.e. all $\mathcal{N}$ objects can move freely in the total volume V_t [31, 32]

$$\varepsilon = \gamma_G A - \Delta p V^\alpha + k_B T \ln \varphi_m \simeq \varepsilon_m + k_B T \ln \varphi_m$$

where k_B is Boltzmann's constant, $\varphi_m \equiv \mathcal{N}/V_t = 1/V$ the volume fraction of objects, and ε_m is the translationally restricted subdivision potential. Thus, at equilibrium, the mechanical work, eqn (2.72), balances the entropy of mixing of the objects. Consequently, the Laplace equation of capillarity, eqn (2.74), amounts at equilibrium to

$$\Delta p = \frac{\gamma_G A}{V^\alpha} - \frac{k_B T}{V^\alpha} \ln V$$

This yields a finite position for the surface of tension in systems with many droplets [33].

REFERENCES

[1] J. Lyklema. *Fundamentals of Interface and Colloid Science*, volume I. Academic Press, 1991.

[2] C.E. Reid. *Chemical Thermodynamics*. McGraw-Hill, 1990.

[3] D.G. Hall and D.J. Mitchell. *J. Chem. Soc. Faraday Trans. 2*, 79:185, 1983.

[4] S. Hyde, S. Andersson, K. Larsson, Z. Blum, T. Landh, S. Lidin, and B.W. Ninham. *The Language of Shape: the role of curvature in condensed matter physics, chemistry and biology*. Elsevier, 1997.

[5] G.B. Arfken and H.J. Weber. *Mathematical Methods for Physicists*. Academic Press, 4th edition, 1995.

[6] M.W. Matsen and F.S. Bates. *Macromolecules*, 29:7641, 1996.

[7] A. Ciach and A. Poniewierski. *Phys. Rev. E*, 52:596, 1995.

[8] A. Ciach. *Phys. Rev. E*, 56:1954, 1997.

[9] J.W. Gibbs. *The Scientific Papers*, volume 1. OxBow Press, 1993.

[10] R.C. Tolman. *J. Chem. Phys.*, 16:758, 1948.

[11] C.L. Murphy. *Thermodynamics of Low Tensions and Highly Curved Interfaces*. PhD thesis, University of Minnesota, 1966.

[12] J.S. Rowlinson and B. Widom. *Molecular Theory of Capillarity*. Clarendon Press, 1982.

[13] J.C. Eriksson and S. Ljunggren. *Progr. Colloid Polym. Sci.*, 81:41, 1990.

[14] F.A.M. Leermakers, J. van Noort, S.M. Oversteegen, P.A. Barneveld, and J. Lyklema. *Faraday Discuss.*, 104:317, 1996.

[15] V.S. Markin, M.M. Kozlov, and S.L. Leikin. *J. Chem. Soc., Faraday Trans. 2*, 84:1149, 1988.

[16] H. Reiss. *Methods of Thermodynamics.* Blaisdell Publishing Company, 1965. reprinted by Dover, 1996.

[17] P. Chen, S.S. Susnar, M. Pasandideh-Fard, J. Mostaghimi, and A.W. Neumann. *Adv. Colloid Interface Sci.*, 63:179, 1996.

[18] P.A. Kralchevsky. *J. Colloid Interface Sci.*, 137:217, 1990.

[19] J. Gaydos, L. Boruvka, Y. Rotenberg, P. Chen, and A.W. Neumann. Generalized theory of capillarity. In A.W. Neumann and J.K. Spelt, editors, *Applied Surface Thermodynamics.* Marcel Dekker, 1996.

[20] M. Pasandideh-Fard, P. Chen, J. Mostaghimi, and A.W. Neumann. *Adv. Colloid Interface Sci.*, 63:151, 1996.

[21] D. Chandler. *Introduction to Modern Statistical Mechanics.* Oxford University Press, 1987.

[22] M.M. Kozlov and V.S. Markin. *J. Chem. Soc., Faraday Trans. 2*, 85:261, 1989.

[23] F.P. Buff. *J. Phys. Chem.*, 23:419, 1955.

[24] S. Kondo. *J. Chem. Phys.*, 25:662, 1954.

[25] J.G. Kirkwood and F.P. Buff. *J. Chem. Phys.*, 17:338, 1949.

[26] T.L. Hill. *Thermodynamics of Small Systems*, volume I. W.A. Benjamin, 1963. reprinted by Dover, 1994.

[27] T.L. Hill. *Thermodynamics of Small Systems*, volume II. W.A. Benjamin, 1964. reprinted by Dover, 1994.

[28] D.G. Hall and B.A. Pethica. Thermodynamics of micelle formation. In M.J. Schick, editor, *Nonionic Surfactants*, volume 1. Marcel Dekker, 1967.

[29] D.G. Hall. Thermodynamics of micelle formation. In M.J. Schick, editor, *Nonionic Surfactants; Physical Chemistry*, volume 23. Marcel Dekker, 1987.

[30] T.L. Hill. *J. Chem. Phys.*, 34:1974, 1961.

[31] H. Reiss, W.K. Kegel, and J. Groenewold. *Ber. Bunsenges. Phys. Chem.*, 100:279, 1996.

[32] H. Reiss and W.K. Kegel. *J. Phys. Chem.*, 100:10428, 1996.

[33] J.Th.G. Overbeek, G.J. Verhoeckx, P.L. de Bruyn, and H.N.W. Lekkerkerker. *J. Colloid Interface Sci.*, 119:422, 1987.

CHAPTER 3

On the Pressure

ABSTRACT

Interfacial characteristics are determined by the pressure profile. A virial and a statistical thermodynamic route to the pressure are considered. Bulk properties of the virial pressure are illustrated by means of molecular dynamics simulations of hard spheres. From a lattice model a statistical thermodynamic pressure is defined and elaborated. Results obtained for the bulk pressure of this model are compared with those from van der Waals and Landau models. The profile of the local pressure across an interface show features that are similar to that of other models in the literature. It is shown that, although the local pressure cannot be determined unambiguously, the mechanical expressions derived in chapter 2 give unequivocal results.

3.1. THE PRESSURE TENSOR

In this section a virial expression for the pressure is derived. It will be shown that the pressure is generally a tensor quantity rather than a scalar as it was used in chapter 2. Properties of the pressure tensor are first analysed for a homogeneous bulk system, supported by molecular dynamic simulations of hard spheres. Subsequently, properties of the pressure tensor are considered for curved interfaces.

3.1.1. Virial route to the pressure

The intuitive notion of pressure is one of molecules colliding with a wall thus exerting a certain force per unit area on the wall. Consider an infinitesimal element of a system. In this element all particles i with mass m_i move with a velocity $\vec{v}_i$ each. An imaginary plane is placed and the momentum that passes that particular plane per time step is counted. For instance, consider a plane of size $dx \times dy$, as depicted in figure 3.1a. Consequently, the momentum $m_i v_{z,i}$ of all particles i passing this plane in the z-direction per time unit is given by

$$P_{zz}^{k} = \sum_{i} \frac{m_i v_{z,i}}{dxdydt}$$

The superscript k indicates that the kinetic contribution to the pressure is considered. The first subscript of P and v denotes the direction the particles moves to, whereas the second subscript of P refers to the plane considered. Multiplying the numerator and

the denominator by the height of the element, dz, and using the elementary equation of motion $v_z = \frac{dz}{dt}$, the equation is rewritten as

$$P^k_{zz} = \sum_i \frac{m_i v_{z,i} v_{z,i}}{dxdydz}$$

Similar analysis can be made for the momentum $m_i v_{x,i}$ and $m_i v_{y,i}$ crossing this plane. Obviously, one can also choose a plane $dx \times dz$ or $dy \times dz$ and count the momentum that goes through these planes per time unit in the three different directions. Hence, for the kinetic contribution to the pressure in an infinitesimal volume element it applies generally that

$$P^k_{\alpha\beta} = \sum_i \frac{m_i v_{\alpha,i} v_{\beta,i}}{dxdydz}$$

where $\alpha, \beta = x, y$ or z. Integration over all elements of volume $dxdydz$ each yields the kinetic contribution to the pressure of the total volume V with N particles

$$P^k_{\alpha\beta} = \frac{1}{V} \sum_{i=1}^{N} m_i v_{\alpha,i} v_{\beta,i} \tag{3.1}$$

This gives the instantaneous kinetic contribution to the pressure. However, by conducting experiments always an average is measured. If the system is ergodic, the time average of eqn (3.1) equals, according to statistical mechanics, the ensemble average. Since the three velocity components are uncorrelated, the ensemble average of eqn (3.1) if $\alpha \neq \beta$ is given by

$$P^k_{\alpha\beta} = 0, \quad \alpha \neq \beta \tag{3.2}$$

Recalling that for not too low temperature velocities have a Maxwell-Boltzmann distribution, the average of the pressure terms $\alpha = \beta$ can be determined term-wise

$$\left\langle m_i v^2_{\alpha,i} \right\rangle = \frac{\int m_i v^2_{\alpha,i} e^{-m_i v^2_{\alpha,i}/2k_B T} dv_{\alpha,i}}{\int e^{-m_i v^2_{\alpha,i}/2k_B T} dv_{\alpha,i}} = k_B T$$

This is equivalent to the equipartition theorem which states that the momentum of each particle contributes $\frac{1}{2} k_B T$ to the internal energy of the system for each degree of freedom [1, 2]. The ensemble average turns out to be independent of the masses of the particles. Hence, each particle contributes $k_B T$ to the pressure. Therefore the sum over all particles finally yields for the ensemble average

$$P^k_{\alpha\alpha} = \frac{N k_B T}{V} \tag{3.3}$$

which is simply the ideal gas law.

In the above analysis only the kinetic contributions of point masses have been considered. Obviously, for the complete expression of the pressure interactions in the system

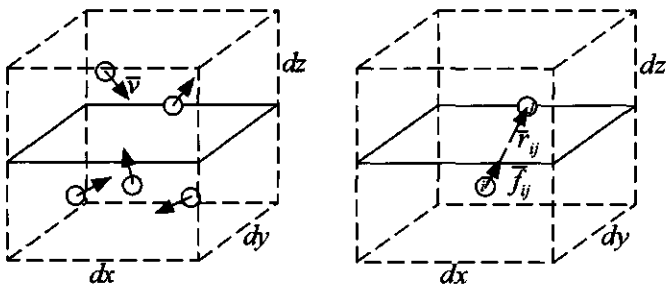

FIGURE 3.1. Contributions to the pressure: (a) the kinetic part is determined by the momentum of the particles passing a certain plane, (b) the interactions are determined by the particles across that plane.

must also be counted for. Consider once again an infinitesimal element of the system and a plane $dx \times dy$. Consider in particular two particles i and j at a distance $\vec{r_{ij}}$ from each other interacting with a certain force $\vec{f_{ij}}$, as depicted in figure 3.1b. The contribution of the interactions to the pressure is the force exerted on the plane by all the pairs of particles, provided that the particles are indeed present on either side of the plane

$$P_{\alpha\beta}^{int} = \frac{1}{2}\sum_i \sum_j \frac{f_{\alpha,ij}}{dxdy}\frac{r_{\beta,ij}}{dz}$$

where the factor $\frac{1}{2}$ comes in to correct for double counting each pair and the superscript *int* refers to the contributions of the interactions. Again, integration over all these elements yields the total contribution of the interactions to the total volume V with N particles

$$P_{\alpha\beta}^{int} = \frac{1}{V}\frac{1}{2}\sum_{i=1}^{N}\sum_{j=1}^{N} f_{\alpha,ij} r_{\beta,ij} \tag{3.4}$$

It follows from the virial theorem, which may be considered as a generalization of the equipartition theorem, that the kinetic contribution and contribution of the interactions are additive [3, 4]. The total instantaneous pressure is therefore in tensor notation given by

$$\mathbf{P}V = \sum_{i=1}^{N} m_i \vec{v_i}\vec{v_i} + \frac{1}{2}\sum_{i=1}^{N}\sum_{j=1}^{N} \vec{f_{ij}}\vec{r_{ij}} \tag{3.5}$$

The ensemble average reads

$$\mathbf{P}V = Nk_BT\mathbf{I} + \frac{1}{2}\sum_{i=1}^{N}\sum_{j=1}^{N} \left\langle \vec{f_{ij}}\vec{r_{ij}} \right\rangle \tag{3.6}$$

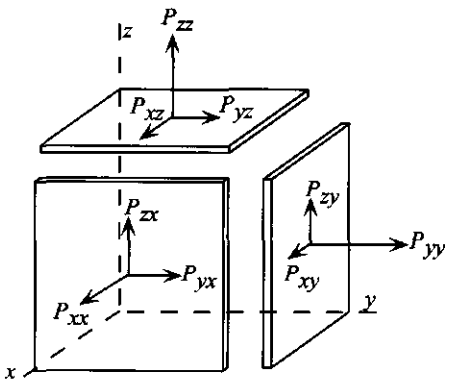

FIGURE 3.2. Elements of the pressure tensor in Cartesian coordinates.

This is the Irving-Kirkwood expression for the pressure based on pairwise additive potentials [5]. Here, it has explicitly been assumed that the particles i and j interact over the straight path $\vec{r_{ij}}$. Although this is an obvious choice, alternative paths are also feasible [6].

Summarising, it is found that the pressure is generally a tensor quantity rather than a scalar [7]. In Cartesian coordinates the respective elements of the tensor can be represented graphically as shown in figure 3.2 as acting on each of the faces of the infinitesimal element. Mathematically the pressure tensor can in that particular case be represented as the matrix

$$\mathbf{P} = \begin{bmatrix} P_{xx} & P_{xy} & P_{xz} \\ P_{yx} & P_{yy} & P_{yz} \\ P_{zx} & P_{zy} & P_{zz} \end{bmatrix}$$

3.1.2. Pressure tensor of homogeneous systems

Since for a homogeneous system the values of the elements of the pressure tensor do not depend on the choice of the orientation of the coordinate system, all diagonal elements must equal the isotropic pressure p. Moreover, because the directions α and β are uncorrelated on longer time scales, the off-diagonal elements $f_{\alpha,ij}r_{\beta,ij}$ of the pressure tensor should cancel in the ensemble average. Therefore, the tensor quantity $\mathbf{P}$ reduces to a scalar quantity p. The average contribution of the interactions to the pressure is found from eqn (3.4)

$$p^{int}V = \frac{1}{3}\frac{1}{2}\sum_i\sum_j \langle f_{x,ij}r_{x,ij} + f_{y,ij}r_{y,ij} + f_{z,ij}r_{z,ij}\rangle = \frac{1}{3}\frac{1}{2}\sum_i\sum_j \left\langle \vec{f_{ij}} \cdot \vec{r_{ij}} \right\rangle$$

Using the definitions $\vec{f}_{ij} \equiv \vec{f}_i - \vec{f}_j$, where $\vec{f}_i$ is the total force acting on particle i, and $\vec{r}_{ij} \equiv \vec{r}_i - \vec{r}_j$, where $\vec{r}_i$ and $\vec{r}_j$ are the positions of particles i and j relative to the origin of the coordinate system, the double sum can be split up into single sums via

$$p^{int}V = \frac{1}{3}\left(\sum_i \left\langle \vec{f}_i \cdot \vec{r}_i \right\rangle - \frac{1}{2}\sum_i \sum_j \left\langle \vec{f}_i \cdot \vec{r}_j \right\rangle\right)$$

In a homogeneous system the particles j are on average equally distributed around particle i. Therefore, on average, the sum over $\vec{f}_i \cdot \vec{r}_j$ does not contribute. It is trivial to determine the average of the kinetic contribution, p^k. Hence, for homogeneous systems the scalar virial pressure $p = p^k + p^i$ is given by

$$pV = Nk_BT + \frac{1}{3}\left\langle \sum_{i=1}^{N} \vec{f}_i \cdot \vec{r}_i \right\rangle \tag{3.7}$$

The sum is referred to as the *(internal) virial* [8, 9].

The scalar virial pressure eqn (3.7) can be recovered from the time average of the quantity $\sum_i m_i \vec{v}_i \cdot \vec{r}_i$ applying the virial theorem [4].

The properties of the pressure tensor will now be demonstrated for a simple, homogeneous system: a hard-sphere liquid. The hard spheres move freely through the system but they interact via collisions due to their finite sizes. These lead to the so-called excluded volume interactions. For an ergodic system the ensemble average of the pressure, given by eqn (3.6), is identical to the time average of eqn (3.5). The latter has been determined by eqn (3.58) for the hard sphere system by means of molecular dynamics simulations in a square box applying periodic boundary conditions, as briefly summarized in appendix 3.A. Applying Newton's third law, $\vec{f}_{ij} = -\vec{f}_{ji}$, as well as $\vec{r}_{ij} = -\vec{r}_{ji}$ it can be seen from eqn (3.4) that the pressure tensor must be symmetrical, i.e. $P_{\alpha\beta} = P_{\beta\alpha}$. The time-averaged values of the diagonal and off-diagonal elements of the pressure tensor of the hard sphere system are given in figure 3.3 as function of the volume fraction of particles. It can be seen that the off-diagonal elements are indeed randomly distributed around zero. Although relatively small compared to the values of the diagonal elements, at higher volume fractions the off-diagonal elements show larger fluctuations than at lower volume fractions. Alternatively, at higher densities the fluctuations relax slowly and hence the liquid is found to be more viscous. From this point of view it can be understood that the decay of the correlation of the off-diagonal elements of the pressure tensor can be related to the viscosity [10, 11].

As can be seen from figure 3.3, the diagonal elements of the pressure tensor approach the ideal gas pressure for low densities. The excluded volume contributions to the pressure can be understood from the distribution of the hard spheres in the system. It

is expected that the distribution is basically a function of all direct pair interactions only. Ornstein and Zernike combined the radial distribution function and the direct correlation function into one integral equation. Since this single equation is a function of two variables, *viz.* the distribution function and the direct correlation function, it cannot be solved; a second relation, a so-called closure, is needed. An example of such a closure is an approximation for the direct correlation-function as suggested by Percus and Yevick (PY). Upon substitution, the Ornstein-Zernike equation can be solved analytically for a hard sphere system yielding an expression for the distribution function. This expression can, in turn, be substituted into both the virial equation of state, eqn (3.7), and the so-called compressibility equation which can be derived from the number fluctuations [2, 9, 12]. Owing to the approximations that were made, these two expressions for the pressure differ. As can be seen in figure 3.3, the PY-compressibility equation overestimates the pressure found from the simulation whereas the PY-virial equation always gives a too low value. However, a weighted average of the pressures obtained by these equations turns out to give a very good fit for the diagonal elements of pressure tensor. This is the so-called Carnahan-Starling (CS) equation

$$\frac{pV}{Nk_BT} = \frac{1+\phi+\phi^2-\phi^3}{(1-\phi)^3} \tag{3.8}$$

It has been shown analytically and by means of molecular dynamics simulation that the ensemble average of the pressure tensor, eqn (3.6), gives unambiguous results for the pressure of the system. One can define the local one-particle density $\phi(\vec{r})$ unambiguously as the probability that there is a particle within the volume $d\vec{r}$ at position $\vec{r}$. The volume integral is the ensemble average of counting all particles at their positions. Obviously, this must yield the number of particles in the system

$$\int \phi(\vec{r})d\vec{r} = \sum_{i=1}^{N} \delta(\vec{r}-\vec{r_i}) = N$$

Unlike the one-particle density or, likewise, the temperature, it is not possible to define a local pressure unambiguously, although the volume integral gives a unique value. This stems from the fact that always pair interactions are considered. As has been mentioned before, the path between the particles i and j can be chosen freely. Moreover, the dyadic term $\vec{f_{ij}}\vec{r_{ij}}$ cannot be unambiguously assigned to one position [13]. It is possible to ascribe half to $\vec{r_i}$ and half to $\vec{r_j}$, but it is equally plausible to assign the whole contribution to, e.g., the average coordinate $(\vec{r_i}+\vec{r_j})/2$ or just to one of the positions [14]. Effort has been made to find unambiguous expressions for the pressure [15], but always led to other difficulties [16]. Although the ambiguity of defining the local pressure has been frequently discussed in the literature (e.g. [5, 6, 17]), this problem is

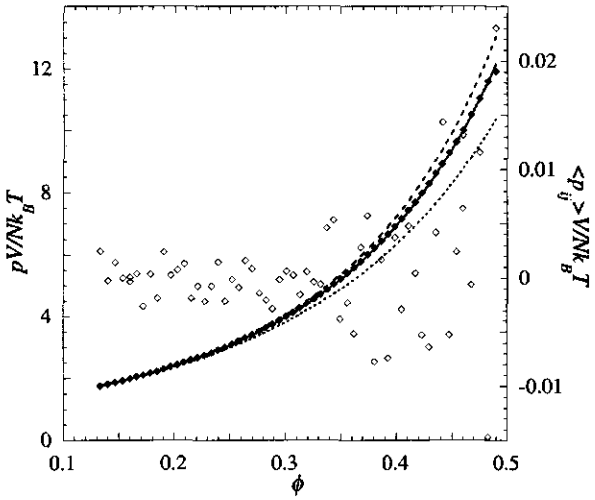

FIGURE 3.3. Hard sphere pressure as a function of the volume fraction from molecular dynamics simulations of 256 particles after 5 million collisions. The filled diamonds are the time averaged diagonal elements, whereas the open diamonds are the time averaged off-diagonal elements. The dotted curve gives the PY-virial equation, whereas the dashed curve gives the PY-compressibility equation. The solid line is the CS-approximation. The diagonal elements recover the results as found in [9].

hardly addressed in calculations where local pressures are used. The consequences for interfacial characteristics as derived in the previous chapter will be discussed below.

3.1.3. Pressure tensor of (curved) interfaces

In the previous section properties of the pressure tensor have been elucidated for a homogeneous bulk system. Here (curved) interfaces are of primary interest. Owing to the inhomogeneity of the interfacial region, the elements of the pressure tensor do depend on the choice of the orientation of the coordinate system, unlike for homogeneous bulk systems. However, since the principal axes of the coordinate system are uncorrelated, it is plausible that the ensemble average of the off-diagonal elements will still vanish [18]. Alternatively, since the decay of the off-diagonal elements is proportional to the viscosity [7, 10], these elements of the pressure tensor must vanish because the viscosity in the interfacial region is finite for liquids. Hence, the averaged pressure tensor has generally a diagonal form with three distinct elements.

The choice of the coordinate system is arbitrary. Here, a Cartesian coordinate system is placed at the interface in such a way that the z-axis is perpendicular to it, i.e. parallel

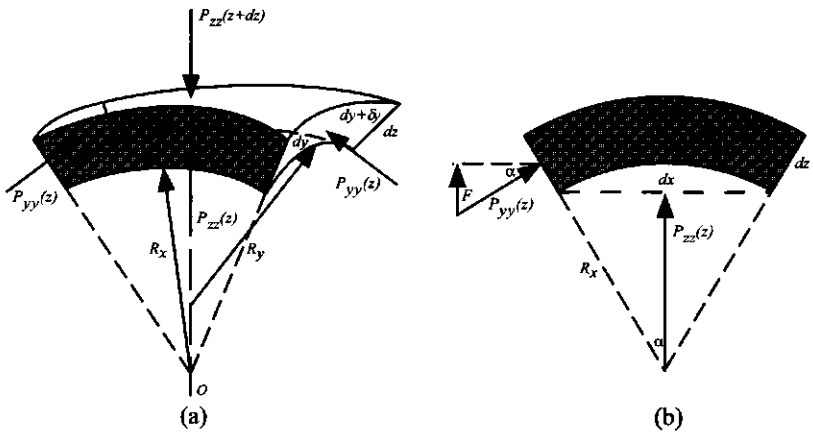

FIGURE 3.4. (a) Infinitesimal segment of an interface with pressure applied on each face. (b) A detail of the pressure on the xz-face.

to the normal vector at the interface. Hence, the two others axes are parallel to the interface. In the interfacial region the normal component P_{zz} will generally differ from the tangential components P_{xx} and P_{yy}. Far away from either side of the interface bulk conditions prevail and all components must be equal to the isotropic (bulk) pressure, as shown in section 3.1.2. This suggests that the components of the pressure tensor are somehow related.

Consider an infinitesimal element of the interface at height z. Each face of the element experiences the pressures applied by adjacent elements, as illustrated in figure 3.4a. At equilibrium the element must apply the same pressure onto all the adjacent elements according to Newton's third law. Consider e.g. the xz-face, the grey area shown in figure 3.4. The fraction F of $P_{yy}(z)$ of the adjacent elements that contributes to the normal direction can be found from similarity of triangles. From figure 3.4b it is seen that

$$\frac{\frac{1}{2}dx}{R_x} = \frac{F}{P_{yy}(z)} \Rightarrow F = \frac{1}{2}P_{yy}(z)\frac{1}{R_x}dx$$

This pressure is exerted on either side of the element with area $dy \times dz$ into the normal direction. Similarly, P_{xx} is applied to both faces with area $dx \times dz$. At equilibrium, the normal force applied at $z + dz$ must balance both the normal force and extra tangential contributions at z

$$P_{zz}(z+dz)A(z+dz) = P_{zz}(z)A(z) + P_{yy}(z)\frac{1}{R_x}A(z)dz + P_{xx}(z)\frac{1}{R_y}A(z)dz \tag{3.9}$$

where $A(z) = dxdy$. Upon substitution of $A(z+dz) = A(z) + dA$ and $P_{zz}(z+dz) = P_{zz}(z) + dP_{zz}$, eqn (3.9) gives after rearranging of terms, dividing by $A(z)$, and ignoring the second order term $dP_{zz}dA$

$$P_{zz}\frac{dA}{A(z)} + dP_{zz} = P_{yy}\frac{1}{R_x}dz + P_{xx}\frac{1}{R_y}dz$$

From eqn (2.29) it follows that $dA = J(z)A(z)dz$, where $J = \frac{1}{R_x} + \frac{1}{R_y}$ is the total curvature. Substitution yields the following differential equation for P_{zz} as function of the position z [19]

$$\frac{dP_{zz}}{dz} = (P_{yy}(z) - P_{zz}(z))\frac{1}{R_x} + (P_{xx}(z) - P_{zz}(z))\frac{1}{R_y} \tag{3.10}$$

If the system is laterally isotropic, the orientation of the axes parallel to spherical or planar interfaces can be chosen freely, i.e. they are invariant under rotation around the z-axis. Therefore, in analogy to the homogeneous bulk system, two diagonal elements must be equal. Hence, there is one component $P_{zz} = p_N$ of the pressure tensor perpendicular to the interface and there are two tangential components $P_{xx} = P_{yy} = p_T$ parallel to the interface. This is shown schematically in figure 3.5 for a segment of the interface. Although this is only exact for laterally isotropic planar and spherical interfaces, it is thought to be a good approximation for other geometries as well [20–22]. This approximation reduces eqn (3.10) to

$$\frac{dp_N}{dz} = (p_T(z) - p_N(z))\,J(z) \tag{3.11}$$

This equilibrium equation can also be derived mechanically, as shown in appendix 3.B.

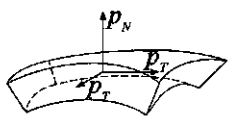

FIGURE 3.5. Elements of the divergence of the pressure tensor acting on a segment of a laterally homogeneous curved interface.

Some properties of the normal and tangential pressure can be derived from this equation. For instance, in the case of a planar interface ($J = 0$) it is seen from eqn (3.11) that the normal pressure does not change and equals the bulk pressure everywhere. For curved interfaces it is known that p_N roughly follows the density profile [8, 23]. If, following van der Waals, a hyperbolic tangent is taken for the normal pressure [6], the tangential pressure can be calculated from eqn (3.11). As depicted in figure 3.6, it turns

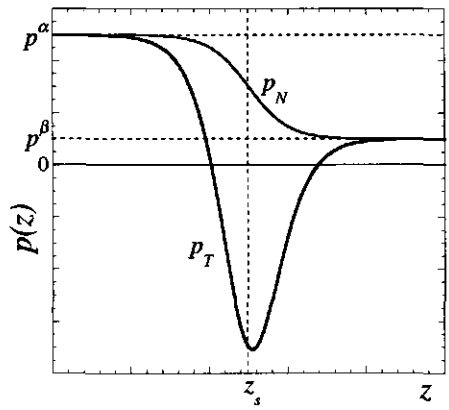

FIGURE 3.6. Possible pressure profile through a curved interface. The normal roughly follows the density profile, here $p_N(z) = \frac{1}{2}\left(p^\alpha + p^\beta\right) - \frac{1}{2}\left(p^\alpha - p^\beta\right)\tanh(z - z_s)$. The tangential pressure follows from differentiation of p_N using eqn (3.11).

out that p_T can locally have negative values in the interfacial region [8, 14]. This means physically that the tangential pressure is locally tensile rather than compressive [23].

Integration of eqn (3.11) from bulk phase α into bulk phase β, gives the Laplace pressure difference [24]

$$\Delta p \equiv p^\alpha - p^\beta = -\int_\alpha^\beta dp_N = \int_\alpha^\beta \left(p_N(z) - p_T(z)\right) J(z) dz \tag{3.12}$$

Integration of eqn (2.31) gives the total curvature as a function of position [25]. Markin *et al.* showed that substitution of this $J(z)$, as well as the bending moments, eqn (2.50), recovers the mechanical expression for γ_G, eqn (2.49) [19]. The normal pressure vanishes upon integrating by parts and gives rise to the bulk pressure term, $p^{\alpha\beta}$. Hence, eqn (3.12) is an alternative version of the generalized Laplace equation.

3.2. LATTICE MODEL

In the preceding section the virial expression for the pressure tensor has been derived. In a particular class of modelling of inhomogeneous systems mean-field and lattice approximations are used. However, a virial route to the pressure in lattice models is, as yet, not found [26]. In this section the grand potential density of the lattice model, as found in section 2.4, is identified as the pressure. Although it is thermodynamically legitimate to identify the grand potential density as the pressure [27], the mechanical properties as outlined in the previous section are not yet clarified for that 'pressure'. In this section these properties are specified for a simple lattice model that contains all

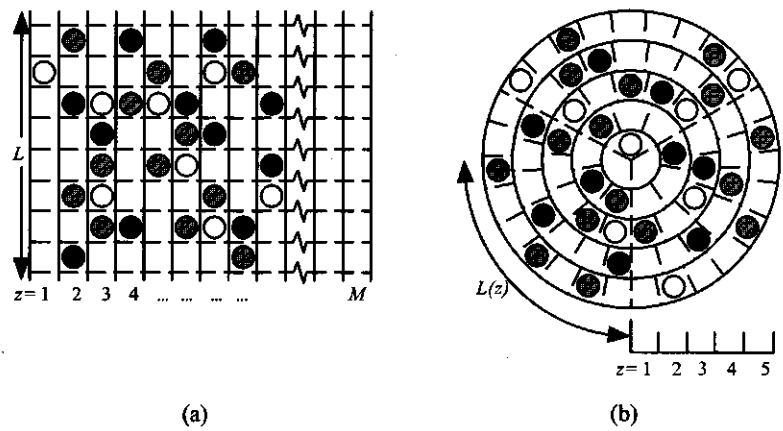

FIGURE 3.7. Schematic section of (a) planar and (b) spherical/cylindrical lattices that consists of $z = 1, \ldots, M$ parallel layers of $L(z)$ sites each. Here, $i = 0, 1, 2, 3$ species are placed on the lattice, where $i = 0$ represents the voids or free volume and the species $i = 1, 2, 3$ are represented by differently coloured beads.

basic features of inhomogeneous liquids. With this model the interfacial parameters of chapter 2 will also be determined and discussed.

3.2.1. Statistical thermodynamics

In order to have an easily accessible partition function, space is divided into sites with equal volume $v_0 = \ell^3$, where ℓ is a characteristic size. From the lattice formed in this way, only $z = 1, \ldots, M$ parallel layers are considered. In the layers $z < 1$ and $z > M$ bulk conditions prevail. Each of these layers consists of L sites, as depicted in figure 3.7a. To describe curved interfaces, space can also be divided into curved elements, as depicted in figure 3.7b. To obtain sites of equal volume, the number of sites per layer, $L(z)$, must be a function of z. It has been derived that [28]

$$v_0 L(z) = \begin{cases} \pi h \left(z^2 - (z-1)^2\right) \ell^3 & \text{cylindrical lattice} \\ \frac{4}{3}\pi \left(z^3 - (z-1)^3\right) \ell^3 & \text{spherical lattice} \end{cases} \tag{3.13}$$

where h is the length of the cylinder in units of ℓ.

In the simplest case, the molecules can be represented as single beads of characteristic size ℓ each. Although this approximation is obviously very crude for real liquids, it accounts satisfactorily for several main physical features of simple liquids. The molecules of the liquid are placed on the lattice. The number of ways to place N_i molecules all of

types i on the whole lattice are given by the degeneracy

$$\Delta = \prod_{z=1}^{M} \frac{L(z)!}{\prod_{i=1} N_i(z)!\,(L(z) - \sum_i N_i(z))!} \tag{3.14}$$

When all molecules have been placed, the internal energy U of the system can be determined. The interactions are assumed to be short ranged such that only adjacent sites have to be accounted for. Now the mean-field approximation is imposed that the $N_i(z)$ molecules of type i in layer z are on average surrounded by a volume fraction $\langle\phi_j(z)\rangle$ of molecules of type j. This so-called contact fraction is defined as [29]

$$\langle\phi_j(z)\rangle \equiv \lambda_{-1}(z)\phi_j(z-1) + \lambda_0(z)\phi_j(z) + \lambda_1(z)\phi_j(z+1) \tag{3.15}$$

Here $\phi_j(z) \equiv N_j(z)/L(z)$ is the volume fraction of molecules of type j in layer z, whereas the transition probability λ is the fraction of adjacent sites in layer z. The fraction λ_0 is the probability of finding an adjacent site in the same layer, whereas λ_{-1} and λ_1 are the probabilities of finding adjacent sites in the previous and next layer, respectively. The values for a planar lattice (i.e., $\lambda_{-1} = \lambda_1$) are commonly derived from Bravais lattices, which are well-known in crystallography. Some examples of frequently used lattices are given in figure 3.8, where the white bead is the central one and the Z grey beads mark all adjacent positions. The transition probabilities of those lattices are given in table 3.1.

Table 3.1. Transition probabilities in different planar lattices.

lattice	λ_0	$\lambda_1 = \lambda_{-1}$
simple cubic	2/3	1/6
hexagonal	1/2	1/4
BCC	1/2	1/4
FCC	1/3	1/3

As can be seen from figure 3.7b, in curved lattices the number of adjacent sites is proportional to the area of the layer z. So, $\lambda_1 = \lambda_1(z) \neq \lambda_{-1} = \lambda_{-1}(z)$. If the lattice is sufficiently large, the outer layer is approximately flat. The area of that layer is

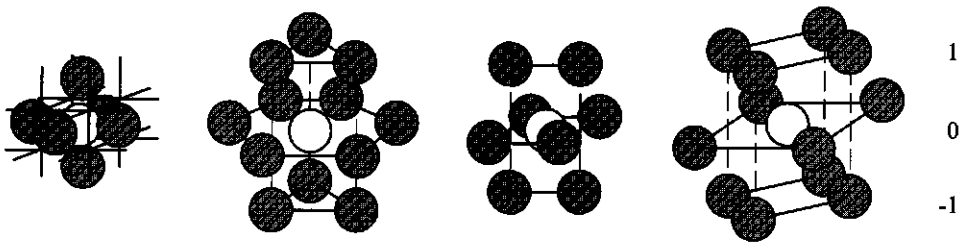

FIGURE 3.8. Frequently used lattice types; (a) simple cubic, $Z = 6$, (b) hexagonal, $Z = 12$, (c) BCC, $Z = 8$ and (d) FCC, $Z = 12$. The Z grey beads give the number of adjacent molecules of the white bead in the previous (-1), the same (0), and next layer (1), respectively.

$a_0 L(M)$, where $a_0 = \ell^2$ is the unit area of a planar site. Hence, [28, 29]

$$\lambda_1(z) = \begin{cases} 2\pi\lambda_1 hz\ell^2/a_0 L(z) & \text{cylindrical lattice} \\ 4\pi\lambda_1 z^2\ell^2/a_0 L(z) & \text{spherical lattice} \end{cases}$$

$$\lambda_{-1}(z) = \begin{cases} 2\pi\lambda_1 h(z-1)\ell^2/a_0 L(z) & \text{cylindrical lattice} \\ 4\pi\lambda_1 (z-1)^2\ell^2/a_0 L(z) & \text{spherical lattice} \end{cases}$$

$$\lambda_0(z) = 1 - \lambda_1(z) - \lambda_{-1}(z) \tag{3.16}$$

It is easily seen that the probability of finding an adjacent site in the next layer, $\lambda_1(z)L(z)$, is equal to the probability of finding an adjacent site in the previous layer relative to the next layer, $\lambda_{-1}(z+1)L(z+1)$. This is the so-called inversion symmetry condition that must always be satisfied on the lattice.

The interaction energy equals $\nu_{ij}k_BT$ per Z contacts between species i and j, where Z is again the coordination number. Within the afore-mentioned mean-field approximation the internal energy of the system is given by

$$\frac{U}{k_BT} = \frac{1}{2}\sum_{z=1}^{M}\sum_{i=0}\sum_{j=0} N_i(z)\nu_{ij}\langle\phi_j(z)\rangle \tag{3.17}$$

where the factor $\frac{1}{2}$ corrects for double counting of the interactions. The summation goes over all species where the free volume is considered as species $i, j = 0$. Thus, the interactions ν_{0j} and ν_{i0} are those between molecules with the free volume which obviously do not contribute.

The energy can also be related to that of the pure amorphous states of each type of molecule, i.e. without free volume. Suppose there are two pure liquids i and j.

One molecule of type i is exchanged with one molecule of type j. To that end, Z pair interactions of $\nu_{ii}k_BT/Z$ and Z pair interactions of $\nu_{jj}k_BT/Z$ are broken but $2Z$ pair interactions of $\nu_{ij}k_BT/Z$ are formed. The total change of interactions in terms of k_BT defines the exchange parameter

$$\chi_{ij} \equiv \frac{1}{2}\left(2\nu_{ij} - \nu_{ii} - \nu_{jj}\right) \tag{3.18}$$

Note that now generally for the interaction with the free volume $\chi_{i0} = \chi_{0i} = -\frac{1}{2}\nu_{ii} \neq 0$. It is equally sensible to give the internal energy relative to these pure reference states rather than the direct pair interactions. This changes eqn (3.17) to

$$\frac{U}{k_BT} = \frac{1}{2}\sum_{z=1}^{M}\sum_{i=0}\sum_{j=0} N_i(z)\chi_{ij}\left\langle\phi_j(z)\right\rangle \tag{3.19}$$

The difference between eqn (3.17) and eqn (3.19) is just a matter of defining the reference state.

When the interaction parameters and the number of particles are known, the internal energy, as given by eqn (3.19), is fixed. Using the degeneracy Δ, eqn (3.14), the Helmholtz energy F of the system is given by

$$\begin{aligned} F &\equiv U - TS = U - k_BT\ln\Delta \\ &= k_BT\sum_{z=1}^{M}\left\{\ln\left(L(z) - \sum_{i=1} N_i(z)\right)! + \sum_{i=1}\ln N_i(z)! - \ln L(z)!\right. \\ &\qquad \left. + \frac{1}{2}\sum_{i=0}\sum_{j=0} N_i(z)\chi_{ij}\left\langle\phi_j(z)\right\rangle\right\} \end{aligned} \tag{3.20}$$

Using the definition of the exchange interaction parameter χ_{ij}, eqn (3.18), the energy term can be expanded in terms of the direct pair interaction parameter ν_{ij}. Recalling that $\nu_{0j} = \nu_{i0} = \nu_{00} = 0$, all sums accounting for the free volume terms ($i, j = 0$) can be replaced by sums over molecules only ($i, j \geq 1$), which will be denoted by i, j. Moreover, applying the Stirling approximation for the logarithm of a factorial, as outlined in appendix 3.C, gives for the Helmholtz energy

$$\begin{aligned} \frac{F}{k_BT} = \sum_{z=1}^{M}\Bigg\{ & L(z)\ln\frac{L(z) - \sum_i N_i(z)}{L(z)} + \sum_i N_i(z)\ln\frac{N_i(z)}{L(z) - \sum_i N_i(z)} \\ & + \frac{1}{2}\sum_i\sum_j N_i(z)\nu_{ij}\left\langle\phi_j(z)\right\rangle - \frac{1}{4}\sum_i N_i(z)\nu_{ii} - \frac{1}{4}\sum_j L(z)\nu_{jj}\left\langle\phi_j(z)\right\rangle\Bigg\} \end{aligned}$$

where use has been made of the definition of the contact fraction, eqn (3.15), and the transition probabilities, eqn (3.16)

$$\begin{aligned}\sum_{j=0}\langle\phi_j(z)\rangle &= \lambda_{-1}(z)\sum_{j=0}\phi_j(z-1)+\lambda_0(z)\sum_{j=0}\phi_j(z)+\lambda_1(z)\sum_{j=0}\phi_j(z+1)\\ &= \lambda_{-1}(z)+\lambda_0(z)+\lambda_1(z)=1\end{aligned}$$

Here, it has taken into account that the sum over $j \geq 0$ includes the free volume and therefore the sum over all sites in a lattice layer. Similarly, $\sum_{i=0} N_i(z) = L(z)$.

Using the definition of the volume fractions, $L(z)$ can be taken from each term in the sum over z, yielding for the Helmholtz energy

$$\frac{F}{k_BT} = \sum_{z=1}^{M} L(z)\left\{\phi_0(z)\ln\phi_0(z)+\sum_i \phi_i(z)\ln\phi_i(z)+\frac{1}{2}\sum_i\sum_j \phi_i(z)\nu_{ij}\langle\phi_j(z)\rangle - \frac{1}{4}\sum_i \nu_{ii}\left(\phi_i(z)+\langle\phi_i(z)\rangle\right)\right\} \tag{3.21}$$

where $\phi_0 \equiv 1 - \sum_i \phi_i$ is the fraction of the free volume.

In the canonical ensemble, equilibrium is found at minimum Helmholtz energy. If the (reduced) volume $V/v_0 = \sum_{z=1}^{M} L(z)$ and temperature T are kept constant, i.e. the number of lattice layers M and the interaction parameters ν_{ij} are fixed, the constraint of constant number of molecules $\{N_i\}$ can be met by introducing a set of undetermined multipliers $\{\mu_i\}$. According to Lagrange the minimum of eqn (3.21) with the given constraint is given by the minimum of the function

$$\Omega = F - \sum_i \mu_i N_i = F - \sum_{z=1}^{M} L(z)\sum_i \mu_i\phi_i(z) \tag{3.22}$$

upon varying the number of molecules as if they were independent [30, 31]. This is obviously a Legendre transformation to the grand potential, as shown section 2.2.1. The undetermined multiplier is identified as the chemical potential. Since at equilibrium the chemical potential of the molecules of type i must be the same throughout the system, μ_i is not a function of the lattice layer z.

The equilibrium condition is found from differentiation of eqn (3.22) with respect to $N_i(z)$ and setting the result to zero

$$\frac{\partial\Omega/k_BT}{\partial N_i(z)} = -\ln\phi_0(z)+\ln\phi_i(z)+\sum_j \nu_{ij}\langle\phi_j(z)\rangle - \frac{1}{2}\nu_{ii} - \frac{\mu_i}{k_BT} = 0 \tag{3.23}$$

where use has been made of the definition of the contact fraction, eqn (3.15), the inversion symmetry, and the fact that the sum of the transition probabilities equals

unity:

$$\begin{aligned}\frac{\partial}{\partial N_i(z)}\sum_{z=1}^{M} L(z)\,\langle\phi_i(z)\rangle &= \frac{\partial}{\partial N_i(z)}\sum_{z=1}^{M} L(z)\left(\lambda_{-1}(z)\phi_i(z-1)+\lambda_0(z)\phi_i(z)+\lambda_1(z)\phi_i(z+1)\right)\\ &= \frac{\partial}{\partial N_i(z)}\left(L(z-1)\lambda_1(z-1)+L(z)\lambda_0(z)+L(z+1)\lambda_{-1}(z+1)\right)\phi_i(z)\\ &= \frac{\partial}{\partial N_i(z)}L(z)\left(\lambda_{-1}(z)+\lambda_0(z)+\lambda_1(z)\right)\phi_i(z)\\ &= L(z)\frac{\partial}{\partial N_i(z)}\phi_i(z) = L(z)\frac{\partial}{\partial N_i(z)}\left(\frac{N_i(z)}{L(z)}\right)=1\end{aligned}$$

Rewriting eqn (3.23), the undetermined multipliers become

$$\frac{\mu_i}{k_BT} = \ln\left(\frac{\phi_i(z)}{\phi_0(z)}\right)+\sum_j \nu_{ij}\,\langle\phi_j(z)\rangle-\frac{1}{2}\nu_{ii} \tag{3.24}$$

Although the terms on the right-hand side are functions of z, the value of μ_i must be constant throughout the system. This can be the case if either $\phi_i(z)$ is also constant throughout the lattice, i.e. bulk conditions, or if a density profile $\phi_i(z)$ varies in such a way that this is satisfied. Note that for a planar two-phase system consisting of one component the chemical potential of the liquid phase is given by

$$\frac{\mu^\alpha}{k_BT} = \ln\left(\frac{\phi}{1-\phi}\right)+\nu\phi-\frac{1}{2}\nu$$

where ϕ is the density in the liquid phase. On the other hand, for the vapour phase then applies

$$\frac{\mu^\beta}{k_BT} = \ln\left(\frac{1-\phi}{\phi}\right)+\nu(1-\phi)-\frac{1}{2}\nu$$

At equilibrium the two chemical potentials should be equal

$$\frac{\mu^\alpha-\mu^\beta}{k_BT} = 2\ln\left(\frac{\phi}{1-\phi}\right)+2\nu\phi-\nu=0$$

which states that $2\mu^\alpha=0$; in a planar, single component two-phase system the chemical potential is zero.

Substitution of eqn (3.24) and eqn (3.21) into eqn (3.22) gives for the equilibrium grand potential

$$\frac{\Omega}{k_BT} = \sum_{z=1}^{M} L(z)\left\{\ln\phi_0(z)-\frac{1}{2}\sum_i\sum_j \phi_i(z)\nu_{ij}\,\langle\phi_j(z)\rangle+\frac{1}{4}\sum_i \nu_{ii}\left(\phi_i(z)-\langle\phi_i(z)\rangle\right)\right\} \tag{3.25}$$

Since the grand potential provides information on the mechanical work, eqn (3.25) is the key equation in the subsequent sections.

3.2.2. Bulk properties of the lattice model

The expression for the grand potential of the lattice model, eqn (3.25), is generally valid for the case that density gradients are present, i.e. when $\phi_i(z)$ varies through the lattice. When bulk conditions prevail, i.e. $\phi_i(z) = \phi_i^b = N_i / \sum_z L(z)$ throughout the lattice, eqn (3.25) can be simplified. From its definition, eqn (3.15), and that of the transition probabilities, eqn (3.16), it is inferred that the contact fraction $\langle \phi_i(z) \rangle = \phi_i^b$. Since the densities do not depend on the layer number, the terms of eqn (3.25) in braces can be shifted in front of the sum. This leaves the sum over all lattice layers of the number of sites per layer $L(z)$, which is simply the reduced volume V/v_0 of the lattice, as defined above. Hence, for a bulk phase the grand potential of the lattice model reduces to

$$\frac{\Omega^b}{k_B T} = \left\{ \ln \phi_0^b - \frac{1}{2} \sum_i \sum_j \phi_i^b \nu_{ij} \phi_j^b \right\} \frac{V}{v_0} \tag{3.26}$$

This should be the same state variable as derived in section 2.2.1. From comparison with eqn (2.16) the bulk pressure can therefore be identified as

$$\frac{p^b v_0}{k_B T} = -\ln \phi_0^b + \frac{1}{2} \sum_i \sum_j \phi_i^b \nu_{ij} \phi_j^b \tag{3.27}$$

Note that this grand potential density, which was defined to be the pressure found from statistical thermodynamics, has an origin that differs from that for the virial expression for the pressure, eqn (3.6). It is therefore not certain whether both 'pressures' have the same physical features. In order to make it plausible that eqn (3.27) indeed represents the bulk pressure, some of its features are now investigated.

When the molecules are indistinguishable ($\sum_i \phi_i^b = \phi^b$) series expansion of the logarithmic term yields for the pressure

$$\frac{p^b v_0}{k_B T} = \frac{1}{2} \nu \phi^{b2} + \phi^b + \frac{1}{2} \phi^{b2} + \frac{1}{3} \phi^{b3} + \ldots = \frac{N}{V} \left(1 + \frac{1}{2} (\nu + 1) \phi^b + \frac{1}{3} \phi^{b2} + \ldots \right) v_0 \tag{3.28}$$

which is the well-known Kamerlingh-Onnes virial expansion of the pressure. This clearly shows the difference between the statistical thermodynamic and virial route to the pressure; the first virial coefficient in eqn (3.28) stems from the configurational entropy only, whereas in eqn (3.6) it has a kinetic origin.

From its definition, $F \equiv U - TS$, and eqn (2.15), the change of the Helmholtz energy of a bulk is given by

$$dF = -SdT - pdV + \sum_i \mu_i dN_i \tag{3.29}$$

Consequently, the pressure is given by

$$p = -\left(\frac{\partial V f}{\partial V}\right)_{N,T} = -f - V\left(\frac{\partial f}{\partial \phi}\right)_T \left(\frac{\partial \phi}{\partial V}\right)_{N,T} = -f + \phi\left(\frac{\partial f}{\partial \phi}\right)_T = -f + \mu\phi \tag{3.30}$$

where $f \equiv F/V$ is the Helmholtz energy per unit volume. For the last step it has been used that

$$\mu = \left(\frac{\partial F}{\partial N}\right)_{T,V} = \left(\frac{\partial F}{\partial \phi}\right)_{T,V}\left(\frac{\partial \phi}{\partial N}\right)_{T,V} = V\left(\frac{\partial f}{\partial \phi}\right)_T \left(\frac{\partial \phi}{\partial N}\right)_{T,V} = \left(\frac{\partial f}{\partial \phi}\right)_T \tag{3.31}$$

According to eqn (3.21), the Helmholtz energy per unit volume of a bulk is given by

$$\frac{f}{k_B T} = \left\{ \phi_0 \ln \phi_0 + \sum_i \phi_i \ln \phi_i + \frac{1}{2}\sum_i \sum_j \phi_i \nu_{ij} \phi_j - \frac{1}{2}\sum_i \nu_{ii}\phi_i \right\} \frac{1}{v_0} \tag{3.32}$$

Substitution of eqn (3.32) into eqn (3.30) recovers the bulk pressure as given in eqn (3.27), which proves the consistency between the lattice expression for the bulk grand potential, eqn (3.26), and its thermodynamic equivalent, eqn (2.16). This thermodynamic result supports the assumption that the expression given for the bulk pressure, eqn (3.27), indeed describes the desired state variable. It is, however, not yet established whether this scalar pressure also has the same spatial properties as the second-order tensor elaborated in section 3.1.3.

The bulk pressure as given by eqn (3.27) can also be used to study the phase behaviour of a mono-molecular liquid. The pressure is plotted as a function of the molecular volume, $1/\phi^b$, as shown in figure 3.9 for a certain value of the interaction parameter ν. Most striking is the loop in the curve which resembles a van der Waals pressure isotherm. This loop contains a region where the pressure increases with increasing volume. This region is unstable since for thermodynamically stable system the Helmholtz energy must be minimal so that $\left(\frac{\partial^2 F}{\partial (1/\phi^b)^2}\right)_{N,T} = -\left(\frac{\partial p^b}{\partial (1/\phi^b)}\right)_{N,T} > 0$. The points where the system is about to become unstable are the so-called spinodals and are given by

$$\frac{\partial p^b}{\partial (1/\phi^b)} = -{\phi^b}^3 \left(\nu + \frac{1}{\phi^b(1-\phi^b)}\right) = 0 \tag{3.33}$$

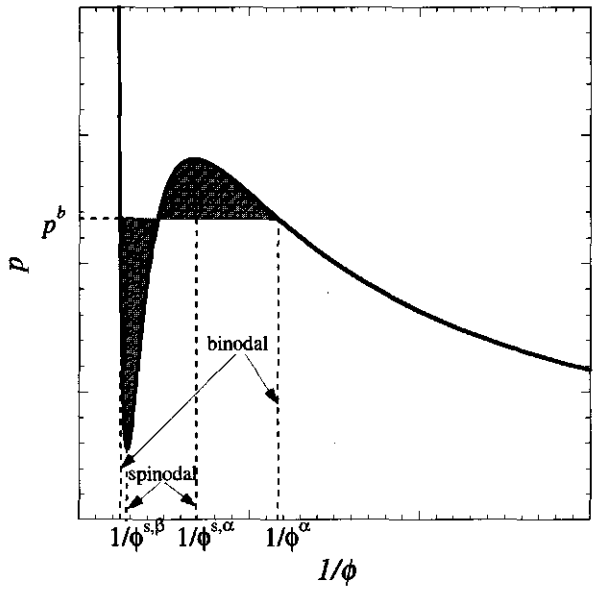

FIGURE 3.9. The bulk pressure of the lattice model, eqn (3.27), plotted as a function of the molecular volume for a certain $\nu < \nu_c$. This curve resembles the familiar van der Waals loop from which phase coexistence can be obtained.

Since $\phi^b = 0$ is not a solution, eqn (3.33) leads to a quadratic equation in the volume fraction from which the two spinodal volume fractions follow

$$\phi^{s,\alpha} = \frac{1}{2} + \frac{1}{2}\sqrt{1 + \frac{4}{\nu}} \tag{3.34a}$$

$$\phi^{s,\beta} = \frac{1}{2} - \frac{1}{2}\sqrt{1 + \frac{4}{\nu}} \tag{3.34b}$$

These spinodals coincide at the critical interaction parameter $\nu_c = -4$ which occurs at the critical density $\phi_c = \phi^{s,\alpha} = \phi^{s,\beta} = \frac{1}{2}$. If $\nu < \nu_c$ both roots are real and distinct and two spinodals values are found. If $0 > \nu > \nu_c$ both roots are imaginary, so no spinodals are found anymore. For $\nu > 0$ the roots have no physical relevance since $0 \leq \phi \leq 1$.

If the volume fraction of the mono-molecular liquid $\phi^{s,\alpha} < \phi < \phi^{s,\beta}$ the liquid is unstable and will phase-separate spontaneously into two phases. The two phases have different volume fractions which are called the binodal volume fractions. At equilibrium the pressure p^b must be equal in both phases. Therefore, in real systems the loop must be replaced by a horizontal line. This line is placed in such a way that the areas above and below the loop are equal. This is a so-called Maxwell construction [11, 32]. Using

eqn (3.27) this reads

$$\int_{1/\phi^\alpha}^{1/\phi^\beta} \left(p^b - p\right) d(1/\phi^b) = \int_{\phi^\alpha}^{\phi^\beta} \frac{1}{2}\nu - \frac{\ln(1-\phi^b)}{\phi^{b2}} - \frac{p^b}{\phi^{b2}} d\phi^b = 0$$

Solving this integral gives

$$\frac{1}{2}\nu\phi^\alpha + \ln\left(\frac{\phi^\alpha}{1-\phi^\alpha}\right) + \frac{\ln(1-\phi^\alpha)}{\phi^\alpha} + \frac{p^\alpha}{\phi^\alpha} = \frac{1}{2}\nu\phi^\beta + \ln\left(\frac{\phi^\beta}{1-\phi^\beta}\right) + \frac{\ln(1-\phi^\beta)}{\phi^\beta} + \frac{p^\beta}{\phi^\beta}$$

Applying eqn (3.27) for p^α and p^β evaluated at ϕ^α and ϕ^β, respectively, and using eqn (3.24) finally yields

$$\nu\phi^\alpha + \ln\left(\frac{\phi^\alpha}{1-\phi^\alpha}\right) = \nu\phi^\beta + \ln\left(\frac{\phi^\beta}{1-\phi^\beta}\right) \Leftrightarrow \mu^\alpha = \mu^\beta \tag{3.35}$$

This is indeed an extra equilibrium condition. Therefore, whereas the spinodal volume fractions are given explicitly by eqn (3.34), the binodals must be determined from the two equilibrium conditions, $p^\alpha = p^\beta$ and $\mu^\alpha = \mu^\beta$, using eqn (3.27) and eqn (3.35), respectively.

Alternatively, one can plot the Helmholtz energy per unit volume as a function of the density. Two different densities, i.e. different phases, are at equilibrium with each other if simultaneously $\mu^\alpha = \mu^\beta$ and $p^\alpha = p^\beta$. According to eqn (3.30) these conditions imply that the slopes μ at both densities are equal and have the same intercept p. That is, both points have a common tangent. Therefore, the binodals can also be found from this so-called common tangent construction from the $f-\phi$-diagram, as shown in figure 3.10 for different values of the interaction parameter. Note that the slope, i.e. chemical potential, in the coexistence points indeed equals zero, as was derived analytically. Apparently, this common tangent construction is identical to the Maxwell-construction in the $p-V$-diagram as will now be proven more generally.

After integration of eqn (3.29), the Helmholtz energy of a single component bulk is given by

$$F^b = -p^b V^b + \mu^b N$$

If the system's volume is reversibly increased from V^α to V^β, the isothermal volume work done is according to eqn (3.29)

$$-\int_{V^\alpha}^{V^\beta} pdV = \int_\alpha^\beta (dF)_{N,T} = -p^\beta V^\beta + \mu^\beta N + p^\alpha V^\alpha - \mu^\alpha N$$

The liquid phase is at mechanical equilibrium with its vapour phase if both phases have equal pressure $p^\alpha = p^\beta = p^b$. This identity gives for the volume work after dividing by

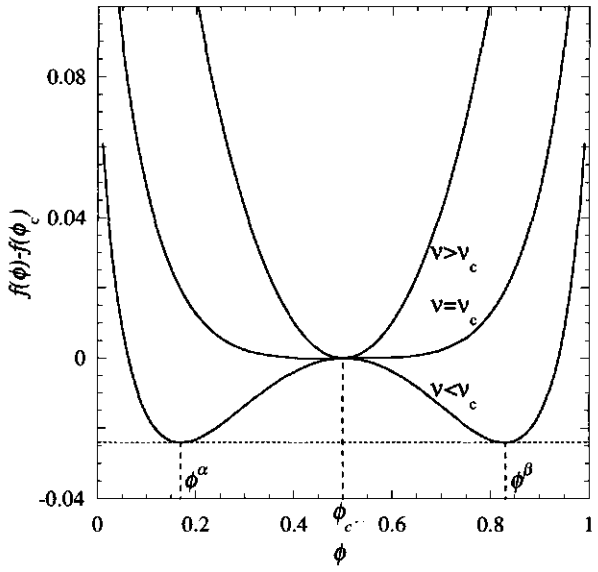

FIGURE 3.10. Helmholtz energy density plotted as a function of the volume fraction below, in, and beyond the critical point. From a common tangent construction phase coexistence can be determined.

the number of molecules N

$$-\int_{v^\alpha}^{v^\beta} pdv = -p^b\left(v^\beta - v^\alpha\right) + \mu^\beta - \mu^\alpha$$

where $v \equiv V/N \equiv 1/\phi$ is the molecular volume. The first term on the right hand side is simply the volume work of enlarging the volume from v^α to v^β of a system at constant bulk pressure p^b. The second term on the right hand side represents the chemical work to bring the molecules from phase α to phase β. Rewriting the volume work gives

$$\int_{v^\alpha}^{v^\beta} (p^b - p)dv = \mu^\beta - \mu^\alpha \tag{3.36}$$

To let the liquid phase α be at chemical equilibrium with a vapour phase β, both phases must have equal chemical potentials $\mu^\alpha = \mu^\beta$. Hence, in the case that a loop in the pressure is replaced by a horizontal line at the equilibrium pressure $p^\alpha = p^\beta = p^b$ such that the areas above and below the lines are equal, this guarantees chemical equilibrium. This is indeed the aforementioned Maxwell construction which yielded the expression for equal chemical potentials, eqn (3.35).

For the above lattice model the binodals and spinodals have been determined for several values of the interaction parameter. The resulting $p-\phi$-phase diagram is shown in figure 3.11. The $\nu-\phi$-phase diagram, figure 3.12, is reminiscent of a van der Waals

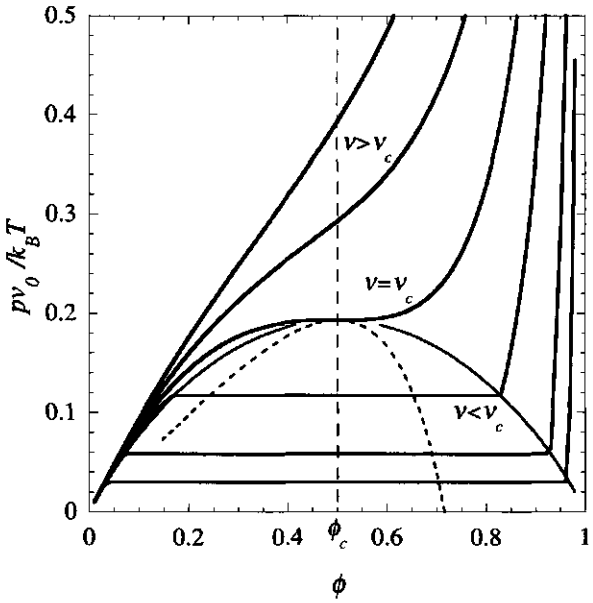

FIGURE 3.11. The bulk pressures of the lattice model as a function of the density. The dashed line is the spinodal, whereas the solid line connects the binodal points.

$T-\phi$-diagram as will be shown in section 3.2.3. It is seen that a low value of the temperature corresponds to a large negative value of the interaction parameter. This makes it plausible that $\nu \propto 1/T$.

3.2.3. Van der Waals pressure

Assuming that the grand potentials in eqn (2.16) and eqn (3.26) are identical, equating them provides an expression for the bulk pressure in the lattice model. This expression indeed shows all features a bulk pressure should have. The presented model and its results are reminiscent of the van der Waals equation of state [2, 9, 33]. Van der Waals modified the ideal gas law for non-ideality. In order to account for the excluded volume of the molecules in the system with molar volume V_m, he introduced a parameter b. Moreover, he accounted for the molecular interactions by adding a $-a/V_m^2$ term to the pressure P [33]

$$P = \frac{Nk_BT}{V_m - b} - \frac{a}{V_m^2} \tag{3.37}$$

As will be shown later, it is convenient to work with reduced variables, i.e. relative to the values in the critical point. The critical point can for instance be found from (*cf.*

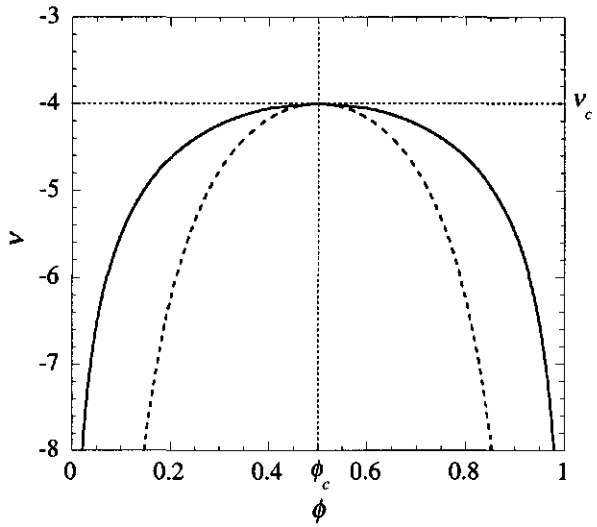

FIGURE 3.12. Phase diagram for the monomolecular lattice model. The solid line gives the binodal whereas the dashed line gives the spinodal. The dotted lines intersect in the critical point.

eqn (3.33)) [12]

$$\left(\frac{\partial P}{\partial V_m}\right)_T = \left(\frac{\partial^2 P}{\partial V_m^2}\right)_T = 0 \tag{3.38}$$

Using

$$\left(\frac{\partial P}{\partial V_m}\right)_T = \frac{2a}{V_m^3} - \frac{Nk_BT}{(V_m - b)^2} \tag{3.39}$$

it is found that

$$\left(\frac{\partial^2 P}{\partial V_m^2}\right)_T = \frac{2Nk_BT}{(V_m - b)^3} - \frac{6a}{V_m^4} \tag{3.40}$$

Substitution of eqn (3.39) and eqn (3.40) into eqn (3.38) gives for the critical point

$$\frac{4a}{V_c^3(V_c - b)} = \frac{2Nk_BT}{(V_c - b)^3} = \frac{6a}{V_c^4}$$

Dividing the first and last term by a/V_c^3 gives a linear equation in V_c which gives straightforwardly $V_c = 3b$. Substitution in eqn (3.39), using eqn (3.38), gives $Nk_BT_c = 8a/27b$. Upon substitution of both variables into eqn (3.37), the critical pressure is given by $P_c = a/27b^2$. Note that V_c, T_c, and P_c are determined by the parameters a and b whereas in the lattice model these have fixed values (*cf.* $\phi_c = \frac{1}{2}$ vs. $1/V_c$ and $\nu_c = -4$ vs. Nk_BT_c). This makes the van der Waals equation more adaptable to experiments than the lattice model.

Introducing the reduced variables $p \equiv P/P_c$, $v \equiv V/V_c$, and $t \equiv T/T_c$, the van der Waals equation eqn (3.37) is rewritten as

$$p = \frac{8t}{3v-1} - \frac{3}{v^2} \tag{3.41}$$

Whereas in eqn (3.37) the variables a and b could be adapted for real gases, the reduced van der Waals equation is independent of these quantities. Indeed, it has been shown experimentally that for systems that can be described by eqn (3.37), all isotherms in reduced units merge [33, 34]. This scaling consideration is called the principle of corresponding states or universality.

Series expansion of the reduced van der Waals equation in terms of the (reduced) density gives

$$\frac{p}{t} = \frac{8}{3v}\left\{1 + \left(\frac{1}{3} - \frac{9}{8t}\right)\frac{1}{v} + \frac{1}{9}\frac{1}{v^2} + \dots\right\} \tag{3.42}$$

This is reminiscent of the Kamerlingh-Onnes virial expansion of the lattice gas pressure, eqn (3.28). Therefore, it is seen that the reduced van der Waals pressure, eqn (3.41), must give similar results as the lattice gas pressure. Moreover, from comparison of eqn (3.42) with eqn (3.28) it is again likely that $\nu \propto 1/T$.

As with eqn (3.27), the binodals are found from the pressure as a function of the (reduced) density. As shown in the previous section, the Maxwell construction, eqn (3.36), gives the expression for equal chemical potentials. In the van der Waals model this yields

$$\int_{v^\alpha}^{v^\beta} (p^b - p)dv = p^b v - \frac{8}{3}t\ln(3v-1) - \frac{3}{v}\Big|_{v^\alpha}^{v^\beta} = 0 \tag{3.43}$$

where

$$p^b = \frac{8t}{3v^\alpha - 1} - \frac{3}{v^{\alpha 2}} = \frac{8t}{3v^\beta - 1} - \frac{3}{v^{\beta 2}} \tag{3.44}$$

Solving both equilibrium conditions simultaneously gives the two reduced binodal volumes v^α and v^β. As outlined in section 3.2.2, the corresponding spinodals are given by

$$\left(\frac{\partial p}{\partial v}\right)_t = 6\left(\frac{1}{v^3} - \frac{4t}{(3v-1)^2}\right) = 0 \tag{3.45}$$

This gives three reduced spinodal volumes, of which only two are physically significant ($v > \frac{1}{3}$). The binodals and spinodals can be found for several temperatures, as shown in figure 3.13. This is equivalent to the $p-\phi$-diagram figure 3.11 where $\phi/\phi_c = 1/v$.

Obviously, from the known binodals and spinodals at different temperatures, a $t-\phi$-phase diagram can also be determined for a van der Waals gas, like has been done in the previous section. As can be seen from figure 3.12, the binodal is approximately a

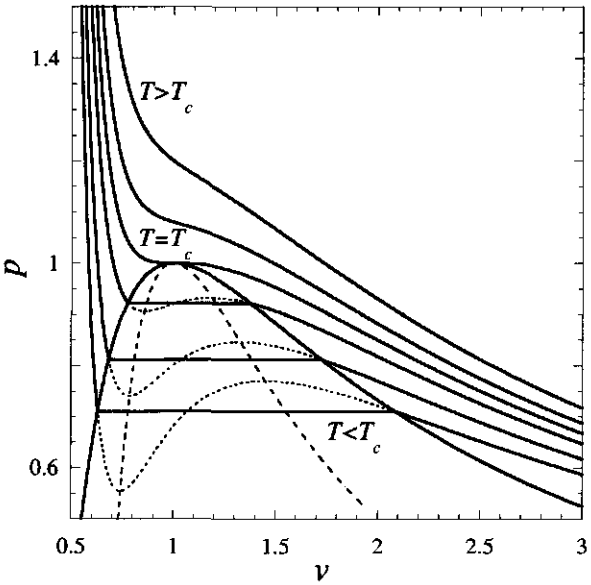

FIGURE 3.13. Van der Waals loops determine the $p-v$-phase diagram. The solid lines gives the pressure for several temperatures below ($t < 1$), in ($t = 1$) and above ($t > 1$) the critical temperature; the dotted regions have been replace by the horizontal (reduced) bulk pressure. The solid line connects these binodal points, whereas the dashed line gives the spinodal.

parabola. This can also be found from mathematics. Series expansion of the chemical potentials, eqn (3.43), around the critical density ($\phi/\phi_c = 1/v = 1$) at constant temperature gives

$$4t - 6 - \frac{8}{3}t\ln 2 + 6(t-1)\left(\frac{\phi}{\phi_c} - 1\right) + \frac{3}{2}t\left(\frac{\phi}{\phi_c} - 1\right)^3\Bigg|_{\phi^\alpha}^{\phi^\beta} = 0$$

Series expansion of the pressure gives

$$4t - 3 + 6(t-1)\left(\frac{\phi}{\phi_c} - 1\right) + 3(t-1)\left(\frac{\phi}{\phi_c} - 1\right)^2 + \frac{3}{2}t\left(\frac{\phi}{\phi_c} - 1\right)^3\Bigg|_{\phi^\alpha}^{\phi^\beta} = 0$$

Subtraction of both series expansions gives

$$\left(\frac{\phi^\alpha}{\phi_c} - 1\right)^2 = \left(\frac{\phi^\beta}{\phi_c} - 1\right)^2$$

This gives only two distinct densities if $\phi^\alpha - \phi_c = \phi_c - \phi^\beta$; the densities are symmetrical with respect to ϕ_c. Substitution of this result in the series expansion of the chemical

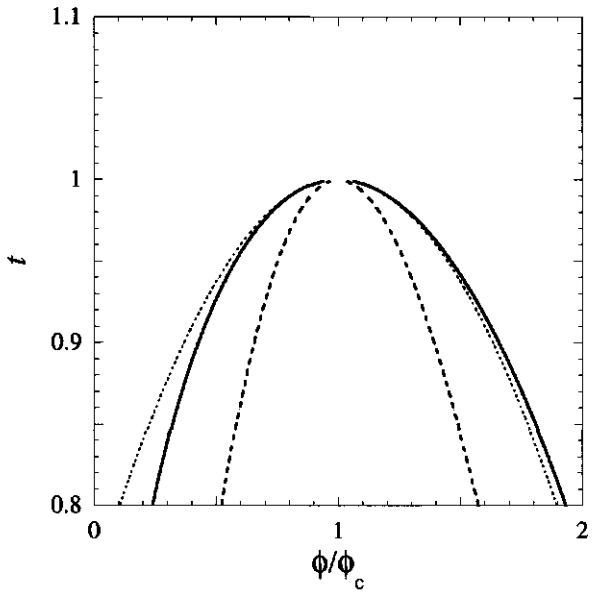

FIGURE 3.14. Van der Waals $t - \phi$-phase diagram. The solid line gives the binodal whereas the dashed line gives the spinodal. The dotted line gives the series expansion around the critical point.

potential gives

$$6(t-1)\left(\frac{\phi^\alpha}{\phi_c}-1\right)+\frac{3}{2}t\left(\frac{\phi^\alpha}{\phi_c}-1\right)^3=-6(t-1)\left(\frac{\phi^\alpha}{\phi_c}-1\right)-\frac{3}{2}t\left(\frac{\phi^\alpha}{\phi_c}-1\right)^3$$

If $\phi^\alpha \neq \phi_c$, rearranging of terms finally yields

$$\left(\frac{\phi^\alpha}{\phi_c}-1\right)^2=\frac{-4(t-1)}{t}$$

Or, alternatively, in the vicinity of a critical point ($t \to 1$)

$$(\phi^\alpha-\phi_c)=2\phi_c(1-t)^{\frac{1}{2}}$$

The fact that the (reduced) density is proportional to the square root of the (reduced) temperature is a well-known scaling result for mean-field models as also will be shown in section 3.2.4. As can be seen in figure 3.14 this approximation for the (reduced) van der Waals binodal seems to fit readily well even for densities beyond the critical point. However, experiments show that in the vicinity of the critical point $(\phi^\alpha - \phi_c) \propto (T_c - T)^{0.34}$ [33, 34].

3.2.4. Landau theory for the lattice model

From figure 3.10 it can be seen that for all values of ν the free energy per unit volume of a bulk phase is an even function which is symmetrical around the critical density. Below the critical temperature three extremum values of the free energy are found. It therefore makes sense to write the free energy density as a fourth order series expansion around the critical density

$$f = f_c - h(\phi - \phi_c) + a_2(\phi - \phi_c)^2 + a_4(\phi - \phi_c)^4 \tag{3.46}$$

This is the so-called Landau expansion of the free energy [35]. Landau omitted the third and higher order odd terms to keep the free energy symmetrical. The linear term is maintained to account for an external field h. Landau found that a_2 vanished at the critical point [34]. It also turns out that if $a_2 > 0$, the system is homogeneous whereas for $a_2 < 0$ the free energy eqn (3.46) has two minima corresponding to two coexisting phases. This gives rise to the approximation that $a_2 \propto (T - T_c)$ [33]. Since a_2 determines the phase behaviour, it is plausible to take a_4 to be constant near the critical point. From a physical point of view this constant must be positive because if $a_4 < 0$ the free energy would have its minima in $\phi = 0$ or $\phi = 1$.

The bulk Helmholtz energy of a lattice model is given by eqn (3.32). The sum can be omitted for a system that consists of only one component. Taylor series expansion up to fourth order around the critical density $\phi_c = \frac{1}{2}$, gives for such a single mono-atomic lattice gas

$$\frac{f}{k_B T} = \left[\frac{1}{8}\nu - \ln 2\right] + \frac{\nu}{2}\left(\phi - \frac{1}{2}\right) + \left(2 + \frac{\nu}{2}\right)\left(\phi - \frac{1}{2}\right)^2 + \frac{4}{3}\left(\phi - \frac{1}{2}\right)^4 \tag{3.47}$$

Indeed, all odd terms in $(\phi - 1/2)$ drop out because both logarithmic, i.e. entropic, terms contribute with opposite signs forcing the system to be symmetric. The linear term stems from the interactions, i.e. it is an energetic term, which accounts for a (mean-)field in the system caused by molecular interactions. Since the energetic term is quadratic in the density, it does not contribute higher order odd terms. Note that in the lattice model the field is always present, unlike a magnetic field that can be externally applied. Nevertheless, magnetism is frequently used as an analogue for a molecular system to illustrate the Landau theory [12, 33, 34].

The quadratic term in eqn (3.47) is proportional to $2 + \frac{\nu}{2}$ and is identified as a_2 from comparison with eqn (3.46). This term vanishes if $\nu = -4$, which indeed coincides with the critical point. For $\nu < -4$ the system will phase separate and for $\nu > -4$ it is homogeneous. This again supports the statement that the interaction parameter is inversely proportional to the temperature. The coefficient of the fourth order term

is indeed a positive constant. So, the series expansion of the free energy of the lattice model and the Landau theory completely agree in this respect.

The chemical potential of the Landau expansion eqn (3.47) can be found from its thermodynamic definition, eqn (3.31)

$$\mu = \left(\frac{\partial f}{\partial \phi}\right)_T = \frac{\nu}{2} + (4+\nu)\left(\phi - \frac{1}{2}\right) + \frac{16}{3}\left(\phi - \frac{1}{2}\right)^3$$

For $\nu < -4$ two coexisting phases with densities ϕ^α and ϕ^β may exist. This requires equal chemical potentials in the two phases. Owing to the symmetry of the Landau expansion, it appears that $\phi^\alpha - \frac{1}{2} = \frac{1}{2} - \phi^\beta$, as can also be seen in figure 3.10. Substitution in the Landau expression for the chemical potential leads to the identity

$$\sqrt{-\frac{6}{32}(\nu+4)} = \phi - \frac{1}{2}$$

Since ν is inversely proportional to the temperature, the classical mean-field scaling result that $(\phi - \phi_c) \propto (\nu_c - \nu)^{1/2}$, as also found in section 3.2.3, is recovered.

In an inhomogeneous system the density is a function of position. In order to account for the spatial variance of the density, Landau added a squared gradient [12, 34] analogous to the van der Waals model for inhomogeneous systems as will be used in section 4.2.2. The total free energy of the inhomogeneous system then reads

$$F = \int \left[f_c - h\left(\phi(\vec{r}) - \phi_c\right) + a_2\left(\phi(\vec{r}) - \phi_c\right)^2 + a_4\left(\phi(\vec{r}) - \phi_c\right)^4 + c\left(\nabla\phi(\vec{r})\right)^2 \right] d\vec{r} \qquad (3.48)$$

The total Helmholtz energy of the lattice model for an inhomogeneous system is given by eqn (3.21). Since $L(z)v_0$ is the volume of a layer, the sum over all layers of the Helmholtz energy density is equivalent to the volume integral in continuous space. For slowly varying densities, the continuous density profile $\phi(\vec{r})$ may be approximated by a second order series expansion around the local discrete density. Substitution in the contact fraction, eqn (3.15), gives

$$\begin{aligned}
\langle\phi(z)\rangle &\equiv \lambda_{-1}\phi(z-1) + \lambda_0\phi(z) + \lambda_1\phi(z+1) \\
&\approx \lambda_{-1}\left(\phi(\vec{r}) - \ell\vec{\nabla}\phi(\vec{r}) + \frac{1}{2}\ell^2\nabla^2\phi(\vec{r})\right) + \lambda_0\phi(\vec{r}) + \lambda_1\left(\phi(\vec{r}) + \ell\vec{\nabla}\phi(\vec{r}) + \frac{1}{2}\ell^2\nabla^2\phi(\vec{r})\right) \\
&= \phi(\vec{r}) + \lambda_1\ell^2\nabla^2\phi(\vec{r})
\end{aligned}$$

Here, a planar lattice has implicitly been assumed, i.e. $\lambda_{-1} = \lambda_1$. Integration by parts gives for the interaction term in eqn (3.21)

$$\sum_{z=1}^{M} \phi(z)\nu\left(\langle\phi(z)\rangle\right) L(z) \approx \int_{\alpha}^{\beta} \nu\phi(\vec{r})^2 d\vec{r} + \int_{\alpha}^{\beta} \nu\lambda_1\ell^2\phi(\vec{r})\nabla^2\phi(\vec{r})d\vec{r}$$
$$= \int_{\alpha}^{\beta} \nu\phi(\vec{r})^2 d\vec{r} - \int_{\alpha}^{\beta} \nu\lambda_1\ell^2 \left|\nabla\phi(\vec{r})\right|^2 d\vec{r}$$

where use has been made of the fact that the density gradient vanishes in both bulk phases α ($z \leq 1$) and β ($z \geq M$). Inserting this result into eqn (3.21) gives for the continuous version of total Helmholtz energy

$$\frac{F}{k_B T} = \int \left[f(\phi(\vec{r})) - \frac{1}{2}\nu\lambda_1\ell^2 \left|\nabla\phi(\vec{r})\right|^2 \right] d\vec{r} \tag{3.49}$$

where the homogeneous Helmholtz energy density $f(\phi(\vec{r})$ is given by eqn (3.47). The term $-\frac{1}{2}\nu\lambda_1\ell^2$ is identified as c of the Landau expansion eqn (3.48). It is concluded that the Landau theory is in complete agreement with the derived lattice model in the vicinity of the critical point. This equivalence will be used in section 4.2 to compare the mechanical expressions for the bending stress and torsion stress, derived in chapter 2, with those found in the literature.

3.2.5. Spatial properties of the pressure in the lattice model

The grand potential of the lattice model for an inhomogeneous system given by eqn (3.25) resembles the state variable derived from thermodynamics, eqn (2.45), as proposed by Buff [36]. Although it has been shown that the latter equation does not yield a unique virial expression for the pressure tensor for different geometries, it can be used to define a local pressure [27]. Upon discretizing eqn (2.45) by replacing the integral by a sum and consequently $d\vec{r}$ by $v_0 L(z)$, as given by eqn (3.13), the grand potential density per layer is identified as the tangential pressure in that layer (*cf.* figure 3.5)

$$\frac{p_T^{\chi}(z)v_0}{k_B T} = -\ln\phi_0(z) + \frac{1}{2}\sum_i\sum_j \phi_i(z)\nu_{ij}\langle\phi_j(z)\rangle - \frac{1}{4}\sum_i \nu_{ii}\left(\phi_i(z) - \langle\phi_i(z)\rangle\right) \tag{3.50}$$

In the Helmholtz energy as given by eqn (3.20), the energy has been expressed in terms of the exchange energies χ_{ij}. If eqn (3.17), the energy based on the direct pair interaction parameter ν_{ij}, had been used instead, the explicit ν_{ii}-terms would drop out in all equations. This would then leave for the pressure

$$\frac{p_T^{\nu}(z)v_0}{kT} = -\ln\phi_0(z) + \frac{1}{2}\sum_i\sum_j \phi_i(z)\nu_{ij}\langle\phi_j(z)\rangle \tag{3.51}$$

Since the contact fractions in the bulk equal the local densities, both expressions for the local pressure (eqn (3.50) and eqn (3.51)) yield the same bulk pressure as given by eqn (3.27). The value of the grand potential of the system is also independent of the choice of the reference state for the internal energy since the extra term vanishes after summing over all layers:

$$\begin{aligned}\sum_{z=1}^{M} L(z)\left\{\phi_i(z)-\langle\phi_i(z)\rangle\right\} &= \ldots + L(z)\phi_i(z) - L(z-1)\lambda_1(z-1)\phi_i(z) \\ &\quad - L(z)\lambda_0(z)\phi_i(z) - L(z+1)\lambda_{-1}(z+1)\phi_i(z) + \ldots \\ &= \ldots + L(z)\left(1-\lambda_{-1}(z)-\lambda_0(z)-\lambda_1(z)\right)\phi_i(z) + \ldots \\ &= 0\end{aligned}$$

where use has been made of the inversion symmetry and the definition of the contact fraction, eqn (3.15). Thus, both eqn (3.50) and eqn (3.51) substituted in eqn (3.25) for the term in braces give the same value for the grand potential and on this basis neither expression for the local pressure can thermodynamically be more correct than the other. That is, they are thermodynamically indistinguishable as one should expect from the pressure defined in this way. However, this is not obvious for a pressure found from the virial route [17].

The ambiguity in the expression for the local pressure has also been encountered for the Irving-Kirkwood expression in section 3.1.2; there is no accepted reasoning to assign the forces uniquely to one particular position. It is in the same way impossible to define the local tangential pressure in the lattice model unambiguously in terms of pair interactions, since eqn (3.50) and eqn (3.51) are believed to be equally correct in that they both yield the same grand potential. Both expressions will be used below to determine properties of the tangential pressure. Note that any other reference state for the energy can be chosen and it is consequently possible to propose various alternative thermodynamically consistent expressions for local pressure.

For a planar lattice containing one type of monomers and free volume, an appropriate density profile can be found satisfying the equilibrium condition that the chemical potential in each lattice layer equals the bulk chemical potential. Such a profile is illustrated in figure 3.15a for a direct interaction parameter which is 1.5 times the critical interaction parameter to obtain phase separation ($\nu=-6$, $\chi=3$).

The tangential pressure profile through the planar lattice as determined by eqn (3.50) is symmetrical with respect to the Gibbs dividing plane at z_{Gibbs} since exchange of all monomers with free volume should give indistinguishable results as it follows from the

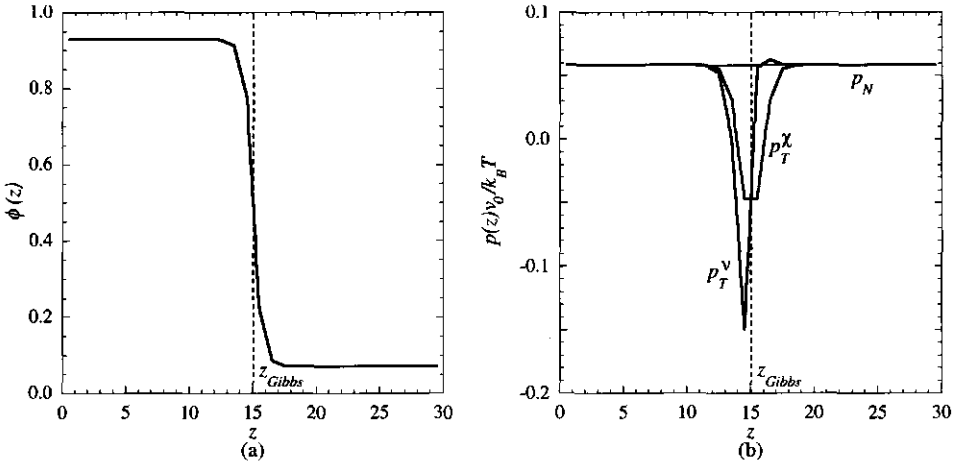

FIGURE 3.15. (a) The density profile and (b) the corresponding pressure profile using either p_T^χ, given by eqn (3.50), or p_T^ν, given by eqn (3.51), for a calculation with $\frac{1}{2}LM$ monomers on a planar lattice, $M = 30$, $\lambda_0 = 2/3$, $\nu = -6$, $\ell = 1$. The discrete values are assigned to the centre of the layer and interpolated linearly.

definition of χ_{ij}, eqn (3.18). On the other hand, the tangential pressure calculated with eqn (3.51) is not symmetrical and has a larger tensile part in the interfacial region. The normal pressure in a planar interface is constant and equals the bulk pressure in order to satisfy mechanical equilibrium as arises mathematically from eqn (3.11). The pressures are illustrated in figure 3.15b for the phase-separated system that corresponds to the aforementioned density profile.

Now a droplet is considered. To that end, $N = \sum_z \varphi^0(z)L(z)$ monomers are placed on a curved lattice where $\varphi^0(z)$ is the previously determined local density of the planar interface. Note that φ^0 has a totally different physical meaning than ϕ_0, which represents the fraction of free volume in the system. Neglecting the curvature dependence of the interfacial tension [37], a Laplace pressure difference $\Delta p = \gamma^0 J$ is applied in order to impose a certain curvature J. According to eqn (2.49), the interfacial tension of the planar interface, γ^0, can be determined from the zeroth bending moment as also found by Kirkwood [22]

$$\gamma^0 = \sum_{z=1}^{M} (p - p_T(z)) \frac{v_0}{a_0} \tag{3.52}$$

With the applied Laplace pressure difference, a density profile similar to figure 3.15a, which satisfies the equilibrium conditions, is found again. From this density profile the

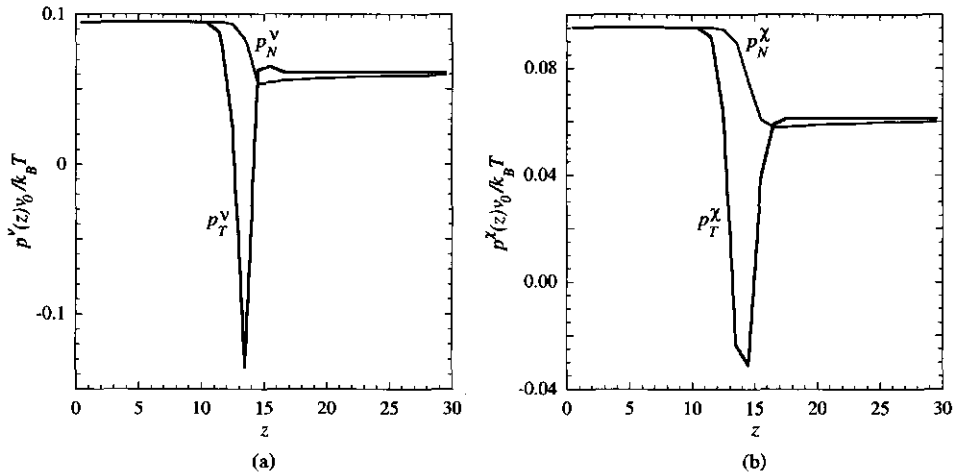

FIGURE 3.16. (a) The tangential pressure profile p_T^ν using eqn (3.51) with the related normal pressure profiel p_N^ν determined from eqn (3.11) and (b) the tangential pressure profile p_T^χ using eqn (3.50) with the related normal pressure profile p_N^χ determined from eqn (3.11), for a calculation with $N = \sum_z \varphi^0(z)L(z)$ monomers on a spherical lattice, where φ^0 is the density profile of the planar interface shown in figure 3.15, $M = 30$, $\lambda_0 = 2/3$, $\nu = -6$, $\ell = 1$.

tangential pressure profiles can be determined using either eqn (3.50) or eqn (3.51). Realising that in the bulk $p_N = p_T$, the normal pressure profile can be determined from integration of the discretization of eqn (3.11), as outlined in appendix 3.D.1. Both components of the pressure tensor are shown in figure 3.16. As for the planar interface, the tangential pressure from eqn (3.51) has a larger tensile part than that determined by eqn (3.50). The calculated normal pressure and the grand potential densities themselves show behaviour similar to the 'real' pressure calculated from molecular dynamics simulations based on the virial expression for the pressure [6] which, in turn, shows a good fit with the hyperbolic tangent expression shown in figure 3.6. This is also found for a van der Waals gradient theory [38].

3.2.6. Calcultation of interfacial properties of the lattice model

In the previous sections knowledge of the local pressure has been gained. The mechanical expressions for the interfacial characteristics found in section 2.4 can now be determined explicitly. As stated in chapter 2, the interfacial tension according to Gibbs, γ_G, depends on the choice of the dividing plane, R_s. In figure 3.17 this dependence is shown for a single component lattice model liquid-vapour equilibrium on the three different lattice types. The number of monomers for each geometry is chosen such that

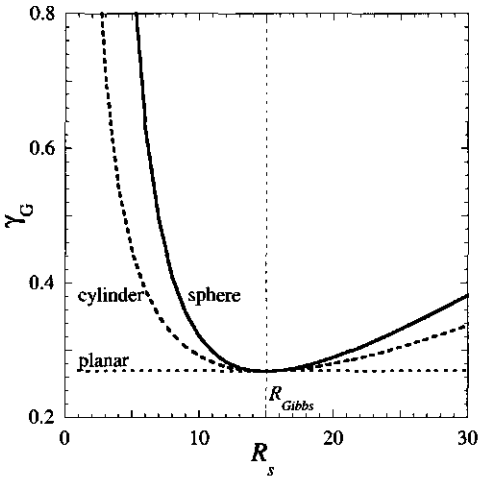

FIGURE 3.17. Interfacial tension according to Gibbs, γ_G, as a function of the position of the dividing plane, R_s, for $\frac{1}{2}LM$ monomers on a planar, and $\sum_z \varphi^0(z)L(z)$ monomers on a cylindrical and spherical lattice, where $\varphi^0(z)$ is the equilibrium density profile of the planar interface, $M = 30$, $\nu = -6$, and $\lambda_0 = 2/3$.

the Gibbs dividing or equimolar plane is approximately at $R_{Gibbs} = M/2$. The value of the interfacial tension according to Gibbs has been determined from eqn (2.49), using both p_T^{ν} and p_T^{χ} for the local pressure profile. Clearly, γ_G is not a function of the choice of the pressure profile. This is due to the fact that $\gamma_G A$ is the excess grand potential (*cf.* eqn (2.17)). Because the area A does not depend on the choice of the pressure profile, neither does γ_G since the grand potential and the bulk pressures have shown to be independent of this choice. With the imposed Laplace pressure difference, $\Delta p = \gamma^0 J$, the surface of tension is found where $\gamma_G = \gamma^0$, as shown in figure 3.17b for a cylindrical and spherical interface. Owing to the curvature of the lattice the surface of tension does not exactly coincide with the Gibbs dividing plane. This small difference may give rise to a dependence of the interfacial tension on the curvature [37], as will be outlined in chapter 4.

Since the local pressure cannot be determined unambiguously, the respective bending moments given by eqn (2.50) can neither be given unambiguously. By term-wise matching of eqn (2.43) and eqn (2.49), the interfacial tension according to Boruvka and Neumann, the bending stress, and the torsion stress equal the zeroth, first, and second bending moments, *viz.* $\gamma_{BN} = \mathbb{P}_0$, $\mathbb{C}_1 = \mathbb{P}_1$, and $\mathbb{C}_2 = \mathbb{P}_2$. As a result, it is concluded

that these thermodynamically well-defined parameters cannot be determined unambiguously. This is physically unacceptable. However, it will now be shown that the mechanical expressions eqn (2.55), eqn (2.56), and eqn (2.57) do give identical results for the given pressures, eqn (3.51) and eqn (3.50), of the lattice model.

Here, a liquid-vapour equilibrium is described for cylindrical droplets. In that case the total curvature J can be varied at constant Gaussian curvature K. Note that in figure 3.17 the curvature of the interface was notionally changed by shifting the dividing plane of a given system. Now the curvature is physically changed for a particular choice of the dividing plane. The Gibbs dividing plane is chosen for the position interface, i.e. $\Gamma = 0$, which is unambiguously determined for a single component system. The mechanical expression for the interfacial tension according Boruvka and Neumann, eqn (2.57), reduces in that case to

$$\gamma_{BN} = \mathbb{P}_0 - \left(\frac{\partial \mathbb{P}_0}{\partial J}\right)_{T,K} J - \left(\frac{\partial \mathbb{P}_1}{\partial J}\right)_{T,K} J^2 \tag{3.53}$$

The mechanical expression for the bending stress, eqn (2.55), reads for a cylindrical interface at the Gibbs dividing plane

$$\mathbb{C}_1 = \mathbb{P}_1 + \left(\frac{\partial \mathbb{P}_0}{\partial J}\right)_{T,K} + \left(\frac{\partial \mathbb{P}_1}{\partial J}\right)_{T,K} J \tag{3.54}$$

To arrive at the interfacial tension according to Boruvka and Neumann, eqn (3.53), and bending stress, eqn (3.54), the derivatives of $\mathbb{P}_0$ and $\mathbb{P}_1$ with respect to the total curvature J are required. The curvature J of the cylindrical geometry is applied analogously as outlined in section 3.2.5 for a spherical droplet. The corresponding zeroth and first bending moment $\mathbb{P}_0$ and $\mathbb{P}_1$ from eqn (2.50) were then determined from the excess pressure profiles. In this way the bending moments can be determined as a function of the curvature. However, the differentiation of the bending moments with respect to J must be carried out numerically and introduces a numerical inaccuracy. In the results presented here, the J-dependence of $\mathbb{P}_0$ is determined from a fit with a third order polynomial, whereas $\mathbb{P}_1$ is fitted with a second order polynomial. From these fits the respective derivatives are determined. Consequently, the results presented here are correct up to second order in the curvature.

From eqn (2.43) it is found that $\gamma_{BN} = \gamma_G$ for a planar interface ($J = K = 0$). Realising that γ_G does not depend on the local pressure profile, it is concluded that the same γ_{BN} must be found from p_T^ν and p_T^χ for a planar interface. However, when $\gamma_{BN} = \mathbb{P}_0$ is applied to a curved interface, as has been done in the literature [23], it is found that using p_T^ν always gives a stronger curvature dependence of γ_{BN} than when p_T^χ is used.

Using eqn (3.53) for γ_{BN} it is seen that within the numerical accuracy of the derivatives p_T^ν and p_T^χ give both the same interfacial tension according to Boruvka and Neumann. This is illustrated for $\nu = 1.5\nu_c$ in figure 3.18a.

If $\mathbb{C}_1 = \mathbb{P}_1$ is taken, as has been done in the literature [23], it is found that the bending stress has qualitatively the same curvature dependence irrespective of whether p_T^ν or p_T^χ is used. However, the values at the planar interface differ significantly. When p_T^ν is used, it gives a finite positive value for the bending stress, whereas p_T^χ gives a vanishing bending stress at the planar interface for all values of the interaction parameter. As will be outlined in chapter 4, the bending stress of the planar interface gives the first order curvature correction to γ_G, the so-called Tolman length [18, 37]. Owing to the symmetry at this single component liquid-vapour equilibrium, the Tolman length and hence the bending stress should vanish [39]. Although the first bending moment using p_T^χ shows this feature for all values of the interaction parameter, there is no (statistical) thermodynamic reasoning why this expression for the local pressure would be more correct than p_T^ν, which shows incorrect physical behaviour. Indeed, eqn (3.54) for the bending stress gives the same values using both p_T^ν and p_T^χ within the numerical accuracy of the derivatives. This is illustrated for $\nu = 1.5\nu_c$ in figure 3.18b. It will be shown in chapter 4 that eqn (2.55) gives identical results for the Tolman length as the well-known van der Waals density functional theory in the vicinity of the critical point.

The torsion stress cannot be evaluated directly in the present model. As can be seen from eqn (2.56), this requires information on the dependence of the bending moments on the Gaussian curvature K at constant total curvature J. In the presented lattice model where only planar, cylindrical, and spherical geometries can be considered, it is not possible to model such a minimal surface. However, the torsion stress can be determined indirectly from comparison of a spherical interface, where J and K are coupled ($c_1 = c_2$), with a cylindrical interface. This requires an extra fit which does not favour the numerical accuracy. Calculations show that within this numerical inaccuracy p_T^χ and p_T^ν also give identical torsion stress in the limit of a planar interface, as will be shown in chapter 4.

3.3. DISCUSSION

A simple lattice model has been elaborated to model liquid-vapour interfaces for planar and curved geometries. The local grand potential density is determined and identified as the local tangential pressure. It was not obvious that this statistical thermodynamic pressure resembled the pressure tensor found from the virial route. Nevertheless, the bulk pressure from the grand potential density is consistent with the

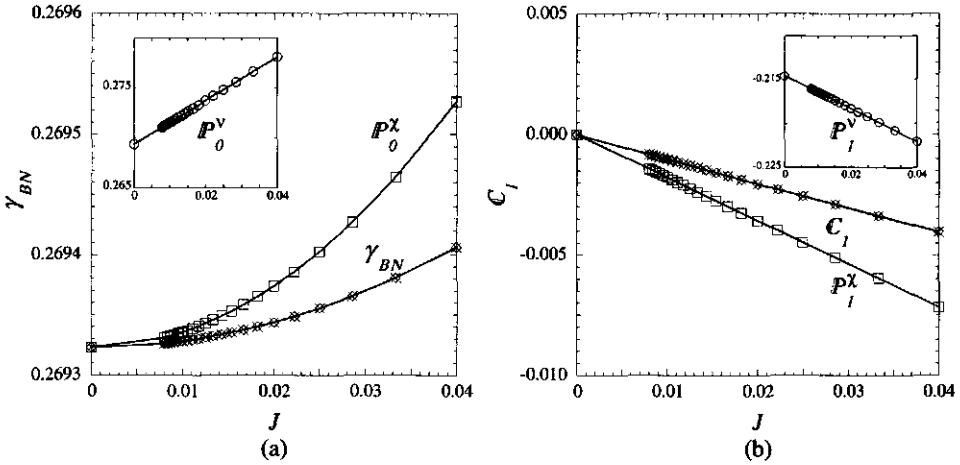

FIGURE 3.18. (a) The interfacial tension according to Boruvka and Neumann of a cylindrical interface evaluated at the Gibbs dividing plane as a function of curvature with $\nu = -6$, $\lambda_0 = 2/3$: the circles give the values for $\gamma_{BN} = \mathbb{P}^{\nu}_0$ using eqn (3.51) for the local pressure, the squares for $\gamma_{BN} = \mathbb{P}^{\chi}_0$ using eqn (3.50) for the local pressure, the diamonds give the values determined by eqn (2.57) using both $\mathbb{P}^{\nu}_0$ and $\mathbb{P}^{\nu}_1$, whereas the crosses give the values determined by eqn (2.57) using both $\mathbb{P}^{\chi}_0$ and $\mathbb{P}^{\chi}_1$. (b) The bending stress of a cylindrical interface evaluated at the Gibbs dividing plane as a function of curvature with $\nu = -6$, $\lambda_0 = 2/3$: the circles give the values for $\mathbb{C}_1 = \mathbb{P}^{\nu}_1$ using eqn (3.51) for the local pressure, the squares for $\mathbb{C}_1 = \mathbb{P}^{\chi}_1$ using eqn (3.50) for the local pressure, the diamonds give the values determined by eqn (2.55) using both $\mathbb{P}^{\nu}_0$ and $\mathbb{P}^{\nu}_1$, whereas the crosses give the values determined by eqn (2.55) using both $\mathbb{P}^{\chi}_0$ and $\mathbb{P}^{\chi}_1$.

thermodynamic definition of the pressure and a virial expansion is found. The tangential pressure profile shows a large compressive, i.e. positive, part in the system but also a tensile, i.e. negative, part in the interfacial region. From eqn (3.52) or, equivalently, eqn (2.49) it can be seen that this tensile part might be necessary to provide a positive interfacial tension. The normal pressure in the lattice model is constructed from the equilibrium condition of the pressure tensor. It has been shown that despite their different origins the same physics apply to the (local) pressure from both the virial route and the statistical thermodynamic route in the above lattice model. The key difference is, however, that in the lattice model the pressure yields by definition the grand potential. This is not the case for the pressure from the virial route in curved interfaces. This difference makes the lattice model an interesting tool for modelling curved interfaces.

The simple lattice model can be extended straightforwardly to chains, as will be done in chapter 5. The chain connectivity is then taken into account by a Green function of a random walk of the segments biased by local mean-field potentials [29]. It is also possible to prevent backfolding in chains [40–42]. Moreover, it is convenient to insert a Lagrange multiplier that satisfies the constraint that the lattice is completely filled; the free volume is then considered as monomeric species in the system. The Lagrange multiplier only biases the statistics of the chain on the lattice but does not affect the physical meaning of the grand potential density. Hence, the pressure in the extended mean-field lattice model also has the physical characteristics of the pressure from the virial route. The compressive and tensile parts in the tangential pressure profile are both found and are completely analogous to the model given above. A detailed understanding of these positive and negative parts is particularly desirable to describe interfaces with very low interfacial tensions, e.g. microemulsions or vesicles. For these systems the tensile and compressive parts balance each other. Given the molecular detail that can be built into the mean-field theory by Scheutjens and Fleer and the basic correctness as ascertained above, it is concluded that this model is particularly useful in modelling the physics of curved interfaces.

It is instructive to discuss briefly the pressure as found in other mean-field models. In the work by Szleifer *et al.* a Lagrange multiplier is also introduced to satisfy packing constraints [43–45]. Although this multiplier indeed represents an energy needed to change the volume, it is actually a generalized pV-term [46] which includes the chemical potentials of the system as well. Hence, their Lagrange multiplier cannot show the same physical features as the tangential pressure as claimed in their work [43–45]. Indeed, the Lagrange multiplier fails to recover the ideal gas limit [47]. Moreover, their Lagrange multiplier vanishes in the region where the average area of the molecules is lower than the available area. However, this lower occupancy would actually allow the chains to redistribute and give a tensile contribution to the pressure. Therefore, by identifying the Lagrange parameter with specified characteristics as the tangential pressure, they ignore a physically important feature by setting this Lagrange multiplier to zero in the region where it is negative.

In a mean-field Landau theory the Helmholtz energy of a system is written as a functional of an order parameter [34]. As shown in section 3.2.4, the Landau functional can be fully recovered from the lattice expression for the Helmholtz energy, eqn (3.21). Consequently, the pressure found from Landau theories also show the mechanical features found from the virial expression. Gompper *et al.* showed that the spatial properties of

the Landau pressure are indeed satisfied [48, 49]. A comparison of the mechanical expressions for interfacial characteristics between the closely related van der Waals model and the lattice model will be made in section 4.2.

The interfacial characteristics, *viz.* the interfacial tension, the bending stress, and the torsion stress, are thermodynamically well-defined. However, the moments of the pressures profile, eqn (2.50), depend on the definition of the local pressure. The origin of this difference is that the interactions used in the expressions for the pressure cannot be uniquely assigned to a certain position. Consequently, identification of the interfacial characteristics as the bending moments, give ambiguous mechanical results. It has been shown that the expressions given in section 2.5 correct for this problem, so no effort to avoid the ambiguities in the local pressure has to be made when it is defined as the grand potential density.

Appendix 3.A. Molecular Dynamics of hard spheres

A collection of hard spheres can only interact via collisions. Therefore, a molecular dynamics simulation of hard spheres can be restricted to tracing the particles from collision to collision. Consider a system of monodisperse hard spheres with uniform mass m and diameter σ. When each particle i is at time t on position $\vec{r}_i$ with velocity $\vec{v}_i$, the shortest collision time t_{ij} between particles i and j can be determined from [8]

$$t_{ij} = \frac{-\vec{r}_{ij} \cdot \vec{v}_{ij} - \sqrt{\left(\vec{r}_{ij} \cdot \vec{v}_{ij}\right)^2 - \vec{v}_{ij}^2 \left(\vec{r}_{ij}^2 - \sigma^2\right)}}{\vec{v}_{ij}^2} \tag{3.55}$$

where $\vec{r}_{ij} \equiv \vec{r}_i - \vec{r}_j$ is the relative position and $\vec{v}_{ij} \equiv \vec{v}_i - \vec{v}_j$ is the relative velocity of particles i and j. When all shortest collision times between the particles at a given moment have been determined, the particles are moved by the shortest collision time t_c. The displacement $\Delta\vec{r}_i$ of all particles i are determined from the elementary equation of motion

$$\Delta\vec{r}_i = \vec{v}_i t_c \tag{3.56}$$

Since there is only one binary collision, only the new velocity of the colliding particles i and j has to be determined. For an elastic collision the change of velocity $\Delta\vec{v}_i$ is given by

$$\Delta\vec{v}_i = -\Delta\vec{v}_j = \frac{\vec{r}_{ij} \cdot \vec{v}_{ij}}{\sigma^2} \vec{r}_{ij} \tag{3.57}$$

With the new positions and velocities, the new collision times of all particles can be determined and the above procedure can be repeated.

For the determination of thermodynamic quantities of the system, an infinite number of molecules should be taken. Obviously, this cannot be carried out in practice. To that end, only a set of N particles is considered in an open box. Each particle that leaves the box on the one side, enters the box on the opposite side. Using this so-called periodic boundary condition, the macroscopic system can be mimicked as an ensemble of exact copies of the central box such that the simulation of N particles represents the whole system.

The time average of the pressure tensor can now be determined by summing the contributions to the pressure over all collisions c. The kinetic contribution is determined from (*cf.* eqn (3.1))

$$\mathbf{P}^k V = \frac{1}{\tau} \sum_c \sum_{i=1}^{N} m \vec{v}_i \vec{v}_i t_c = \frac{m}{\tau} \sum_c \sum_{i=1}^{N} \vec{v}_i \Delta \vec{r}_i$$

where $\tau \equiv \sum_c t_c$ is the total simulation time.

The contribution of the interactions follow from (*cf.* eqn (3.4))

$$\mathbf{P}^{int} V = \sum_c \frac{1}{2} \sum_{i=1}^{N} \sum_{j=1}^{N} \vec{f}_{ij} \vec{r}_{ij} = \sum_c m \frac{d\vec{v}_{ij}}{dt} \vec{r}_{ij} \delta(t_c) = \sum_c m \frac{\Delta \vec{v}_i}{t_c} \vec{r}_{ij} = \frac{m}{\tau} \sum_c \Delta \vec{v}_i \vec{r}_{ij} \delta(t_c)$$

where the Dirac delta function $\delta(t_c)$ denotes that only the binary collision between particles i and j at t_c has to be accounted for.

Consequently, the time average of the (reduced) pressure tensor of a collection of N hard spheres after a simulation time τ of c collisions is given by

$$\frac{\mathbf{P}V}{Nk_BT} = \frac{m}{Nk_BT} \frac{1}{\tau} \sum_c \left\{ \sum_{i=1}^{N} \vec{v}_i \Delta \vec{r}_i + \vec{r}_{ij} \Delta \vec{v}_i \delta(t_c) \right\} \tag{3.58}$$

The pre-factor on the right-hand side of eqn (3.58) can at equilibrium be determined from the equipartition theorem $\sum_i \frac{1}{2} m \vec{v}_i^2 = \frac{3}{2} N k_B T$. Since elastic collisions are considered, this factor is constant throughout the simulation.

For a more detailed review on molecular dynamics simulations the reader is referred to the literature [8, 50].

APPENDIX 3.B. NORMAL PRESSURE FROM PRESSURE TENSOR

The force acting on an infinitesimal area dA is given by $\mathbf{P} \cdot \hat{n} dA$, where $\hat{n}$ is the normal vector on that particular area. At equilibrium, all forces on the total interface ∂A are balanced. Using Gauss's theorem this is mathematically represented as

$$\int_{\partial A} \mathbf{P} \cdot \hat{n} dA = \int_V \vec{\nabla} \cdot \mathbf{P} dV = 0$$

where the nabla operator is defined as

$$\vec{\nabla} \equiv \vec{e_1}\frac{\partial}{\partial x_1} + \vec{e_2}\frac{\partial}{\partial x_2} + \vec{e_3}\frac{\partial}{\partial x_3}$$

Here, $\vec{e_i}$ are the unit vectors of the coordinate system in the directions i.

As stated in section 3.1.3, the equilibrium condition must apply to each infinitesimal element. Hence, the divergence of the pressure tensor must vanish term-wise

$$\vec{\nabla} \cdot \mathbf{P} = 0 \tag{3.59}$$

3.B.1. Cylindrical geometry

If the interface has a cylindrical geometry, it is convenient to transform to cylindrical coordinates $\{r, \phi, z\}$

$$\left.\begin{aligned} x_1 &= r\cos\phi \\ x_2 &= r\sin\phi \\ x_3 &= z \end{aligned}\right\} \Rightarrow \left\{\begin{aligned} \vec{e_1} &= \cos\phi\,\vec{e_r} - \sin\phi\,\vec{e_\phi} \\ \vec{e_2} &= \sin\phi\,\vec{e_r} + \cos\phi\,\vec{e_\phi} \\ \vec{e_3} &= \vec{e_z} \end{aligned}\right\}$$

This converts the nabla operator to

$$\vec{\nabla} = \vec{e_r}\frac{\partial}{\partial r} + \frac{1}{r}\vec{e_\phi}\frac{\partial}{\partial \phi} + \vec{e_z}\frac{\partial}{\partial z}$$

After straightforward expansion using tensor analysis, the divergence of the pressure tensor becomes (*cf.* for symmetrical tensors [51])

$$\begin{aligned} \vec{\nabla} \cdot \mathbf{P} = &\left[\frac{P_{rr} - P_{\phi\phi}}{r} + \frac{\partial P_{rr}}{\partial r} + \frac{\partial P_{zr}}{\partial z} + \frac{1}{r}\frac{\partial P_{\phi r}}{\partial \phi}\right]\vec{e_r} \\ &+ \left[\frac{P_{r\phi} + P_{\phi r}}{r} + \frac{\partial P_{r\phi}}{\partial r} + \frac{\partial P_{z\phi}}{\partial z} + \frac{1}{r}\frac{\partial P_{\phi\phi}}{\partial \phi}\right]\vec{e_\phi} \\ &+ \left[\frac{1}{r}P_{rz} + \frac{\partial P_{rz}}{\partial r} + \frac{\partial P_{zz}}{\partial z} + \frac{1}{r}\frac{\partial P_{\phi z}}{\partial \phi}\right]\vec{e_z} \end{aligned}$$

In a cylindrical geometry the r-direction is normal to the interface. Since in the present scope only the normal pressure has to be considered, only the term proportional to $\vec{e_r}$ is of interest. Recall that at equilibrium the off-diagonal elements of the pressure tensor vanish: $P_{\phi r} = P_{zr} = 0$. Substitution of this equilibrium condition in eqn (3.59) gives for the term proportional to $\vec{e_r}$

$$\frac{P_{rr} - P_{\phi\phi}}{r} + \frac{\partial P_{rr}}{\partial r} = 0 \tag{3.60}$$

Since r is perpendicular and ϕ is parallel to the cylindrical interface, $P_{rr} = p_N$ and $P_{\phi\phi} = p_T$. Recall moreover that for a cylinder the total curvature $J = 1/r$ (*cf.* section 2.1.2), so that eqn (3.60) corresponds to eqn (3.11). Furthermore, it is seen with the vanishing off-diagonal elements, that both $P_{\phi\phi} = P_{zz} = p_T$ are constant for each r.

3.B.2. Spherical geometry

For a spherical interface, a transformation to spherical coordinates $\{r, \phi, z\}$ is convenient

$$\left.\begin{aligned} x_1 &= r\sin\theta\cos\phi \\ x_2 &= r\sin\theta\sin\phi \\ x_3 &= r\cos\theta \end{aligned}\right\} \Rightarrow \left.\begin{aligned} \vec{e_1} &= \sin\theta\cos\phi\ \vec{e_r} + \cos\theta\cos\phi\ \vec{e_\theta} - \sin\phi\ \vec{e_\phi} \\ \vec{e_2} &= \sin\theta\sin\phi\ \vec{e_r} + \cos\theta\sin\phi\ \vec{e_\theta} + \cos\phi\ \vec{e_\phi} \\ \vec{e_3} &= \cos\theta\ \vec{e_r} - \sin\theta\ \vec{e_\theta} \end{aligned}\right\}$$

Substitution into the nabla operator gives in spherical coordinates

$$\vec{\nabla} = \vec{e_r}\frac{\partial}{\partial r} + \frac{1}{r}\vec{e_\theta}\frac{\partial}{\partial\theta} + \frac{1}{r\sin\theta}\vec{e_\phi}\frac{\partial}{\partial\phi}$$

From tensor analysis, the divergence of the pressure tensor is given by (*cf.* for symmetrical tensors [51])

$$\begin{aligned} \vec{\nabla}\cdot\mathbf{P} = &\left[\frac{\partial P_{rr}}{\partial r} + \frac{2}{r}P_{rr} + \frac{1}{r}\frac{\partial P_{\theta r}}{\partial\theta} - \frac{1}{r}P_{\theta\theta} + \frac{1}{r\sin\theta}\frac{\partial P_{\phi r}}{\partial\phi} + \frac{\cot\theta}{r}P_{\theta r} - \frac{1}{r}P_{\phi\phi}\right]\vec{e_r} \\ &+ \left[\frac{2}{r}P_{r\theta} + \frac{\partial P_{r\theta}}{\partial r} + \frac{1}{r}P_{\theta r} + \frac{1}{r}\frac{\partial P_{\theta\theta}}{\partial\theta} + \frac{1}{r\sin\theta}\frac{\partial P_{\phi\theta}}{\partial\phi} + \frac{\cot\theta}{r}P_{\theta\theta} - \frac{\cot\theta}{r}P_{\phi\phi}\right]\vec{e_\theta} \\ &+ \left[\frac{\partial P_{r\phi}}{\partial r} + \frac{2}{r}P_{r\phi} + \frac{1}{r}\frac{\partial P_{\theta\phi}}{\partial\theta} + \frac{1}{r\sin\theta}\frac{\partial P_{\phi\phi}}{\partial\phi} + \frac{\cot\theta}{r}P_{\theta\phi} + \frac{1}{r}P_{\phi r} + \frac{\cot\theta}{r}P_{\phi\theta}\right]\vec{e_\phi} \end{aligned}$$

Again, only the term proportional to $\vec{e_r}$ is of current interest since the r-direction is normal to the interface. It has been shown that the off-diagonal elements $P_{\alpha\beta} = 0$, $\alpha \neq \beta$ vanish at equilibrium. Substitution of these values for the off-diagonal elements in eqn (3.59) gives for the term proportional to $\vec{e_r}$

$$\frac{2P_{rr} - P_{\phi\phi} - P_{\theta\theta}}{r} + \frac{\partial P_{rr}}{\partial r} = 0 \tag{3.61}$$

Since r is perpendicular to the spherical interface, $P_{rr} = p_N$. Analogously, because both θ and ϕ are parallel to the spherical interface, $P_{\theta\theta} = P_{\phi\phi} = p_T$. In has been shown in section 2.1.2 that the total curvature $J = 2/r$ for a sphere. Consequently, eqn (3.61) is equivalent to eqn (3.11). Moreover, since the off-diagonal elements vanish and $P_{\theta\theta} = P_{\phi\phi} = p_T$ it is found that p_T is constant at each r.

APPENDIX 3.C. STIRLING'S APPROXIMATION

A factorial is given by the well-known Γ-function

$$N! = \int_0^\infty x^N e^{-x}dx = \int_0^\infty e^{-x+N\ln x}dx \tag{3.62}$$

The exponent of the last term is approximated by a second order Taylor series around it maximum $x = N$

$$-x + N\ln x = -N + N\ln N + 0 - \frac{1}{2}\frac{N}{N^2}(x-N)^2 + \mathcal{O}(x^3)$$

Substitution into eqn (3.62) gives

$$N! \approx \int_0^\infty \exp\left\{-N + N\ln N - \frac{(x-N)^2}{2N}\right\} dx$$
$$= \frac{1}{2} e^{N\ln N - N} \int_{-\infty}^{\infty} \exp\left\{-\frac{(x-N)^2}{2N}\right\} dx$$

Using the error function yields

$$N! = e^{N\ln N - N}\sqrt{2\pi N}$$

From this it follows that

$$\ln N! = N\ln N - N + \frac{1}{2}\ln 2\pi N \approx N\ln N - N \tag{3.63}$$

The last expression on the right hand side is the so-called Stirling approximation, where the term $\ln 2\pi N$ is negligible if N is sufficiently large.

The relative error of the Stirling approximation is less than 2% if $N > 50$. Therefore, in the thermodynamic limit ($N \approx 10^{23}$) this approximation is sufficiently accurate. However, the relative error is rather large for small values of N. In that case the accuracy can be improved considerably by adding the $\ln 2\pi N$-term. The error is then less than 2% if $N > 3$. So, this correction term might be introduced for expressions where N is not sufficiently large (e.g., $N < 100$) to have a better approximation.

APPENDIX 3.D. DISCRETIZED INTERFACIAL PROPERTIES

The expressions in chapter 2 were all derived in continuous space. Owing to the discretization of space, imposed by the lattice model, they must be rewritten. Here the discretized version of the normal pressure on the lattice will be derived as well as the expressions for the bending moments and the generalized Laplace equation.

3.D.1. Discretized normal pressure

As the tangential pressure was identified with the grand potential density, it is constant within each lattice layer. Therefore, this also holds for the normal pressure. The change of the normal pressure from one layer to another is according to eqn (3.11) given by the difference equation

$$\int_z^{z+1} dp_N = p_N(z+1) - p_N(z) = (p_T(z) - p_N(z)) \int_z^{z+1} J(z)dz$$

Using the total curvature of a sphere, $J(z) = 2/z$, this reads

$$p_N(z+1) = p_N(z) + 2\left(p_T(z) - p_N(z)\right) \ln\left(1 + \frac{1}{z}\right)$$

For a cylinder, the difference equation for the normal pressure is given by

$$p_N(z+1) = p_N(z) + \left(p_T(z) - p_N(z)\right) \ln\left(1 + \frac{1}{z}\right)$$

because $J(z) = 1/z$. For a planar geometry this implies that the normal pressure of all layers are equal to the bulk pressure since $J(z) = 0$.

3.D.2. Discretized bending moments

In section 2.5 thermodynamically consistent mechanical expressions for the bending moments were found as given by eqn (2.50). As stated before, the tangential pressure is constant within each lattice layer. Consequently, a bending moment can be written as a sum over all layers. The zeroth bending moment, eqn (2.50a), is simply given by

$$\mathbb{P}_0 = \int (p^{\alpha\beta} - p_T) dR = \sum_z \int_{z-1}^{z} (p^{\alpha\beta} - p_T(z)) dR = \sum_z (p^{\alpha\beta} - p_T(z)) \tag{3.64}$$

As before, $p^{\alpha\beta}$ equals p^α up to the dividing plane and p^β beyond, where both bulk pressures are given by eqn (3.27). Either bulk pressure p^α and p^β is evaluated by applying $\phi_i^\alpha = \phi_i(1)$ and $\phi_i^\beta = \phi_i(M)$, respectively. The integral in eqn (2.50a) is thus effectively replaced by a sum. However, this cannot be done for the first bending moment, eqn (2.50b)

$$\begin{aligned}\mathbb{P}_1 &= \int (R - R_s)(p^{\alpha\beta} - p_T) dR = \sum_z \int_{z-1}^{z} (R - R_s)(p^{\alpha\beta} - p_T(z)) dR \\ &= \sum_z \frac{1}{2} R^2 - R_s R \Big|_{z-1}^{z} (p^{\alpha\beta} - p_T(z)) = \sum_z \left(z - R_s - \frac{1}{2}\right) (p^{\alpha\beta} - p_T(z))\end{aligned} \tag{3.65}$$

Owing to the discretization, an extra factor half enters. Analogously, it is found that the second bending moment, eqn (2.50c), is given by

$$\mathbb{P}_2 = \sum_z \left((z - R_s)^2 - (z - R_s - \frac{1}{3})\right) (p^{\alpha\beta} - p_T(z)) \tag{3.66}$$

Applying the relation between the bending moments and the interfacial tension according to Gibbs, eqn (2.43), as well as using eqn (2.28) with $z = R_s + \Delta R_s$, the excess grand potential, given by eqn (2.17), becomes

$$\Omega^s = \gamma_G A = \sum_z A(z)(p^{\alpha\beta} - p_T(z)) \left(1 - \frac{\frac{1}{2}J + K(z - R_s - \frac{1}{3})}{1 + J(z - R_s) + K(z - R_s)^2}\right)$$

It is easily seen that for a planar geometry ($J = 0$, $K = 0$) this recovers eqn (3.64) since $A(z) = A$ throughout the lattice. For a spherical lattice ($J = \frac{2}{R_s}$, $K = \frac{1}{R_s^2}$, $A(z) = 4\pi z^2$) it is found that

$$\begin{aligned}\gamma_G A &= \sum_z 4\pi z^2 \left(1 - \frac{1}{z} + \frac{1}{3z^2}\right)\left(p^{\alpha\beta} - p_T(z)\right) \\ &= \sum_z \frac{4}{3}\pi \left(z^3 - (z-1)^3\right)\left(p^{\alpha\beta} - p_T(z)\right) \end{aligned} \tag{3.67}$$

Using eqn (3.13) for $L(z)$, eqn (3.67) recovers the excess grand potential as given by eqn (3.25)

$$\Omega^s = \gamma_G A = \sum_{z=1}^{M} L(z)\left(p^{\alpha\beta} - p_T(z)\right)$$

In the cylindrical case ($J = \frac{1}{R_s}$, $K = 0$, $A(z) = h\pi z^2$) the excess grand potential is recovered analogously. This shows that the discretized expressions for the bending moments as given by eqn (3.64), eqn (3.65), and eqn (3.66) form a consistent set of equations.

3.D.3. Discretized generalized Laplace equation

The generalized Laplace equation was derived from the invariance of the grand potential with respect to the choice of the arbitrary dividing plane. This implies (*cf.* eqn (2.18))

$$\begin{aligned}-p^\alpha V^\alpha(R_{s,1}) - p^\beta V^\beta(R_{s,1}) + \gamma_G(R_{s,1})A(R_{s,1}) \\ = -p^\alpha V^\alpha(R_{s,2}) - p^\beta V^\beta(R_{s,2}) + \gamma_G(R_{s,2})A(R_{s,2})\end{aligned}$$

where $R_{s,1}$ and $R_{s,2}$ are the two choices of the dividing plane. For a sphere this equation reduces to

$$\Delta p = \frac{\gamma_G(R_{s,1})R_{s,1}^2 - \gamma_G(R_{s,2})R_{s,2}^2}{\frac{1}{3}\left(R_{s,1}^3 - R_{s,2}^3\right)} \tag{3.68}$$

In continuous space, one could take $R_{s,2} = R_{s,1} + dR_s$, such that $\gamma_G(R_{s,2}) = \gamma_G(R_{s,1}) + d\gamma_G$. Neglecting higher order terms, this reduces eqn (3.68) to

$$\Delta p = \gamma_G(R_s)\frac{2}{R_s} + \frac{\partial \gamma_G}{\partial R_s}$$

which recovers the generalized Laplace equation eqn (2.36). Analogously, the generalised discrete Laplace equation for a cylindrical geometry reads

$$\Delta p = \frac{\gamma_G(R_{s,1})R_{s,1} - \gamma_G(R_{s,2})R_{s,2}}{\frac{1}{2}\left(R_{s,1}^2 - R_{s,2}^2\right)}$$

For a planar geometry this gives $\gamma_G(R_{s,1}) = \gamma_G(R_{s,2})$ because $\Delta p = 0$.

REFERENCES

[1] D. Chandler. *Introduction to Modern Statistical Mechanics.* Oxford University Press, 1987.

[2] H.T. Davis. *Statistical Mechanics of Phases, Interfaces, and Thin Films.* Advances in Interfacial Engenineering. VCH Publishers, Inc., 1996.

[3] R.P. Feynman. Statistical mechanics: A set of lectures. In D. Pines, editor, *Frontiers in Physics*, volume 36, pages 55–57. Addison-Wesley, 1972.

[4] H. Goldstein. *Classical Mechanics.* Addison-Wesley, 1959.

[5] P. Schofield and J.R. Henderson. *Proc. R. Soc. Lond.*, A379:231, 1982.

[6] S.M. Thompson, K.E. Gubbins, J.P.R.B. Walton, R.A.R. Chantry, and J.S. Rowlinson. *J. Chem. Phys.*, 81:530, 1984.

[7] D.A. McQuarrie. *Statistical Mechanics.* Harper and Row, 1976.

[8] M.P. Allen and D.J. Tildesley. *Computer Simulation of Liquids.* Oxford University Press, 1987.

[9] J.P. Hansen and I.R. McDonald. *Theory of Simple Liquids.* Academic Press, 1976.

[10] E. Helfand. *Phys. Rev.*, 119:1, 1960.

[11] G.C. Maitland, M. Rigby, E.B. Smith, and W.A. Wakeham. *Intermolecular Forces: Their Origin and Determination*, volume 3 of *International Series of Monographs on Chemistry.* Clarendon Press, 1987.

[12] N. Goldenfeld. Lectures on phase transitions and the renormalization group. In D. Pines, editor, *Frontiers in Physics*, volume 85. Addison-Wesley, 1992.

[13] J.S. Rowlinson. *Chem. Soc. Rev.*, 12:251, 1983.

[14] J.S. Rowlinson. *Pure Appl. Chem.*, 65:873, 1993.

[15] R. Lovett and M. Baus. *J. Chem. Phys.*, 106:635, 1997.

[16] J.S. Rowlinson. *J. Phys.: Condens. Matter*, 6:A1, 1994.

[17] J.K. Percus, L.A. Pozhar, and K.E. Gubbins. *Phys. Rev. E*, 51:261, 1995.

[18] J.S. Rowlinson and B. Widom. *Molecular Theory of Capillarity.* Clarendon Press, 1982.

[19] V.S. Markin, M.M. Kozlov, and S.L. Leikin. *J. Chem. Soc. Faraday Trans. 2*, 84:1149, 1988.

[20] L. Boruvka, Y. Rotenberg, and A.W. Neumann. *J. Phys. Chem.*, 90:125, 1986.

[21] M. Pasandideh-Fard, P. Chen, J. Mostaghimi, and A.W. Neumann. *Adv. Colloid Interface Sci.*, 63:151, 1996.

[22] J.G. Kirkwood and F.P. Buff. *J. Chem. Phys.*, 17:338, 1949.

[23] J. Gaydos, L. Boruvka, Y. Rotenberg, P. Chen, and A.W. Neumann. Generalized theory of capillarity. In A.W. Neumann and J.K. Spelt, editors, *Applied Surface Thermodynamics.* Marcel Dekker, 1996.

[24] E.M. Blokhuis and D. Bedeaux. *J. Chem. Phys.*, 97:3576, 1992.

[25] S. Hyde, S. Andersson, K. Larsson, Z. Blum, T. Landh, S. Lidin, and B.W. Ninham. *The Language of Shape: the role of curvature in condensed matter physics, chemistry and biology.* Elsevier, 1997.

[26] J.R. Henderson. *Mol. Phys.*, 95:187, 1998.

[27] A.J.M. Yang, P.D. Flemming, and J.H. Gibbs. *J. Chem. Phys.*, 64:3732, 1976.

[28] P.P.A.M. van der Schoot and F.A.M. Leermakers. *Macromolecules*, 21:1876, 1988.

[29] G.J. Fleer, M.A. Cohen Stuart, J.M.H.M. Scheutjens, T. Cosgrove, and B. Vincent. *Polymers at Interfaces.* Chapman and Hall, 1993.

[30] H. Reiss. *Methods of Thermodynamics.* Blaisdell Publishing Company, 1965. reprinted by Dover, 1996.

[31] G.B. Arfken and H.J. Weber. *Mathematical Methods for Physicists.* Academic Press, 4th edition, 1995.

[32] P.W. Atkins. *Physical Chemistry.* Oxford University Press, fifth edition, 1994.

[33] J.M. Yeomans. *Statistical Mechanics of Phase Transitions.* Oxford University Press, 1992.

[34] S.K. Ma. Modern theory of critical phenomena. In *Frontiers in Physics*, volume 46. Benjamin, 1976.

[35] L.D. Landau and E.M. Lifshitz. *Statistical Physics*, volume 1. Pergamon Press, 3rd edition, 1980.

[36] F.P. Buff. *J. Phys. Chem.*, 23:419, 1955.

[37] R.C. Tolman. *J. Chem. Phys.*, 17:333, 1949.

[38] A.H. Falls, L.E. Scriven, and H.T. Davis. *J. Chem. Phys.*, 75:3986, 1981.

[39] M.P.A. Fisher and M. Wortis. *Phys. Rev. B*, 29:6252, 1984.

[40] C.M. Wijmans, F.A.M. Leermakers, and G.J. Fleer. *J. Chem. Phys.*, 101:8214, 1994.

[41] C.C. van der Linden, F.A.M. Leermakers, and G.J. Fleer. *Macromolecules*, 29:1172, 1996.

[42] F.A.M. Leermakers and J.M.H.M. Scheutjens. *J. Chem. Phys.*, 89:3264, 1988.

[43] I. Szleifer, D. Kramer, A. Ben-Shaul, W.M. Gelbart, and S.A. Safran. *J. Chem. Phys.*, 92:6800, 1990.

[44] I. Szleifer and M.A. Carignano. In I. Prigogine and S.A. Rice, editors, *Advances in Chemical Physics*, volume XCIV, page 165. John Wiley and Sons, 1996.

[45] A.D. Mackie, A.Z. Panagiotopoulos, and I. Szleifer. *Langmuir*, 13:5022, 1997.

[46] A. Ben-Shaul and W.M. Gelbart. Statistical thermodynamics of amphiphile self-assembly: Structure and phase transitions in micellar solutions. In W.M. Gelbart, A. Ben-Shaul, and D. Roux, editors, *Micelles, Membranes, Microemulsions and Monolayers.* Springer-Verlag, 1994.

[47] E.P.K. Currie, F.A.M. Leermakers, M.A. Cohen Stuart, and G.J. Fleer. *Macromolecules*, 32:487, 1999.

[48] G. Gompper and S. Zschocke. *Phys. Rev. A*, 46:4836, 1992.

[49] Gompper. G. and M. Schick. Self-assembling amphiphilic systems. In C. Domb and J.L. Lebowitz, editors, *Phase Transitions and Critical Phenomena*, volume 16. Academic Press, 1994.

[50] D.C. Rapaport. *The Art of Molecular Dynamics simulation.* Cambridge University Press, 1995.

[51] R.B. Bird, W.E. Stewart, and E.N. Lightfoot. *Transport Phenomena.* Wiley and Sons, Inc., 1960.

CHAPTER 4

Mechanical Properties of Curved Interfaces

ABSTRACT

The change of the interfacial tension according to Gibbs as a function of the physical curvature is described by an expansion up to first and second order in the curvature leading to a definition of the Tolman length and the Helfrich constants, respectively. Generally valid expressions for the Helfrich constants in terms of the local pressure profile are found which seem to differ from those in the literature. These discrepancies are attributed to different definitions of the local pressure. Using a lattice model, the descriptions are applied to a simple liquid-vapour interface. It is found that the mechanical quantities, derived in this way, evaluated at the Gibbs dividing plane give unambiguous results for the Helfrich constants. The constants that were found reproduce a direct fit to the interfacial tension within numerical accuracy. The results of the lattice model are compared to the results found from the van der Waals model and from an analytical expansion of the van der Waals model around the critical point. The three approaches are in agreement in the regions where these theories apply. The practical relevance of the Helfrich constants is discussed.

4.1. BENDING AN INTERFACE

In chapter 2 it is shown that the interfacial tension can be obtained from the excess pressure profile. Although the pressure could locally not be determined unambiguously, a unique value for the interfacial tension according to Gibbs is found, as shown in chapter 3. Nevertheless, the interfacial tension has shown to be a function of the notional position of the chosen dividing plane. This is caused by the fact that by changing the notional position of the dividing plane, the chosen interface has a different area and principal curvatures and both phases occupy different volumes. Since this mathematical choice of the dividing plane does not change the system physically, the grand potential cannot change and thus the interfacial tension must change accordingly. However, for a fixed particular choice of the dividing plane the interfacial tension is determined unambiguously.

In this chapter the change of the interfacial tension is investigated as a function of a physical change in the curvature of the interface for a given choice of the mathematical dividing plane. As derived in section 2.5, the isothermal change of the interfacial tension

according to Gibbs is given by the Gibbs-Duhem relation

$$(d\gamma_G)_T = \left(\mathbb{C}_1 - \sum_i \Gamma_i \left(\frac{\partial \mu_i}{\partial J}\right)_{T,K}\right) dJ + \left(\mathbb{C}_2 - \sum_i \Gamma_i \left(\frac{\partial \mu_i}{\partial K}\right)_{T,J}\right) dK \tag{4.1}$$

where it has been assumed that the chemical potentials of the system will generally change upon the physical change of the dividing plane. Obviously, in the case that the chemical potentials are constant upon bending, the terms containing μ_i vanish.

Two phenomenological descriptions of the change of the interfacial tension will be given below. One description, up to first order in the curvature, is by Tolman [1]. The Tolman description has been elaborated among others by using the penetrable-sphere model [2, 3] and molecular dynamics simulations [4, 5]. A more generally applicable description, up to second order in the curvature, was given by Helfrich [6]. Several models, e.g. a molecular model [7–9] and a Ginzburg-Landau model [10, 11], have been proposed to describe complex surfactant systems this way. Blokhuis and Bedeaux gave a thorough overview of the application of both phenomenological descriptions using various models [12].

4.1.1. First order discription: the Tolman length

The curvature terms in the expression for the internal energy vanish by definition at the surface of tension, as discussed in section 2.2. Therefore, at that particular interface the isothermal Gibbs adsorption equation, eqn (4.1), reduces for a single-component system to

$$d\gamma_{G,s} = -\Gamma_s d\mu \tag{4.2}$$

Here the subscript s refers to the quantities with respect to the surface of tension. From the Gibbs-Duhem relation derived from eqn (3.29) and eqn (3.30) it is found that, at constant temperature

$$(d\mu)_T = \frac{1}{\phi^\alpha} dp^\alpha = \frac{1}{\phi^\beta} dp^\beta$$

where ϕ^α and ϕ^β are the densities in the respective bulk phases. Substitution into eqn (4.2) yields

$$d\gamma_{G,s} = -\Gamma_s \frac{1}{\phi^\alpha} dp^\alpha = \frac{-\Gamma_s}{\phi^\alpha - \phi^\beta}\left(1 - \frac{\phi^\beta}{\phi^\alpha}\right) dp^\alpha = \frac{-\Gamma_s}{\phi^\alpha - \phi^\beta} d\left(p^\alpha - p^\beta\right)$$

Using the classical expression for the Laplace pressure difference $p^\alpha - p^\beta$, eqn (2.11), valid at the surface of tension only, this gives

$$d\gamma_{G,s} = \frac{-\Gamma_s}{\phi^\alpha - \phi^\beta} d\left(\gamma_{G,s} J_s\right) = \frac{-\Gamma_s}{\phi^\alpha - \phi^\beta} \gamma_{G,s} dJ_s + \frac{-\Gamma_s}{\phi^\alpha - \phi^\beta} J_s d\gamma_{G,s}$$

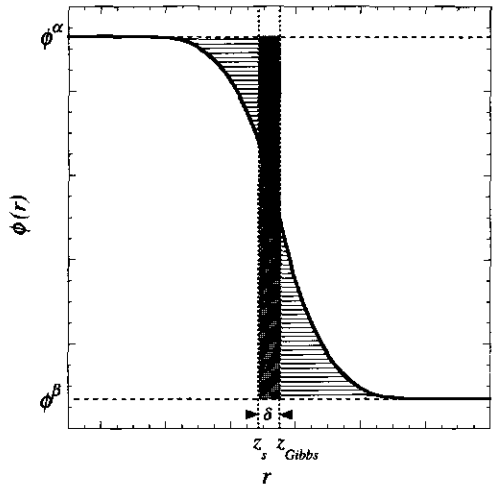

FIGURE 4.1. A possible density profile of a planar interface; the hatched areas are equal for the Gibbs dividing plane z_{Gibbs} whereas the grey bar indicates the extra adsorbed amount by shifting the dividing plane over a distance δ to the surface of tension z_s.

After rearranging terms, the following differential equation is obtained

$$\frac{1}{\gamma_{G,s}} d\gamma_{G,s} = \frac{\dfrac{-\Gamma_s}{\phi^\alpha - \phi^\beta}}{1 + \dfrac{\Gamma_s}{\phi^\alpha - \phi^\beta} J_s} dJ_s \tag{4.3}$$

At the Gibbs dividing plane, z_{Gibbs}, the interfacial excess vanishes by definition, i.e. for a planar interface

$$\int_{-\infty}^{z_{Gibbs}} (\phi^\alpha - \phi(r))\, dr = -\int_{z_{Gibbs}}^{\infty} \left(\phi^\beta - \phi(r)\right) dr \tag{4.4}$$

However, if the dividing plane is shifted to the surface of tension, z_s, the adsorbed amount changes. As can be seen from figure 4.1, this change is given by

$$\Gamma_s = \left(\phi^\alpha - \phi^\beta\right)(z_{Gibbs} - z_s) \equiv \left(\phi^\alpha - \phi^\beta\right)\delta \tag{4.5}$$

which defines the so-called Tolman length $\delta \equiv z_{Gibbs} - z_s$. This derivation is completely analogous to that of eqn (2.62) in section 2.5.1, where the pressures have been replaced by densities. There it has been made plausible that a mathematical derivation, as given by Tolman [1], indeed gives the same result as the above graphical construction.

Substitution of eqn (4.5) into the differential equation eqn (4.3) gives

$$\frac{1}{\gamma_{G,s}} d\gamma_{G,s} = \frac{-\delta}{1 + \delta J_s} dJ_s$$

The Tolman length has been defined from the density profile of a planar interface. However, for a curved interface one also has to account for the change of the interfacial area when the dividing plane is shifted. This leads to a differential equation that is difficult to solve. However, since the Tolman length is thought to be of the order of molecular distances [1], this change is negligible for weakly curved interfaces and hence δ is assumed to be constant. Integrating at constant temperature from the planar interface ($J_s = 0$) with an interfacial tension γ^0 to a certain, albeit weak, curvature J_s gives for the interfacial tension

$$\frac{\gamma_{G,s}}{\gamma^0} = \frac{1}{1 + \delta J_s} \tag{4.6}$$

Since the assumption of a constant Tolman length is only valid for weak curvatures ($J_s \approx 0$), eqn (4.6) can be written in a power series up to first order in curvature as [2]

$$\gamma_{G,s} = \gamma^0 (1 - \delta J_s) \tag{4.7}$$

The Tolman length is defined to be the distance between the Gibbs dividing plane and the surface of tension of the planar interface. The position of the Gibbs dividing plane of a planar interface can be found from its definition, eqn (4.4). The surface of tension was defined to be at that position where the curvature terms vanish, i.e. where the generalised Laplace equation, eqn (2.33), reduces to the classical Laplace equation, eqn (2.11), that is, when

$$\mathbb{C}_1 \left(J_s^2 - 2K_s \right) + \mathbb{C}_2 J_s K_s = 0 \tag{4.8}$$

If spherical droplets are considered ($J = \frac{2}{R_s}$, $K = \frac{1}{R_s^2}$), the surface of tension is found at $\left(\mathbb{C}_1 + \mathbb{C}_2 \frac{1}{R_s} \right) = 0$. Hence, in the limit of of a planar interface ($R_s \to \infty$), the surface of tension is found where the bending stress of a planar interface vanishes; $\mathbb{C}_1^0 = 0$. Tolman derived a mechanical expression for the position of the surface of tension of planar interfaces as $\mathbb{P}_1^0 = 0$ [13]. Using $\gamma^0 = \gamma_G = \gamma_{BN} = \mathbb{P}_0^0$ for a planar interface [14], eqn (4.8) leads after rearranging of terms to

$$\gamma^0 z_s = \int z \left(p^0 - p_T^0(z) \right) dz \tag{4.9}$$

where the superscript $\alpha\beta$ has been dropped since $p^\alpha = p^\beta = p_N(z)$ throughout a planar interface, as outlined in section 3.1.3. The superscript 0 refers again to evaluation at the planar interface. This equation is often found in the literature, although it has been acknowledged that it gives ambiguous results [2, 14]. Although eqn (4.9) provides an equation to an interface where the tension acts [15] (*cf.* the way to find the position of the fulcrum where a lever is balanced), it is not clear that this surface coincides with the surface of tension from its thermodynamic definition, $[d\gamma_G/dR] = 0$, as found in

section 2.2.2. Applying eqn (2.55) for the bending stress of the planar interface, the mechanical expression for the position of the surface of tension is found to be

$$\gamma^0 z_s = \int z \left(p^0 - p_T^0(z)\right) dz + \left(\frac{\partial \mathbb{P}_0}{\partial J_s}\right)^0_{T,K_s} + \sum_i \Gamma_i^0 \left(\frac{\partial \mu_i}{\partial J_s}\right)^0_{T,K} \tag{4.10}$$

In contrast to eqn (4.9), the surface of tension at the planar interface has to be invoked in order to obtain it. Therefore, eqn (4.10) has to be solved self-consistently. Moreover, it remains to be established whether the same mechanical expression for the surface of tension holds for other geometries, e.g. cylindrical ($J = 1/R_s, K = 0$). Therefore, eqn (4.10) is not an easy way to assess the position of the surface of tension and hence the mechanical route to the position of the surface of tension is not recommended. Since at the surface of tension the Laplace equation of capillarity reduces to $\Delta p = \gamma J$, the surface of tension can straightforwardly be found from eqn (2.18) once the grand potential and the bulk pressures are known. This provides a much easier, unambiguous way to locate the surface of tension.

4.1.2. Second order description: the Helfrich equation

The thermodynamic analysis in the previous section only holds for a single-component system. For a multi-component system the position of the Gibbs dividing plane will generally depend on the component to which it refers to. Consequently, the Tolman length cannot uniquely be defined. Moreover, the Tolman description as given by eqn (4.7) is an approximation which is only valid up to first order in the curvature. It can be seen from eqn (4.1) that a description of the interfacial tension of second order in the curvature is more appropriate. Therefore, a more general description up to higher order is desirable.

Consider the interfacial work needed to bend a planar interface at constant temperature. The requires integration of eqn (4.1) from the planar interface to an interface with a certain curvature (J, K)

$$\int_{\gamma^0}^{\gamma_G} d\gamma'_G = \int_0^J \left(\mathbb{C}_1 - \sum_i \Gamma_i \left(\frac{\partial \mu_i}{\partial J'}\right)_{T,K}\right) dJ' + \int_0^K \left(\mathbb{C}_2 - \sum_i \Gamma_i \left(\frac{\partial \mu_i}{\partial K'}\right)_{T,J}\right) dK' \tag{4.11}$$

It is generally impossible to evaluate these integrals without a model. Considering the interface as a harmonic spring, the work per unit area to deform it, γ_G, may phenomenologically be given by a series expansion up to second order in the curvature. For small differences between x_0 and x, an integral of a function $f(x)$ can be approximated up to

second order as

$$\int_{x_0}^{x} f(x')dx' = F(x) - F(x_0) \approx \left(\frac{dF}{dx}\right)_{x=x_0}(x-x_0) + \frac{1}{2}\left(\frac{d^2F}{dx^2}\right)_{x=x_0}(x-x_0)^2$$
$$= f(x_0)(x-x_0) + \frac{1}{2}\left(\frac{df}{dx}\right)_{x=x_0}(x-x_0)^2$$

Applying this expansion up to second order in curvature to eqn (4.11) yields

$$\gamma_G(J,K) - \gamma_G^0 \approx \left(\mathbb{C}_1 - \sum_i \Gamma_i \left(\frac{\partial \mu_i}{\partial J}\right)_{T,K}\right)^0 J + \frac{1}{2}\left(\frac{\partial}{\partial J}\left\{\mathbb{C}_1 - \sum_i \Gamma_i \left(\frac{\partial \mu_i}{\partial J}\right)_{T,K}\right\}\right)^0 J^2$$
$$+ \left(\mathbb{C}_2 - \sum_i \Gamma_i \left(\frac{\partial \mu_i}{\partial K}\right)_{T,J}\right)^0 K \tag{4.12}$$

Helfrich gave a similar expression for a phenomenological description of the undulation of lipid bilayers [6]

$$\gamma_G(J,K) - \gamma_0 = \frac{1}{2}k_c J^2 - k_c J_0 J + \overline{k}K \tag{4.13}$$

where J_0 is the so-called *spontaneous curvature*. The *saddle-splay modulus* $\overline{k}$ determines the topology of the interface rather than its rigidity, which is in turn determined by the *bending modulus* k_c. The Helfrich equation, eqn (4.13), has frequently been used in the literature to describe curved interfaces, undulation forces, and predict phase transitions in multi-component, e.g. surfactant, systems like vesicles and microemulsions [9, 16]. Since the coefficients of J and K in eqn (4.12) are constants, matching with the Helfrich equation, eqn (4.13), is allowed

$$-k_c J_0 = \left(\mathbb{C}_1 - \sum_i \Gamma_i \left(\frac{\partial \mu_i}{\partial J}\right)_{T,K}\right)^0 \tag{4.14a}$$

$$k_c = \left(\frac{\partial}{\partial J}\left\{\mathbb{C}_1 - \sum_i \Gamma_i \left(\frac{\partial \mu_i}{\partial J}\right)_{T,K}\right\}\right)^0 \tag{4.14b}$$

$$\overline{k} = \left(\mathbb{C}_2 - \sum \Gamma_i \left(\frac{\partial \mu_i}{\partial K}\right)_{T,J}\right)^0 \tag{4.14c}$$

Using eqn (2.55) and eqn (2.56) for, respectively, the bending stress and torsion stress in terms of the excess pressure profile, the following mechanical expressions for the

Helfrich constants are obtained

$$-k_c J_0 = \mathbb{P}_1{}^0 + \left(\frac{\partial \mathbb{P}_0}{\partial J}\right)^0_{T,K} \tag{4.15a}$$

$$k_c = 2\left(\frac{\partial \mathbb{P}_1}{\partial J}\right)^0_{T,K} + \left(\frac{\partial^2 \mathbb{P}_0}{\partial J^2}\right)^0_{T,K} \tag{4.15b}$$

$$\overline{k} = \mathbb{P}_2{}^0 + \left(\frac{\partial \mathbb{P}_0}{\partial K}\right)^0_{T,J} \tag{4.15c}$$

At first sight, all second terms on the right-hand sides of eqn (4.15) are extra compared to the expressions given in the literature, *viz.* $-k_c J_0 = \mathbb{P}_1^0$, $k_c = \left(\frac{\partial \mathbb{P}_1}{\partial J}\right)^0$, and $\overline{k} = \mathbb{P}_2^0$ [9, 12, 16]. Moreover, in the first term on the right hand side of eqn (4.15b) a factor 2 comes in compared to the literature due to differentiation of the extra terms in eqn (2.55). The extra terms make the thermodynamic variables independent of the choice of the expression for the local pressure, as demonstrated in section 3.2.6. In addition, these terms require that one has to do real bending work. Hence, according to eqn (4.15), evaluation of the planar interface only, as found in the literature [9, 12, 16], is not sufficient when the pressure is thermodynamically defined.

Safran [16] derived mechanical expressions for the bending and saddle-splay moduli from virtual work. He first determined the tangential volume work $-p_T dV$ needed to bend an element of a planar interface to certain curvatures J and K. Then the volume work $-p_N dV$ is applied perpendicular to the interface in order to recover the original volume of the planar interface; this guarantees that there is no net volume work thus satisfying the principle of virtual work [17]. The change in the pressure profile upon curvature is found from a first order series expansion around the pressure profile of the planar interface. Consequently, he assigned all the work done to the pressure tensor. The generally allowed change of the chemical potentials are embodied in the pressure, which is not consistent with its thermodynamical definition. As outlined in section 3.3, something similar occurs in the work by Szleifer *et al.* [8]. Their pressure enters as a Lagrange multiplier introduced to satisfy packing constraints; this is not obviously identical to the local pressure. Inserting this constraint into the partition function only adds a generalized pV-term [9], also accounting for the chemical potentials. Gompper *et al.* [10, 11] define the Ginzburg-Landau free energy density as the excess pressure profile. All these local pressures differ from the thermodynamic definition as found from eqn (2.45) on which the above analysis leading to eqn (4.15) has been based. The differences between eqn (4.15) and the expressions given in the literature may thus stem from the different definitions of the local pressure.

The Helfrich equation, eqn (4.13), was derived by series expansion up to second order in the curvature. If only the first order terms are evaluated, the approximated Tolman equation, eqn (4.7), is recovered. Comparison of both equations yield for a one-component system

$$\delta\gamma^0 = k_c J_0 = -\mathbb{P}_1^0 - \left(\frac{\partial \mathbb{P}_0}{\partial J}\right)_{T,K=0}^0 \tag{4.16}$$

The Tolman length can be replaced by its thermodynamic definition, $\delta \equiv z_{Gibbs} - z_s$. Subsequently, eqn (4.10) can be substituted for $\gamma^0 z_s$. Using $\gamma^0 = \mathbb{P}_0^0$, eqn (4.16) gives after rearranging terms

$$(z_{Gibbs} - z_s)\,\gamma^0 = \delta\gamma^0 = \Gamma^0 \left(\frac{\partial \mu}{\partial J}\right)_{T,K=0}^0 \tag{4.17}$$

This is an alternative expression for the bending modulus times the spontaneous curvature. Here, it has implicitly been assumed that $(z_{Gibbs} - z_s)$ is constant within first order in the curvature, i.e. eqn (4.6) is consistent with eqn (4.7). It follows from eqn (4.17) that bending an interface is a thermodynamic rather than a completely mechanical process.

Note that for a one-component system the Tolman length is a fixed distance between two well-defined dividing planes, *viz.* the Gibbs dividing plane and the surface of tension. Moreover, it can be seen from eqn (2.50a) that $\gamma^0 = \mathbb{P}_0^0$ does not depend on the choice of the dividing plane. Hence, the product $\delta\gamma^0$, and consequently $k_c J_0$, is independent of the choice of the dividing plane. However, the bending modulus k_c, as given by eqn (4.15b), and the saddle-splay modulus $\overline{k}$, found from eqn (4.15c), are a function of the position the interface. Alternatively, it is found from eqn (4.13) that whereas the first order curvature correction to the interfacial tension is independent of the choice of the interface, the second order curvature corrections do depend on that choice. This might be the basic reason that the Helfrich equation is still in dispute [18–20].

4.2. APPLICATION TO A SIMPLE LIQUID-VAPOUR INTERFACE

The curvature corrections to the interfacial tension in the previous section were phenomenological. These descriptions have frequently been used to describe the phase behaviour of complex interfaces [9, 16]. It is, however, illuminating to elaborate the phenomenological descriptions for a simple, i.e. monomeric, liquid-vapour interface. The practical relevance of such simple interfaces is among others found in the understanding of nucleation phenomena [21].

In this section the curvature corrections are determined from eqn (4.15) using the lattice model as elaborated in chapter 3. Subsequently, the results are verified by the well-known van der Waals theory of interfaces, which has been employed before [22].

4.2.1. Lattice model for curved interfaces

In section 3.2.1 the grand potential of a multi-component lattice has been derived. For a single component system, the grand potential as given by eqn (3.22) reduces to

$$\frac{\Omega[\phi]}{k_B T} = \sum_{z=1}^{M} L(z) \left[f(\phi(z)) - \mu \phi(z) \right] \tag{4.18}$$

where the Helmholtz energy density $f(\phi)$ follows from eqn (3.21)

$$f(\phi) = \phi \ln \phi + (1-\phi) \ln (1-\phi) - \phi \chi \langle \phi \rangle + \frac{1}{2} \chi \{ \phi + \langle \phi \rangle \} \tag{4.19}$$

Here, it has been used that for a single component system the exchange parameter is given by $\chi = -\frac{1}{2}\nu$, using eqn (3.18). It has also been shown that if the direct interaction parameter ν had been used, the last term in eqn (4.19) vanishes. Although this has led to a unique bulk pressure, eqn (3.27), two different expressions for the local pressure, eqn (3.50) and eqn (3.51), were found. Consequently, the bending moments, eqn (2.50), cannot be given unambiguously.

The chemical potential can be found from its definition, eqn (3.31)

$$\mu = \left(\frac{\partial f}{\partial \phi} \right)_T = \ln \left(\frac{\phi(z)}{1-\phi(z)} \right) - 2\chi \langle \phi(z) \rangle + \chi \tag{4.20}$$

which recovers eqn (3.24) for a single component system. The density profile varies spatially in such a way that the chemical potential is constant throughout the lattice. Considering the chemical potential as an undetermined Lagrange multiplier, it has been seen that this density profile minimizes the Helmholtz energy.

In order to obtain a certain curvature J of an interface, a Laplace pressure difference $\Delta p = \gamma^0 J'$ is imposed. The interfacial tension of the planar interface, γ^0, is determined from the zeroth bending moment, as given by eqn (3.52). The total curvature J' is an approximation for the desired curvature J. The bulk chemical potential corresponding to the applied pressure difference is determined and subsequently molecules are 'titrated' on a curved simple cubic lattice until the chemical potential of the phase separated system, as given by eqn (4.20), equals the desired bulk chemical potential. This procedure prevents so-called lattice artefacts [23], as outlined in appendix 4.A. After that, the equilibrium density profile of the curved system is known, so that all state variables can be determined.

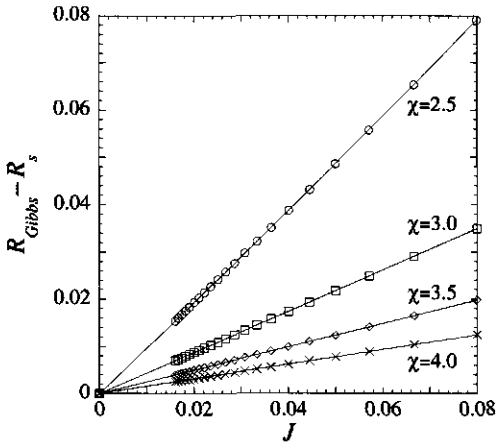

FIGURE 4.2. The distance in units of ℓ between the Gibbs dividing plane R_{Gibbs} and the surface of tension R_s of a spherical interface as a function of the total curvature J, determined from the Gibbs dividing plane, for four values of the interaction parameter χ. The limiting value for a planar interface yields a zero Tolman length for each value of χ.

It follows from eqn (2.11) that the value of interfacial tension according to Gibbs evaluated at the surface of tension is given by $\gamma_G = \Delta p/J$. Consequently, the position of the surface of tension R_s can be found from the grand potential, eqn (2.18), if the bulk pressures are known. With the given density profile, the position of the Gibbs dividing plane R_{Gibbs} can be determined from eqn (4.4). Note that although space has been discretized, neither the surface of tension nor the Gibbs dividing plane are necessarily integers. In figure 4.2 the distance between these dividing planes has been plotted as a function of the total curvature $J = 2/R_{Gibbs}$ of a spherical interface for several values of the interaction parameter χ. Recalling that the Tolman length δ is the distance between the Gibbs dividing plane and the surface of tension of a planar interface, δ may alternatively be given by [2]

$$\delta = \lim_{J \to 0} (R_{Gibbs} - R_s)$$

Using this definition, it is found from figure 4.2 that the Tolman length vanishes for all values of the interaction parameter, as should be the case from symmetry considerations [24]. It is easily seen from eqn (4.19) that exchange of species (with volume fraction $\phi(z)$) and free volume $(1-\phi(z))$ gives the same minimal Helmholtz energy of the planar interface.

The discretized bending moments $\mathbb{P}_0$, $\mathbb{P}_1$, and $\mathbb{P}_2$ are evaluated at the Gibbs dividing plane as outlined in appendix 3.D.2 for several curvatures in cylindrical and spherical drops. This has been carried out for the two definitions of the local pressure, eqn (3.50) and eqn (3.51). The interfacial tension according to Gibbs is determined from these bending moments, using eqn (2.49). As stated in section 3.2.6, γ_G does not depend on the choice of the local pressure profile. The interfacial tension according to Gibbs as a function of the curvature is shown by the symbols in figure 4.3. Obviously, the curvature dependence of the interfacial tension is very weak but noticeable. This explains the lack of experimental evidence for the existence of second order curvature corrections to the interfacial tension of simple liquid-vapour interfaces [19].

The spontaneous curvature $k_c J_0$ and the bending modulus k_c can only be determined from a cylindrical interface because in order to evaluate the derivatives of the bending moments, as given in eqn (4.15), the total curvature J must be varied at constant Gaussian curvature K. Third order polynomials were fit through the bending moments of the cylindrical interface as a function of curvature in order to evaluate the derivatives numerically. The values for $k_c J_0$, determined from eqn (4.15a), and k_c, determined from eqn (4.15b), are given in table 4.1 for four values of the interaction parameter. Both expressions for the local pressure yielded the same results for $k_c J_0$ and k_c within numerical accuracy. The values of $\mathbb{P}_0^0$ and $\left(\frac{\partial \mathbb{P}_0}{\partial J}\right)^0$, from both eqn (3.50) and eqn (3.51), are also given in table 4.1 to compare the calculated values with the ones if the expression from the literature were used uncarefully, i.e. $-k_c J_0 = \mathbb{P}_1^0$ and $k_c = \left(\frac{\partial \mathbb{P}_0}{\partial J}\right)^0$.

The saddle-splay modulus cannot be determined from a consideration of the cylindrical interface only, since, according to eqn (4.15c), K must be varied at constant J. Neither can this be done from a spherical interface since $1/R_1 = 1/R_2 = 1/R$ such that J and K are no longer independent state variables, as demonstrated in section 2.1.1. Consequently, for a spherical interface one of the curvature terms in the starting thermodynamic equation of the interface, eqn (2.12), is redundant and the thermodynamic analysis should be gone through again. However, it is easily seen that this leads to only one new state variable conjugated to the total curvature that incorporates both the bending and torsion stress. Only one *'effective' modulus*, $k_c + \frac{1}{2}\bar{k}$, is then found from eqn (4.14b) for the Helfrich equation. Consequently, the mechanical expression for the effective modulus is given by eqn (4.15b), where the respective bending moments are found from a spherical interface. From the effective bending modulus, determined completely analogously to the bending modulus from a cylindrical geometry, the saddle-splay modulus $\bar{k}$ can be extracted since k_c was already known from the cylindrical interface. The bending modulus, k_c, and the effective modulus, $k_c + \frac{1}{2}\bar{k}$, were

TABLE 4.1. Helfrich constants of a simple liquid-vapour interface determined from a lattice model using (a) a parabolic fit through the actual values of the interfacial tension, (b) eqn (4.15) for both expression for the local pressure, and the expressions $k_c J_0 = \mathbb{P}_1^0$, $k_c = \left(\frac{\partial \mathbb{P}_0}{\partial J}\right)^0$, and $\overline{k} = \mathbb{P}_2^0$ where (c) p_T^ν, as given by eqn (3.51), and (d) p_T^χ from eqn (3.50) have been used for the local pressure. The units are chosen such that $k_B T = 1$ and $\ell = 1$

	χ	(a)	(b)	(c)	(d)
$-k_c J_0$	2.5	0.0000	0.0000	-0.1480	0.0000
	3.0	0.0000	0.0000	-0.2146	0.0000
	3.5	0.0000	0.0000	-0.2696	0.0000
	4.0	0.0000	0.0000	-0.3191	0.0000
k_c	2.5	-0.0946	-0.0943	-0.1392	-0.1392
	3.0	-0.1028	-0.1035	-0.1785	-0.1785
	3.5	-0.0908	-0.0907	-0.1968	-0.1968
	4.0	-0.0749	-0.0733	-0.2101	-0.2101
$\overline{k}$	2.5	0.0535[1]	0.0506[1]	0.1883	0.1883
	3.0	0.0571[1]	0.0583[1]	0.2367	0.2367
	3.5	0.0497[1]	0.0489[1]	0.2603	0.2603
	4.0	0.0397[1]	0.0371[1]	0.2784	0.2784

[1] from comparison of cylindrical and spherical geometry

determined from a third order polynomial fit through the respective bending moments. Consequently, the extracted value for the saddle-splay modulus is subject to relatively much numerical noise. However, within numerical accuracy the two expressions for the pressure gave identical results. The (average) values of $\overline{k}$ that are found in this way are given in table 4.1 for some values of the interaction parameter. The values of $\mathbb{P}_2^0$ for the two definitions of the local pressure are also given for comparison with the value if the expression from the literature had been applied imprudently, i.e. $\overline{k} = \mathbb{P}_2^0$.

On the basis of the calculated values of the spontaneous curvature, the bending modules, and the saddle-splay modulus, the Helfrich equation, eqn (4.13), can be plotted for several values of the interaction parameter χ. These are the solid lines in figure 4.3. Alternatively, the Helfrich constants can also be determined from a direct parabolic fit through the symbols in figure 4.3. Those values are listed in table 4.1. For the sake of completeness, the Helfrich descriptions using the expressions from the literature carelessly are included in figure 4.3 as dashed and dotted lines for the two definitions of the pressure, respectively.

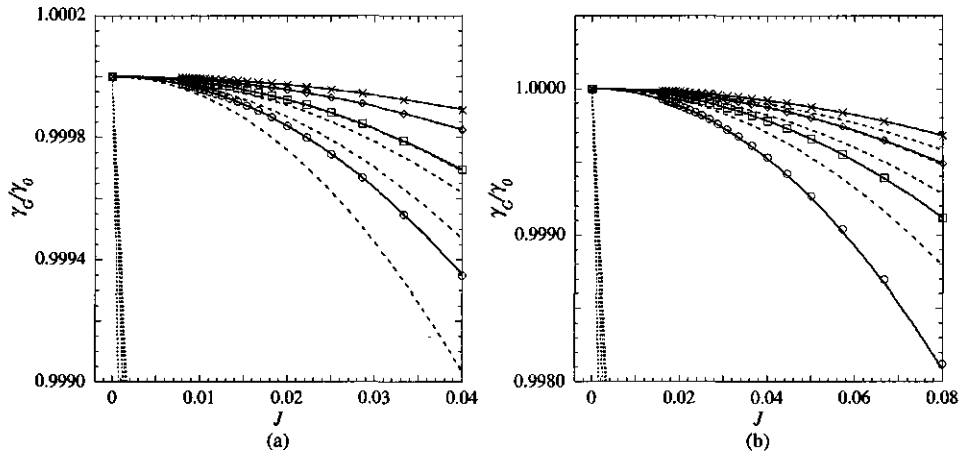

FIGURE 4.3. The curvature dependence of the interfacial tension according to Gibbs for a (a) cylindrical and (b) spherical liquid-vapour interface. The symbols give the interfacial tension according to eqn (2.49); ○: $\chi = 2.5$, □: $\chi = 3.0$, ◇: $\chi = 3.5$, ×: $\chi = 4.0$. The solid lines give the Helfrich description as found by eqn (4.15). The dashed and dotted lines give the Helfrich description using $k_c J_0 = \mathbb{P}_1^0$, $k_c = \left(\frac{\partial \mathbb{P}_0}{\partial J}\right)^0$, and $\overline{k} = \mathbb{P}_2^0$ where eqn (3.50) (dashed) and eqn (3.51) (dotted) have been used for the local pressure. The units are chosen such that $k_B T = 1$ and $\ell = 1$.

It is concluded that the phenomenological description using the parameters as given by eqn (4.15) is consistent with the thermodynamic data for the liquid-vapour interface from the lattice model. The values of k_c and $\overline{k}$ are identical for the two choices of the local pressure when the expressions from the literature are used imprudently. Nevertheless, these are in poor agreement with the parabolic fit to the curvature dependence of the interfacial tension. Moreover, the pressure profile p_T^ν, based on direct contact interactions, fails to reproduce a zero Tolman length from $k_c J_0 = \mathbb{P}_1^0$. This failure is due to the fact that p_T^ν is asymmetric, as can be seen from figure 3.16. The interactions are rather assigned to the inner part of the droplet emphasizing the tensile part inside the droplet. This causes $\mathbb{P}_1^0$ to become asymmetric around the Gibbs dividing plane, yielding a finite value for the surface of tension. Consequently, the surface where the tension acts does not coincide with the surface of tension.

The values for the interfacial tension of the planar interface, γ^0, are determined from eqn (3.52) for several values of the interaction parameter, as shown in figure 4.4. It has been shown in section 3.2.2 that for $\chi < \chi_c = -\frac{1}{2}\nu_c = 2$ no phase separation can be obtained. Since the two faces become identical at the critical point, the interfacial

tension vanishes. For $\chi > 2$ the interface becomes sharper such that the interfacial entropy becomes less important with increasing χ. Eventually, the interfacial tension is completely energetic: $\gamma^0 = \chi\lambda_1$.

The bending modulus k_c is also determined as a function of the interaction parameter and shown by the symbols in figure 4.5a. The bending modulus in the lattice model as given by eqn (4.15b) vanishes in the critical point. Beyond the critical point, for larger values of the interaction parameter, an interface is formed and the system is affected by the applied curvature. This yields a finite bending modulus. The bending modulus from the lattice model goes through a minimum. For very large χ it appears that the bending modulus goes to zero. This physically means that in the lattice model the free energy of the interface is for large χ apparently dominated by the interfacial tension rather than by the curvature.

The results for the saddle-splay modulus as a function of the interaction parameter are shown in figure 4.5b and give the same qualitative behaviour as the bending modulus. In the spherical geometry the interactions are in two directions affected by bending, whereas in the cylindrical only in one direction. Consequently, a simple liquid-vapour interface is more resilient against bending into a spherical geometry than into a cylindrical geometry. Consequently, the effective bending modulus is less negative than the bending modulus, which leads to a positive saddle-splay modulus that goes through a maximum.

4.2.2. Van der Waals theory of curved interfaces

Since $L(z)v_0$ is the volume of a layer, the sum over all layers of the grand potential density, as given by eqn (4.18), is equivalent to a volume integral in continuous space. Consequently, the grand potential of a lattice model can be regarded as the discretized version of the well-known free energy functional as given by van der Waals. In that continuous limit the discrete density profile $\phi(z)$ reduces to $\rho(\vec{r})$. For slowly varying densities, the contact fraction $\langle\phi(z)\rangle$ may be replaced by a squared gradient of the density profile, as outlined in section 3.2.4. In units such that $k_BT = 1$, $\ell = 1$, and $\lambda_1 = \frac{1}{6}$, the continuous version of the grand potential, eqn (4.18), then reads

$$\Omega[\rho] = \int d\vec{r}\,[\,\frac{\chi}{6}\,|\vec{\nabla}\rho(\vec{r})|^2 + f(\rho) - \mu\,\rho(\vec{r})\,] \tag{4.21}$$

with the free energy density $f(\rho)$

$$f(\rho) = \rho\ln(\rho) + (1-\rho)\ln(1-\rho) + \rho\chi(1-\rho) \tag{4.22}$$

As demonstrated analytically and graphically in section 3.2, the chemical potential of a planar interface is zero. Consequently, the chemical potential μ gives the distance to

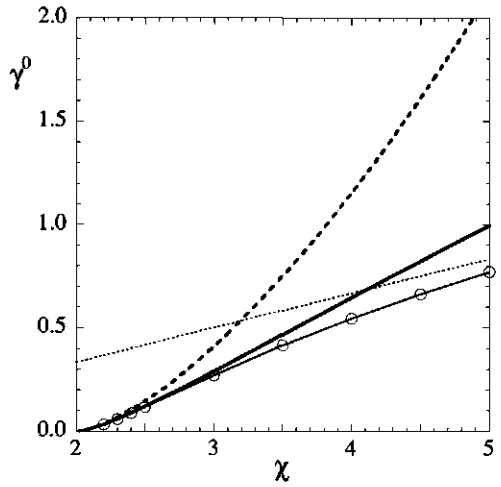

FIGURE 4.4. The interfacial tension of the planar interface as a function of the exchange interaction parameter in such units that $k_BT = 1$ and $\ell = 1$. The symbols are determined by the lattice model using a simple cubic lattice. The dotted line gives the limiting value $\gamma^0 = \chi/6$. The solid line gives the corresponding van der Waals description, eqn (4.26a), whereas the dashed line gives the asymptotic values, eqn (4.32a), valid in the vicinity of the critical point $\chi = 2$.

liquid-vapour coexistence. It will hence be used in the calculation to vary the curvature of the liquid-vapour interface.

As shown in section 2.2.2, the volume element $d\vec{r}$ depends on the geometry of the system. The Euler-Lagrange equation that minimizes the above grand potential in spherical geometry is given by [25, 26]

$$\frac{\chi}{3}\rho_s''(r) = -\frac{4\chi}{3}\frac{1}{r}\rho_s'(r) + f'(\rho_s) - \mu_s \tag{4.23}$$

where r is the radial distance. The subscript s denotes the fact that a spherical interface is considered, whereas the prime denotes the derivative with respect to its argument. In order to relate the grand potential to the curvature coefficients γ^0, k_c, and $\overline{k}$, an expansion is made in the reciprocal radius, $1/R$, of the spherical droplet. The density and chemical potential expanded to first order are

$$\rho_s(r) = \rho_0(r) + \rho_1(r)\frac{1}{R} + \mathcal{O}(\frac{1}{R^2}) \tag{4.24a}$$

$$\mu_s = \mu_1\frac{1}{R} + \mathcal{O}(\frac{1}{R^2}) \tag{4.24b}$$

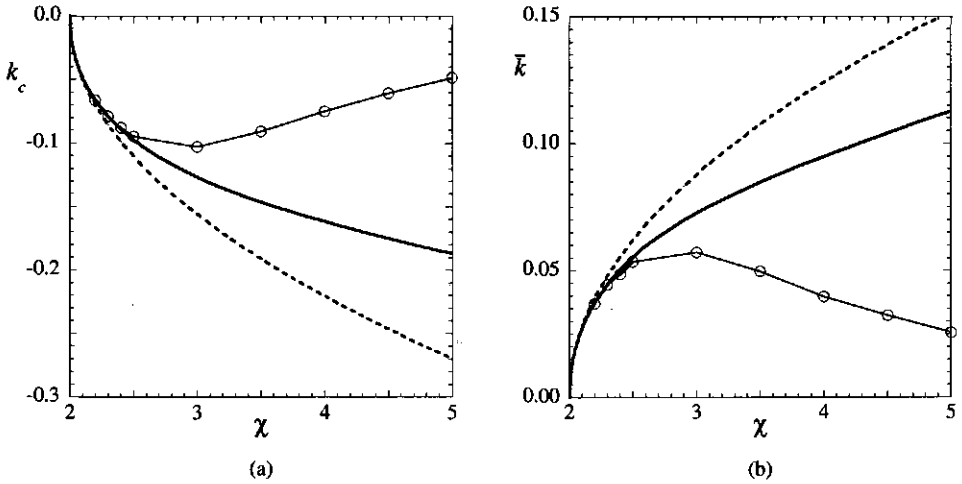

FIGURE 4.5. (a) The bending modulus and (b) the saddle-splay modulus as a function of the interaction parameter in units such that $k_BT=1$ and $\ell=1$. The symbols are determined on a simple cubic lattice. The solid line gives the corresponding van der Waals description, eqn (4.26c) and eqn (4.26d), whereas the dashed line gives the asymptotic values, eqn (4.32b) and eqn (4.32c).

where it can be shown that $\mu_1=2\gamma^0/\Delta\rho$ [24], with $\Delta\rho\equiv\rho_\ell-\rho_v$ the density difference between the liquid ($\rho_\ell\cong\phi^\alpha$) and vapour ($\rho_v\cong\phi^\beta$) phase at coexistence. The Euler-Lagrange equation in eqn (4.23) is also expanded to first order in the reciprocal radius

$$\frac{\chi}{3}\rho_0''(z)=f'(\rho_0) \tag{4.25a}$$

$$\frac{\chi}{3}\rho_1''(z)=-\frac{2}{3}\chi\,\rho_0'(z)+f''(\rho_0)\,\rho_1(z)-\mu_1 \tag{4.25b}$$

where it has been defined that $z\equiv r-R$, which must not be confused with the lattice index in the previous sections. Using the above differential equations, the grand potential of the interface can be extracted from eqn (4.21) up to second order in the curvature. Comparison with the Helfrich equation, eqn (4.13), yields the interfacial tension of the planar interface and Helfrich constants expressed in terms of the density profiles $\rho_0(z)$

and $\rho_1(z)$ [22]

$$\gamma^0 = \frac{\chi}{3}\int_{-\infty}^{\infty} dz\,[\rho_0'(z)]^2 \tag{4.26a}$$

$$k_c J_0 = \frac{\chi}{3}\int_{-\infty}^{\infty} dz\, z\,[\rho_0'(z)]^2 \tag{4.26b}$$

$$k_c = -\frac{\chi}{6}\int_{-\infty}^{\infty} dz\,\rho_1(z)\rho_0'(z) + \frac{\mu_1}{4}\int_{-\infty}^{\infty} dz\, z^2\rho_0'(z) \tag{4.26c}$$

$$\overline{k} = \frac{\chi}{3}\int_{-\infty}^{\infty} dz\, z^2\,[\rho_0'(z)]^2 \tag{4.26d}$$

Similar expressions were previously derived from Landau theory [10, 24]. As also found in section 4.2.1, k_c and $\overline{k}$ depend, unlike γ^0 and $k_c J_0$, on the choice of the position of the dividing plane. In order to make a fair comparison with the lattice model, the above expressions were derived by locating the interface at the equimolar plane, defined by

$$\Gamma = \int d\vec{r}\,[\rho_s(z) - \rho_{bulk}(z)] = 0 \tag{4.27}$$

where $\rho_{bulk} \equiv \rho_\ell\,\theta(-z) + \rho_v\,\theta(z)$. Expanded to first order in $1/R$, eqn (4.27) gives the following set of conditions for the profiles $\rho_0(z)$ and $\rho_1(z)$

$$\int_{-\infty}^{\infty} dz\,[\rho_0(z) - \rho_{0,bulk}(z)] = 0$$

$$\int_{-\infty}^{\infty} dz\,[\rho_1(z) - \rho_{1,bulk}(z)] = \int_{-\infty}^{\infty} dz\, z^2\rho_0'(z)$$

With these two conditions, the differential equations in eqn (4.25) have been solved numerically for the density profiles $\rho_0(z)$ and $\rho_1(z)$, using the explicit expression for $f(\rho)$ in eqn (4.22). The resulting density profiles have then been substituted into the expression for the interfacial tension and Helfrich constants as given by eqn (4.26). The results of this numerical approach are shown as the solid lines in figure 4.4 and figure 4.5.

The lattice model and the van der Waals theory both required a numerical solution of the density profiles. However, in the vicinity of the critical point, $\chi_c = 2$, analytical solutions for the interfacial tension of the planar interface and Helfrich constants can be derived [18]. To that end, the density is expanded around the critical density, $\rho_c = \frac{1}{2}$. Analogously as it was found in the Landau expansion of the free energy density,

eqn (3.46), $f(\rho)$ can be expanded to fourth order in $(\rho - \rho_c)$

$$f(\rho) = f(\rho_c) - (\chi - \chi_c)(\rho - \rho_c)^2 + \frac{4}{3}(\rho - \rho_c)^4 + \mathcal{O}((\rho - \rho_c)^6) \tag{4.28}$$

Solving the Euler-Lagrange equation for $\rho_0(z)$ in eqn (4.25) with the above form for $f(\rho)$, yields the well-known hyperbolic-tangent profile [2, 16]

$$\rho_0(z) = \rho_c - \frac{\Delta\rho}{2}\tanh(z/2\xi) \tag{4.29}$$

where the density difference $\Delta\rho$ and bulk correlation length ξ, which is a measure of the thickness of the interface, are given by

$$(\Delta\rho)^2 = \frac{3}{2}(\chi - \chi_c) \tag{4.30}$$

and

$$\xi = \frac{1}{6}\sqrt{6}\,(\chi - \chi_c)^{-\frac{1}{2}} \tag{4.31}$$

Within the van der Waals theory, the expressions for the interfacial tension of the planar interface and Helfrich constants have already been determined by eqn (4.26) [22]. The above expression for ρ_0 can simply be substituted, using eqn (4.30) and eqn (4.31) for $\Delta\rho$ and ξ, respectively. This gives

$$\gamma^0 = \frac{\chi_c}{18}\frac{(\Delta\rho)^2}{\xi} = \frac{1}{6}\sqrt{6}\,(\chi - \chi_c)^{\frac{3}{2}} \tag{4.32a}$$

$$k_c = -\frac{\chi_c}{54}(\pi^2 - 3)(\Delta\rho)^2\xi = \frac{-1}{108}\sqrt{6}\,(\pi^2 - 3)\,(\chi - \chi_c)^{\frac{1}{2}} \tag{4.32b}$$

$$\overline{k} = \frac{\chi_c}{54}(\pi^2 - 6)(\Delta\rho)^2\xi = \frac{1}{108}\sqrt{6}\,(\pi^2 - 6)\,(\chi - \chi_c)^{\frac{1}{2}} \tag{4.32c}$$

The familiar mean-field result for the interfacial tension of the planar interface [2] is recovered by eqn (4.32a). The asymptotic expressions eqn (4.32) are the dashed curves in figure 4.4 and figure 4.5.

4.3. DISCUSSION

The change of the interfacial tension according to Gibbs as a function of an imposed curvature is described phenomenologically using the Tolman and the Helfrich descriptions. The former applies up to first order in the curvature whereas the latter is up to second order in curvature.

The Tolman length is found thermodynamically as the distance between the Gibbs dividing plane and the surface of tension of a single-component planar interface and is assumed to be constant within first order of the curvature. As a consequence of the mechanical expression for the bending stress as found in section 2.5, the position of

the surface of tension of a planar interface can only be found self-consistently from the mechanical route. However, it can be found straightforwardly from the grand potential if the bulk pressures are known. In the limit of planar interfaces, it turns out that the distance between the two planes vanishes for a single-component monomer lattice gas, i.e. the interfacial tension is up to first order independent of the curvature. This feature must result case from symmetry considerations [24] and has indeed also been found mechanically for the first order curvature correction in the Helfrich description.

The Helfrich constants are found from the moments of the pressure profile and derivatives thereof evaluated at the flat interface. Calculations for a simple liquid-vapour interface from the lattice model show that the given Helfrich constants yield unambiguous results that are in agreement with the values found from a direct parabolic fit to the interfacial tension as a function of the curvature. This correspondence shows that when the pressure is defined from the grand potential density, it gives fully consistent results.

It has been shown that the grand potential of this lattice model is the discretized version of the well-known van der Waals free energy functional. The continuous version of this free energy is expanded up to second order in the curvature. Comparison with the Helfrich equation yields independent expressions for the interfacial tension of the planar interface and the Helfrich constants in terms of (derivatives of) the density profile of the planar interface. These results are given by the solid lines in figure 4.4 and figure 4.5. Substitution of a series expansion of the free energy density up to fourth order around the critical density in the van der Waals expressions, yields analytical expressions for the interfacial tension of the planar interface and the Helfrich constants. These are given by the dashed lines in figure 4.4 and figure 4.5.

The interfacial tension of the planar liquid-vapour interface, γ^0 has been studied extensively before [2]. As clearly shown in figure 4.4 all three models have the same known mean-field behaviour in the vicinity of the critical point $\chi_c = 2$. Away from the critical point non-local effects must be included and the analytical solution, which does not account for that, deviates from the other two. Further away from the critical point ($\chi \gtrsim 1.2\chi_c$) the density profile in the interfacial region becomes steeper and the square gradient term in the van der Waals expression for the free energy is no longer sufficient to account for this rapidly varying density profile and higher order derivatives of the density profile should be included. In the lattice gas expression for the Helmholtz energy the contact fraction also accounts for rapidly varying density gradients, as can be seen from the truncated series expansion in section 3.2.4. Consequently, only the lattice model gives the appropriate linear behaviour of γ^0 far away from the critical point. This

recovers the differences between square gradient and the more exact integral-functional theory as already known in the literature [27]. Some progress in the van der Waals description can be made by adding a square Laplacian [22, 28].

The bending modulus, k_c, determined from the lattice model using eqn (4.15b), is in good quantitative agreement with the ones found from the van der Waals theory, eqn (4.26c), up to the interaction parameter where the higher order derivatives of the density profile become important ($\chi \lesssim 1.2\chi_c$). The saddle-splay modulus, $\overline{k}$, is also in good qualitative agreement with the ones found from the van der Waals theory, eqn (4.26d), in the region where the latter is valid.

In the region where all the above-mentioned theories are valid they gave identical and physically relevant results for the interfacial tension of the planar interface and the bending constants. Within the mean-field approximation for the pair density, the van der Waals expressions for the Helfrich constants, eqn (4.26), are consistent with the those found from the virial route [22]. Gompper *et al.* [10, 11] derived expressions that were very reminiscent of eqn (4.26). They defined a free energy density, in this particular case for instance $\frac{\chi}{3}[\rho_0']^2$, as the tangential pressure profile, $p_T(z)$. Szleifer *et al.* did the same with their free energy density [8] to arrive at the same expressions for the Helfrich constants as from the principle of virtual work [16]. It is therefore concluded that the Helfrich constants as given by eqn (4.15) are consistent with all previously mentioned models within the mean-field approximation.

The first order curvature correction to the interfacial tension turned out to be independent of the choice of the dividing plane. However, the generally applicable second order curvature corrections as given by eqn (4.15) depend on the position of the interface. In the above analyses the Gibbs dividing plane is chosen for the location of the single-component liquid-vapour interface. However, in a multi-component system, this choice is ambiguous because for each of the different species that are in surface excess an equimolar plane can be allocated. Although the surface of tension provides a unique choice for the position of the dividing plane, it cannot be located for, e.g., microemulsions when the translational entropy is neglected, as shown in section 2.6.2. For the curvature dependence of the adsorption of polymer brushes to a solid interface, the surface of the substrate seems an obvious choice for the position of the dividing plane [29]. Something similar has been done in the work of Szleifer *et al.* where surfactants are adsorbed at a predefined interface for the formation of a surfactant (bi-)layer [8]. The ambiguity regarding the position of the interface may lead to confusion in the calculation of the Helfrich constants from a model. Nevertheless, the existence of the Helfrich

constants is experimentally clearly established, see e.g. [30, 31]. However, with Rowlinson [19], it is believed that the thermodynamic meaning of these measured moduli is restricted. The series expansions that led to eqn (4.12) are up to second order in the curvature around the planar interface, which means that its validity is restricted to relatively small curvatures. It is therefore doubtful whether this quasi-thermodynamic description also holds for highly curved interfaces like in microemulsions. Although it is quite successful in a phenomenological way [32], one should be very cautious in the thermodynamic interpretation of the constants obtained from a fit to second order in the curvature.

One should also be careful with a thermodynamic interpretation of J_0 from a model. This 'spontaneous curvature' is thought to be the curvature that minimizes the free energy. This condition is in the grand canonical ensemble given by the minimum of the interfacial tension, although it is yet unclear how this is generally realised in practice at constant chemical potential. From eqn (4.13) it is found indeed that

$$\frac{d\gamma_G}{dJ} = -k_c J_0 + k_c J = 0 \;\Rightarrow\; J = J_0$$

However, the spontaneous curvature does not give a complete description of the preferred geometry of an interface since this is also determined by the preferred Gaussian curvature, K_0. The latter drops out in the Helfrich equation owing to that the fact that the expansion is only up to second order in the curvature [33]. For a spherical interface, where a description in terms of J is sufficient, the above condition gives for the 'preferred curvature'

$$\frac{d\gamma_{G,s}}{dJ} = -k_c J_0 + \left(k_c + \frac{1}{2}\overline{k}\right) J = 0 \;\Rightarrow\; J = \frac{k_c J_0}{k_c + \frac{1}{2}\overline{k}}$$

The curvature in the last term is sometimes referred to as the 'natural curvature' and only equals the spontaneous curvature J_0 if $\overline{k}$ vanishes. Moreover, in real systems the curvature of droplets has a certain distribution [34] which is among others entropically favourable.

When the interfacial tension is the characteristic function, the sign of the (effective) bending modulus indicates whether a curved interface is stable or not. In the grand canonical ensemble the stability condition is given by

$$\frac{\partial^2 \gamma_G}{\partial J^2} = \begin{cases} k_c > 0 & \text{general curved interfaces} \\ k_c + \frac{1}{2}\overline{k} > 0 & \text{spherical interfaces} \end{cases}$$

Note that the calculations for the simple liquid-vapour interface were in a canonical ensemble. The chemical potential had not been fixed; it was in the van der Waals

theory actually used to vary the curvature. Therefore, a negative (effective) bending modulus in conjunction with a positive interfacial tension is feasible for simple liquid-vapour interfaces.

Note that from the Helfrich equation, eqn (4.13), the generalized Laplace equation of capillarity, eqn (2.36), can be given in terms of the Helfrich constants

$$\Delta p = \gamma^0 J + 2k_c (J - J_0) K - \frac{1}{2} k_c J^3 + \frac{1}{2} \left[\frac{dk_c}{dR_s}\right] J^2 + \left[\frac{d\bar{k}}{dR_s}\right] K$$

where the square brackets denote again a notional change of the position of the dividing plane.

ACKNOWLEDGEMENT

Edgar M. Blokhuis is gratefully acknowledged for the discussions on the mechanical expressions for the Helfrich constants in general and in particular for providing the equations and data on the van der Waals calculations and the analytical expansion around the critical point.

APPENDIX 4.A. MEAN-FIELD LATTICE CALCULATIONS

In an inhomogeneous system, consisting of C components, the chemical potential of species i, given by eqn (3.24), must be equal in each of the M lattice layers to guarantee chemical equilibrium; $\mu_i(1) = \mu_i(2) = \ldots = \mu_i(M)$. These equilibrium conditions give $C(M-1)$ equations for the CM variables $\phi_i(z)$. The C mass balances complete the set of equations

$$\sum_{z=1}^{M} L(z)\phi_i(z) = N_i$$

The set of equations can be solved numerically; the N_i molecules are distributed over the lattice in such a way that their mean-field interactions result a constant chemical potential throughout the lattice. Hence, the field caused by the presence of the molecules is made self-consistent.

In the above calculation technique, the N_i molecules are 'squeezed' on the lattice. Alternatively, owing to the discretization of space, molecules are forced to take place in one layer or the other. Consequently, an extra field is introduced as a result of the presence of the lattice which causes a spurious Laplace pressure difference, $\Delta p_{lattice}$ [23]. In order to study the actual physics of the lattice model, this so-called lattice artefact must be eliminated. To that end, the true chemical potentials of the bulk phases are determined.

The chemical potential of species i in the bulk phases $b = \alpha$ or β are according to eqn (3.24) given by

$$\frac{\mu_i^b}{k_B T} = \ln\left(\frac{\phi_i^b}{\phi_0^b}\right) + \sum_j \nu_{ij}\phi_j^b - \frac{1}{2}\nu_{ii} \tag{4.33}$$

In order to guarantee chemical equilibrium, the chemical potentials of the two phases must be equal; $\mu_i^\alpha = \mu_i^\beta$. For a two-phase system this equilibrium condition gives a set of C equations, with $2C$ variables, *viz.* ϕ_i^α and ϕ_i^β for each of the components $i = 1, \ldots, C$. The applied Laplace pressure difference $\Delta p = p^\alpha - p^\beta$, that can be determined from eqn (3.27), provides another equation. In order to give a complete set of equations, a mass balance for each of the components is also required

$$r\phi_i^\alpha + (1-r)\,\phi_i^\beta = \frac{N_i}{M} \tag{4.34}$$

where the variable r is the relative extent of phase α. Consequently, a set of $2C+1$ equations has been obtained for the $2C+1$ variables which can be solved numerically. Since r is not restricted to discrete lattice layers, the solution is free of artefacts. Note that the mass balance is not required for a single component system since $\mu^\alpha = \mu^\beta$ and $\Delta p = p^\alpha - p^\beta$ already provide the two equations for the unknowns ϕ^α and ϕ^β.

Now the number of particles on the lattice can be adjusted until the chemical potential, that is determined self-consistently, equals the chemical potentials in the bulk phases. This guarantees that the Laplace pressure difference equals the applied Δp, or, alternatively, $\Delta p_{lattice} = 0$. The difference between the chemical potential of the bulk phase and that of the homogeneous system as a function of the number of molecules is shown in figure 4.6a for three types of planar lattices for a single component liquid-vapour equilibrium. Clearly, the artefact oscillates by a periodic deviation that is approximately the thickness of a lattice layer. The artefact is relatively large for $\lambda_0 = 2/3$, smaller for $\lambda_0 = 1/2$, and small for $\lambda_0 = 1/3$. Two situations can be distinguished at which $\mu^b = \mu$; one zero in a descending and one in an ascending branch. The former, where $\left(\frac{\partial \mu}{\partial N}\right)_{T,V} = \left(\frac{\partial^2 F}{\partial N^2}\right)_{T,V} < 0$, corresponds to a maximum in the Helmholtz energy, whereas the latter corresponds to a minimum in the Helmholtz energy since $\left(\frac{\partial \mu}{\partial N}\right)_{T,V} = \left(\frac{\partial^2 F}{\partial N^2}\right)_{T,V} > 0$. Consequently, only the ascending branch must be considered.

In a curved system the oscillations are superimposed on the thermodynamic change of the chemical potential, as shown in figure 4.6b. From the isothermal Gibbs-Duhem relation $N d\mu^\alpha = V^\alpha dp^\alpha$ it can be derived that

$$(d\mu^\alpha)_T = -c_d \frac{d-1}{d} N^{-(d+1)/d} dN \tag{4.35}$$

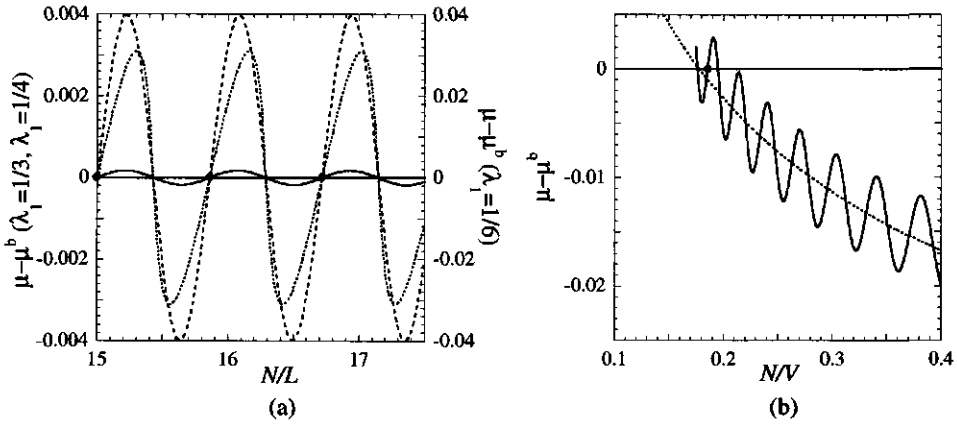

FIGURE 4.6. (a) The lattice artefact measured by the difference between the chemical potential of the bulk and that of the self-consistent system for a planar liquid-vapour interface with $\nu = -6$ in units so that $k_BT = 1$ and $\ell = 1$. The solid line gives the lattice artefact for $\lambda_1 = 1/3$, the dashed one for $\lambda_1 = 1/4$, and the dotted one for $\lambda_1 = 1/6$. The dots indicate the artefact-free points. (b) An example of the lattice artefact for a spherical liquid-vapour interface with $\nu = -6$ and $\lambda_0 = 1/2$. The lattice artefact of the planar interface is superimposed on the dotted line given by eqn (4.36) with $d = 3$ for the spherical interface. The only artefact free point is indicated by the thick dot

where d is the dimensionality of the system and the constant c_d includes the interfacial tension of the planar interface, γ^0, and the molecular volume. It has been assumed that $\Delta p = \gamma^0(d-1)/R$, that the bulk pressure p^β is constant, and that all molecules N are in the phase α. Integration of eqn (4.35) yields

$$\mu = c_d(d-1)N^{-1/d} + \mu_\infty \tag{4.36}$$

For a planar interface ($d = 1$) it is indeed found from this simple scaling consideration that the chemical potential should be constant. In the case that the oscillations are very weak, it is very well possible that there is no ascending branch that goes through zero. Consequently, in the vicinity of the critical point or $\lambda_1 = 1/3$ there are no artefact-free points found for curved interfaces. However, the oscillations for the lattice $\lambda_1 = 1/3$ are so small, that for some calculations the 'artefact poor' points may suffice.

REFERENCES

[1] R.C. Tolman. *J. Chem. Phys.*, 17:333, 1949.

[2] J.S. Rowlinson and B. Widom. *Molecular Theory of Capillarity.* Clarendon Press, 1982.

[3] S.J. Hemingway, J.S. Rowlinson, and J.P.R.B. Walton. *J. Chem. Soc. Faraday Trans. 2*, 79:1689, 1983.

[4] M.J.P. Nijmijer, C. Bruin, A.B. van Woerkom, and A.F. Bakker. *J. Chem. Phys.*, 96:565, 1992.

[5] S.M. Thompson, K.E. Gubbins, J.P.R.B. Walton, R.A.R. Chantry, and J.S. Rowlinson. *J. Chem. Phys.*, 81:530, 1984.

[6] W. Helfrich. *Z. Naturforsch*, 28c:693, 1973.

[7] E.M. Blokhuis and D. Bedeaux. *Physica A*, 184:42, 1992.

[8] I. Szleifer, D. Kramer, A. Ben-Shaul, W.M. Gelbart, and S.A. Safran. *J. Chem. Phys.*, 92:6800, 1990.

[9] A. Ben-Shaul and W.M. Gelbart. Statistical thermodynamics of amphiphile self-assembly: Structure and phase transitions in micellar solutions. In W.M. Gelbart, A. Ben-Shaul, and D. Roux, editors, *Micelles, Membranes, Microemulsions and Monolayers*. Springer-Verlag, 1994.

[10] G. Gompper and S. Zschocke. *Phys. Rev. A*, 46:4836, 1992.

[11] G. Gompper and M. Schick. Self-assembling amphiphilic systems. In C. Domb and J.L. Lebowitz, editors, *Phase Transitions and Critical Phenomena*, volume 16, pages 97–115. Academic Press, 1994.

[12] E.M. Blokhuis and D. Bedeaux. *Heterog. Chem. Rev.*, 1:55, 1994.

[13] R.C. Tolman. *J. Chem. Phys.*, 16:758, 1948.

[14] J.G. Kirkwood and F.P. Buff. *J. Chem. Phys.*, 17:338, 1949.

[15] J.S. Rowlinson. *Chem. Soc. Rev.*, 12:251, 1983.

[16] S.A. Safran. Statistical thermodynamics of surfaces, interfaces, and membranes. In D. Pines, editor, *Frontiers in Physics*, volume 90. Addison-Wesley, 1994.

[17] C. Lanczos. *The Variational Principles of Mechanics*. University of Toronto Press, 4th edition, 1970. reprinted by Dover, 1986.

[18] A.E. van Giessen, E.M. Blokhuis, and D.J. Bukman. *J. Chem. Phys.*, 108:1148, 1998.

[19] J.S. Rowlinson. *J. Phys.: Condens. Matter*, 6:A1, 1994.

[20] S. Hyde, S. Anderson, K. Larsson, Z. Blum, T. Landh, S. Lidin, and B.W. Ninham. *The Language of Shape: the role of curvature in condensed matter physics, chemistry and biology*. Elsevier, 1997.

[21] R.J. Hunter. *Foundations of Colloid Science*, volume I. Oxford University Press, 1986.

[22] E.M. Blokhuis and D. Bedeaux. *Mol. Phys.*, 80:705, 1993.

[23] P.A. Barneveld, J.M.H.M. Scheutjens, and J. Lyklema. *Langmuir*, 8:3122, 1992.

[24] M.P.A. Fisher and M. Wortis. *Phys. Rev. B*, 29:6252, 1984.

[25] G.B. Arfken and H.J. Weber. *Mathematical Methods for Physicists*. Academic Press, 4th edition, 1995.

[26] H. Goldstein. *Classical Mechanics*. Addison-Wesley, 1959.

[27] B. Widom. *J. Chem. Phys.*, 88:6508, 1984.

[28] V. Romero-Rochín, C. Varea, and A. Robledo. *Phys. Rev. A*, 44:8417, 1991.

[29] J. Brooks, C. Marques, and M. Cates. *J. Phys. II France*, 1:673, 1991.

[30] D. Langevin and J. Meunier. Interfacial tension: Theory and experiment. In W.M. Gelbart, A. Ben-Shaul, and D. Roux, editors, *Micelles, Membranes, Microemulsions and Monolayers*. Springer-Verlag, 1994.

[31] M. Gradzielski, D. Langevin, and B. Farago. *Phys. Rev. E*, 53:3900, 1996.

[32] R. Strey. *Colloid Polym. Sci.*, 272:1005, 1994.

[33] F.A.M. Leermakers, J. van Noort, S.M. Oversteegen, P.A. Barneveld, and J. Lyklema. *Faraday Discuss.*, 104:317, 1996.

[34] W.K. Kegel and H. Reiss. *Ber. Bunsenges. Phys. Chem.*, 100:300, 1996.

CHAPTER 5

Thermodynamics and Mechanics of Bilayer Membranes

ABSTRACT

A mean-field lattice model is applied to chain molecules for the study of surfactant systems. As an example, $C_{12}E_5$ surfactants, modelled as $C_{12}O(C_2O)_5$ chains, are forced into cylindrical and spherical shaped vesicles in a monomer solvent. These aggregates are used to obtain the Helfrich constants of the bilayers as a function of the hydrophilicity of the surfactant's headgroup from both a thermodynamic and mechanical route. The magnitude and sign of the Helfrich constants are interpreted to gain insight into features of the experimentally well-established phase diagram. It is concluded that the lattice model is a potentially valuable tool to help understand the generic phase behaviour of surfactant systems.

5.1. INTRODUCTION

In an aqueous environment surfactants self-assemble into finite-sized aggregates if their concentration exceeds the so-called critical micellization concentration. The characteristic length scale of these aggregates, e.g. the radius of spherical or cylindrical micelles, is comparable to that of the surfactant molecules. The formation dynamics [1] and interfacial geometry [2] of the aggregates can be related to this common length scale, as has also been made plausible in chapter 1. This chapter will be focused on bilayer membranes, in which a double sheet of surfactants separates two aqueous phases. The exterior of the sheet consists of the hydrophilic headgroups, whereas the interior is formed by the hydrophobic tails of the surfactants. The thickness of the membrane is comparable to the size of the constituting surfactant molecules. Bilayer systems are of interest for industrial applications, e.g. cleaning and catalysis [3], and in life sciences, e.g. as models for biomembranes.

The headgroups of the surfactants are hydrated on the one hand but also overlap to some extent with the conformationally disordered tails. Consequently, the conformational fluctuations within the various parts of the surfactant molecules are correlated. If the headgroups are well-hydrated, i.e. swollen, their relatively large headgroup area

allows for a disorder of the tail region. Conversely, a collapsed headgroup induces more conformational order in the tails.

Bilayer membranes are also subject to collective, wave-like, thermal motions of the constituting surfactant molecules. These so-called undulations give rise to a conformational disorder on the level of the membrane. When two bilayers approach each other, the undulations are confined which gives a loss of conformational entropy. This loss leads to a repulsive steric interaction between the bilayers. A low rigidity allows for large shape fluctuations of a membrane and yields a strong steric repulsion. This suggests that the contribution to the Helmholtz energy per unit area owing to undulations, f_u, is inversely proportional to the bending rigidity of the bilayer membrane. Since the bending modulus k_c as introduced in section 4.1.2 is of the order k_BT, dimensional analysis gives

$$f_u \propto \left(\frac{k_BT}{k_c}\right)^{\alpha} \frac{k_BT}{r^2} \tag{5.1}$$

Here α is a numerical constant and r is the distance between two adjacent membranes. Indeed, Helfrich showed that $\alpha = 1$ [4] and has been confirmed by others [1, 5]. However, the proportionality constant is still disputed [6]. Depending on the magnitude of k_c, and the prefactor in eqn (5.1), the repulsive undulation energy, eqn (5.1), may overcome the attractive van der Waals energy $f_{vdW} \propto -A/r^2$, where A is the Hamaker constant [1]. In those cases the stability of bilayer membranes largely depends on the bending rigidity. Hence, it is of interest to determine k_c for these types of surfactant systems.

The saddle-splay modulus $\overline{k}$, introduced in section 4.1.2, is of interest for the phase behaviour of the surfactant layer as well. If $\overline{k}$ is positive, the free energy of the interface can be lowered by forming saddle planes which have negative Gaussian curvatures K (*cf.* eqn (4.13)). It follows from the Gauss-Bonnet theorem [5, 7]

$$\int K dA = 4\pi (1 - g)$$

that g handles can be formed on a closed interface. For instance, $g = 0$ for a spherical interface ($K = 1/R^2$). Consequently, a positive saddle-splay modulus favours the formation of handles. Hence, $\overline{k}$ determines the topology of surfactant layers.

The phase behaviour of surfactants can thus be understood in terms of the Helfrich constants [8]. In order to study these constants k_c and $\overline{k}$ of a bilayer membrane, the free energy of the interface has to be considered as a function of curvature, as outlined in chapter 4. This can best be done by considering closed bilayers or so-called vesicles. Vesicles are of interest for many biological purposes and are used as, e.g., drug delivery vehicles [1–3, 7]. In the case of vesicles there are no end-cap contributions to the free

energy of the bilayer [2]. This also allows the application of the lattice model as derived in chapter 3, where spherically and cylindrically shaped structures have been studied.

In this chapter the phase behaviour of the non-ionic surfactant dodecyl penta(ethylene oxide), or briefly $C_{12}E_5$, will be considered. This non-ionic surfactant forms vesicles and is widely used as an emulsifying agent and detergent. It exhibits the same characteristic features as more complex, multi-component surfactant systems [9]. Consequently, much experimental data is available for this system [9, 10]. In order to study surfactants, the lattice model as previously elaborated will be extended to chain molecules in section 5.2. Subsequently, in section 5.3 the Helfrich constants of $C_{12}E_5$ vesicles will be investigated as a function of the hydrophilicity of the headgroup. From the obtained values possible implications for the phase behaviour will be discussed in section 5.4. Finally, recommendations for further study are given.

5.2. EXTENSION OF THE LATTICE MODEL

Surfactant molecules typically have an amphiphilic nature. Consequently, the surfactants must be modelled as consisting of at least two different, connected, species. Hence, the monomer lattice model derived in section 3.2 must be extended to include chain molecules. To that end, consider a diffusing monomer on a lattice of $z = 1, \ldots M$ layers, each consisting of $L(z)$ indistinguishable sites of volume v_0. The path covered by the particle on the lattice may be regarded as a chain; the next segment of the chain emerges from the previous segment like an unfolding accordion or fan.

5.2.1. Diffusing monomer on a lattice

Consider first the diffusion of a monomer alone. The (unnormalized) probability to find that monomer in layer z at time t, given it was in layer z_0 at time t_0, is given by the Green function

$$G(z,t|z_0,t_0) = \delta(z - z_0)\,\delta(t - t_0) \tag{5.2}$$

where $\delta(z)$ is the Dirac delta function. The probability that the particle, originally in z_0 at t, arrives in layer z via z' at time $t + \Delta t$ is given by the Chapmann-Kolmogorov equation [11]

$$G(z,t+\Delta t|z_0,t_0) = \int G(z,t+\Delta t|z',t)G(z',t|z_0,t_0)dz' \tag{5.3}$$

This describes a so-called first-order Markov process in which the probability at $t + \Delta t$ only depends on t and not on the completed path. Consequently, the monomer can come back to positions where it has already been.

Series expansion of $G(z, t + \Delta t|z', t_0)$ up to first order in Δt yields for infinitesimal Δt the Fokker-Planck or Smoluchowski equation [12, 13]

$$\frac{\partial}{\partial t}G(z,t) = \mathcal{L}_S G(z,t) \tag{5.4}$$

where $\mathcal{L}_S$ is the Smoluchowski operator [14] which includes the interactions present in the system given by the energy $u(z)$. Note that $u(z)$ represents the complete mean field that a segment of the emerging chain encounters. Hence, within the mean-field approximation, it is not profitable to distinguish between intra and intermolecular forces, albeit suggested otherwise in the literature [15, 16].

The stationary, i.e. equilibrium, solution of eqn (5.4) yield for the Green function [13, 14]

$$G(z) = \exp\left(-\frac{u(z)}{k_B T}\right) \tag{5.5}$$

This gives the probability to find a monomer in layer z.

5.2.2. Chain statistics

Upon each discrete time step t the chain, created by the random walk of monomers on the lattice, emerges a new segment. Consequently, in the equations of section 5.2.1 the time t may be replaced by the segment number s. Note that the chain of monomers created this way is *not* self-avoiding. Since each segment can be accounted for individually, they can be of different types. When the first segment of a chain of type i is in an arbitrary layer z_0, the discretization of the Chapmann-Kolmogorov equation, eqn (5.3), yields after summation over all z_0 the following recurrence relation for the probability $G_i(z, s|z_0, 1)$ to find segment s of chain type i in layer z

$$G_i(z, s|1) = G_i(z, s)\,\langle G_i(z, s-1|1)\rangle \tag{5.6}$$

The boundary condition of this recurrence relation is given by $G_i(z, 1|1) = G_i(z, 1)$ (*cf.* eqn (5.2)). In equilibrium, the so-called *segment weighting factor* is according to eqn (5.5) given by

$$G_i(z, s) = \sum_A G_A(z)\delta^i_{s,A} = \sum_A \exp\left(-\frac{u_A(z)}{k_B T}\right)\delta^i_{s,A} \tag{5.7}$$

where the Kronecker delta function $\delta^i_{s,A} = 1$ when segment s of molecule i is of type A and $\delta^i_{s,A} = 0$ otherwise.

The energy $u_A(z)$ a segment of type A encounters at z is, relative to the bulk phase β, given by (*cf.* eqn (3.19)) [17]

$$u_A(z) = u'(z) + k_B T \sum_B \chi_{AB}\left(\langle\phi_B(z)\rangle - \phi_B^\beta\right) \tag{5.8}$$

Here ϕ_B is the volume fraction of all other segment types B. Since exchange energies χ_{AB} are used, the free volume is accounted for as species such that the lattice must be completely filled. The energy $u'(z)$ comes in to account for this constraint.

The angular brackets in eqn (5.6) denote averaging over adjacent layers, like it has been done for the contact fraction in eqn (3.15)

$$\langle G_i(z,s|1)\rangle \equiv \lambda_{-1}(z)G_i(z-1,s|1) + \lambda_0(z)G_i(z,s|1) + \lambda_1(z)G_i(z+1,s|1)$$

For any position of the last segment N_i, the probability to find segment s of chain type i in layer z reads

$$G_i(z,s|N_i) = G_i(z,s)\,\langle G_i(z,s+1|N_i)\rangle \tag{5.9}$$

Here the boundary condition $G_i(z,N_i|N_i) = G_i(z,N_i)$ must be satisfied. The total volume fraction of segments of type A stemming from all chain types i in layer z follows from connecting the subchains of segments $1,\ldots s$ in layer z with the subchains $s,\ldots N_i$ [17]

$$\phi_A(z) = \sum_i C_i \sum_{s=1}^{N_i} \frac{G_i(z,s|1)G_i(z,s|N_i)}{G_i(z,s)}\delta^i_{s,A} \tag{5.10}$$

The denominator corrects for the double counting of segment s that came in from both subchains, as can be seen from eqn (5.6) and eqn (5.9). Considering that the sum over all layers of the volume fractions yields the total number of monomers, $\sum_z L(z)\phi_i(z) = n_i N_i$, it follows that the normalization factor C_i reads

$$C_i = \frac{n_i}{\sum_z L(z)G_i(z,N_i|1)} = \frac{\phi_i^\beta}{N_i} \tag{5.11}$$

The second normalization factor on the right hand side of eqn (5.11) is actually the same as the first albeit evaluated in the reference bulk phase. The first normalization factor allows for calculations with a fixed number of molecules of type i, n_i, whereas the second one may be used to fix the bulk concentration of type i, ϕ_i^β.

The volume fractions of type A can be determined from the segment weighting factors eqn (5.7), which follow from the energies $u_A(z)$. However, as can be seen from eqn (5.8), the energies $u_A(z)$ depend, in turn, on the volume fractions. Consequently, the set of equations has to be solved iteratively until the energies and volume fraction are consistent.

The grand potential relative to its bulk value can be derived in terms of the volume fraction profiles from statistical thermodynamics [17, 18]

$$\begin{aligned}\frac{\Omega + p^\beta V}{k_B T} &= \sum_z L(z) \left\{ \sum_i \frac{\phi_i^\beta - \phi_i(z)}{N_i} - \sum_A \frac{\phi_A(z) u_A(z)}{k_B T} \right. \\ &\qquad \left. + \frac{1}{2} \sum_A \sum_B \chi_{AB} \left[\phi_A(z) \left(\langle \phi_B(z) \rangle - \phi_B^\beta \right) - \phi_A^\beta \left(\phi_B(z) - \phi_B^\beta \right) \right] \right\} \\ &= \sum_z L(z) \left\{ p^\beta - p_T(z) \right\}\end{aligned} \tag{5.12}$$

The factor $1/2$ enters to correct for double counting the interactions while summing over all species A and B. This means that the interactions between species A and B are effectively locally averaged over both species. However, one can also perform the double sum $\frac{1}{2} \sum_A \sum_B$ as $\sum_A \sum_{B>A}$, using the property that $\phi_A(z) \langle \phi_B(z) \rangle = \phi_B(z) \langle \phi_A(z) \rangle$ when summing over all layers. In this way the interactions are assigned to only one of the species. Although both ways of counting the interactions yield the same grand potential, the excess pressure profile $p^\beta - p_T(z)$ is locally different. Still other schemes to calculate the double sum can be thought of, each yielding the same grand potential but different excess pressure profiles. Consequently, like it has been shown in chapter 3, the local pressure is ambiguous although it yields a unequivocal value for the grand potential.

5.3. BENDING A BILAYER

5.3.1. Thermodynamics of bilayer membranes

As outlined in section 5.1, the rigidity of a bilayer determines the phase behaviour of bilayer membranes to some extent. The Helfrich constants can be derived from the curvature dependence of the interfacial tension, as expressed in the Helfrich equation, eqn (4.13) [19]. Thermodynamically the interfacial tension follows from (*cf.* eqn (2.19))

$$\Omega + p^\beta V = -\Delta p V^\alpha + \gamma_G A \tag{5.13}$$

where A is the area of the bilayer and V^α the volume enclosed by the membrane. Since the inner bulk phase α, enclosed by the bilayer, is identical to the continuous outer phase β, there is no Laplace pressure drop, i.e., $\Delta p = 0$. An equilibrium system of membranes that forms spontaneously from the surfactant solution can adapt its own number of bilayers with the corresponding interfacial area A. Consequently, as outlined in section 2.6, it follows from the thermodynamics of small systems that for

an equilibrium bilayer membrane (*cf.* eqn (2.72), eqn (2.73), and eqn (2.69))

$$\Omega + p^\beta V = \varepsilon = \gamma_G A = 0$$

Consequently, if the translational entropy of the membrane is neglected, the equilibrium bilayer is tensionless, i.e. $\gamma_G = 0$ [18]. Moreover, it is easily seen from symmetry considerations that the equilibrium membrane has on average a planar geometry [20], i.e., $J_0 = 0$. In conjunction with the previously found result that the equilibrium membrane is tensionless, neglecting the translational entropy of the membrane, the Helfrich equation eqn (4.13) reduces to

$$\frac{\Omega + p^\beta V}{A} = \gamma_G = \frac{1}{2} k_c J^2 + \overline{k} K \tag{5.14}$$

where J and K are the total and Gaussian curvature, respectively.

5.3.2. Mechanics of bilayer membranes

It has been shown in section 4.1.2 that the Helfrich constants can also be obtained mechanically, i.e. in terms of the (excess) pressure profile. The bending modulus k_c and spontaneous curvature J_0 can be found directly from the cylindrical bilayer. The saddle-splay modulus $\overline{k}$ can only be determined from comparison of the bending modulus and the effective modulus of the spherical vesicle (*cf.* eqn (4.15))

$$-k_c J_0 = \mathbb{P}_1^{c,0} + \left(\frac{\partial \mathbb{P}_0^c}{\partial J}\right)_T^0 \tag{5.15a}$$

$$k_c = 2\left(\frac{\partial \mathbb{P}_1^c}{\partial J}\right)_T + \left(\frac{\partial^2 \mathbb{P}_0^c}{\partial J^2}\right)_T^0 \tag{5.15b}$$

$$k_c + \frac{1}{2}\overline{k} = 2\left(\frac{\partial \mathbb{P}_1^s}{\partial J}\right)_T + \left(\frac{\partial^2 \mathbb{P}_0^s}{\partial J^2}\right)_T^0 + \frac{1}{2}\mathbb{P}_2^{s,0} \tag{5.15c}$$

where the superscripts ^{c} and ^{s} refer to evaluation at the cylindrical and spherical interface, respectively. As it follows from appendix 3.D.2, for the lattice model the bending moments are given by

$$\mathbb{P}_0 = \Delta p R_s + \sum_{z=1}^{M} (p^\beta - p_T(z)) \tag{5.16a}$$

$$\mathbb{P}_1 = -\frac{1}{2}\Delta p R_s^2 + \sum_{z=1}^{M} \left(z - R_s - \frac{1}{2}\right)(p^\beta - p_T(z)) \tag{5.16b}$$

$$\mathbb{P}_2 = \frac{1}{3}\Delta p R_s^3 + \sum_{z=1}^{M} \left((z - R_s)^2 - (z - R_s - \frac{1}{3})\right)(p^\beta - p_T(z)) \tag{5.16c}$$

where the excess pressure profile $p^\beta - p_T(z)$ is given by eqn (5.12). Using the fact that there is no Laplace pressure difference, all first terms on the right-hand side of eqn (5.16) vanish for bilayer membranes.

5.3.3. Results for $C_{12}E_5$ in water

Using the lattice model, the $C_{12}E_5$ surfactants will be modelled as the chain molecule $C_{12}O(C_2O)_5$. Here, C stand for CH_2 or CH_3 groups, which will not be discriminated, and O mimics the oxygen or hydroxyl groups in the surfactant. The water molecules will be modelled by a simple monomer solvent W. Obviously, this is a poor model for water but can be improved by accounting the orientation-dependent interactions [21]. Given the three monomer types C, O, and W, three exchange parameters χ_{CO}, χ_{CW}, and χ_{OW} need to be specified. Indicating that the interactions with the C group are hydrophobic, the exchange parameters are positive and are taken to be constant $\chi_{CO} = \chi_{CW} = 1.6$ [22–25]. However, owing to the hydration of the hydrophilic O groups by the water molecules, χ_{OW} is more strongly temperature dependent. Consequently, varying χ_{OW} may be regarded as changing the temperature. Moreover, an FCC lattice type will be used, i.e. $\lambda_0 = \lambda_1 = 1/3$. As shown in appendix 4.A, this lattice type in conjunction with the relatively low exchange parameters χ, suppresses the lattice artefact.

In order the determine the interfacial tension from the bending moments, eqn (5.16) (*cf.* eqn (2.49)), the position of the dividing plane R_s remains to be defined. Although both the inner and outer radius of the bilayer are possible choices, the dividing plane is here found from

$$\sum_{z=1}^{M} (z - R_s) \left(\phi_s(z) - \phi_s^\beta\right) = 0 \tag{5.17}$$

where $\phi_s = \phi_C + \phi_O$ is the total surfactant volume fraction. The volume fraction profiles $\phi_C(z)$, $\phi_O(z)$, and $\phi_W(z)$ are illustrated in figure 5.1a for a cylindrical vesicle, where $\chi_{OW} = -0.5$ and the centre of the vesicle is located at $z = 0$. Using eqn (5.17), the dividing plane is located in the middle of the membrane. The contributions to the C groups come from both the headgroups and the tails and are distributed over the complete bilayer. However, the O segments of the headgroups prefer the exterior of the vesicle but are relatively diffusively distributed because they are bound to the hydrophobic C groups. Furthermore, the vesicle is asymmetric due to the curvature; the O groups are slightly more densely packed inside the vesicle ($z < R_s$) than the groups on the outside. This forces the tails outwards, hence the maximum of the C groups is found for $z > R_s$. Note the relatively large penetration of the monomeric water in the centre of the membrane due to the lack of specific interactions.

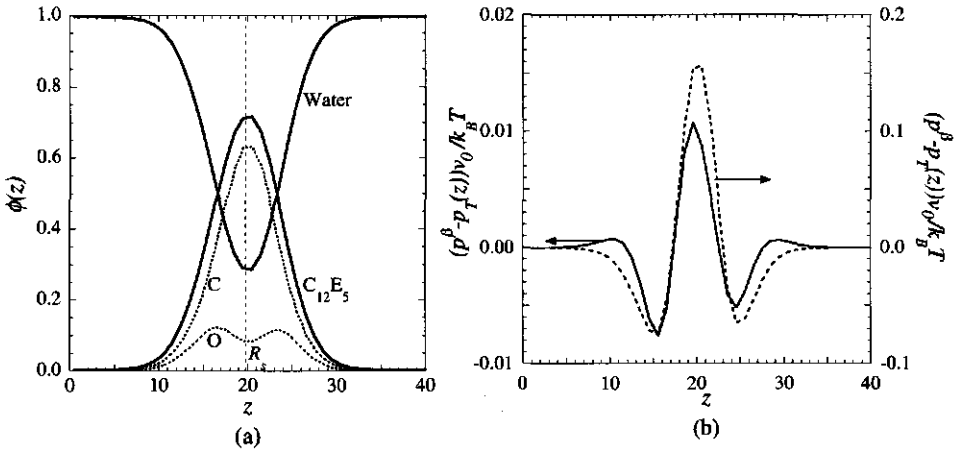

FIGURE 5.1. (a) Volume fraction profiles of a cylindrical $C_{12}E_5$ vesicle in water. The surfactant $C_{12}E_5$ is modelled as $C_{12}O(C_2O)_5$, where the C represents CH_2 or CH_3 groups and the O mimics the O or OH groups. Water has been treated as a monomer with orientation-independent interactions. A lattice of 40 layers has been used with $\lambda_0 = 1/3$, $\chi_{CW} = \chi_{CO} = 1.6$, and $\chi_{OW} = -0.5$. The dividing plane at R_s is chosen to be in the middle of the bilayer, whereas the centre of the vesicle is located at $z = 0$. (b) The tangential excess pressure profile corresponding to the density profiles as given in (a) can be determined in various ways yielding the same grand potential. The excess pressure represented by the solid line (left vertical axis) effectively averages the interactions over adjacent layers, whereas the dashed line (right vertical axis) gives the excess pressure where the interactions with adjacent layers is assigned to either one of the layers. Note that the scales differ one order of magnitude.

Given the volume fractions, the excess profile can be determined from eqn (5.12). As stated, several ways to perform the double sum counting the interactions can be considered. Note the different features of the two examples given in figure 5.1b. For instance, the two examples differ one order of magnitude and the pressure given by the solid line has three maxima whereas the one given by the dashed line only one. Nevertheless, both excess pressure profiles are slightly more tensile, i.e. negative, inside the vesicle than outside due to the curvature. The tensile parts are needed to compensate for the compressive, i.e. positive, parts resulting in the typical small interfacial tension, as discussed in section 3.3.

With the above set of parameters, eqn (5.12), and eqn (5.14), the Helfrich constants can be determined from the curvature dependence of the interfacial tension as a function

of the hydrophilicity χ_{OW} of the headgroup. The curvature of a bilayer is varied by changing the number of surfactants in the system. Given the number of surfactants, n_i, the constrained equilibrium density profiles are found from eqn (5.10), using the first normalization factor of eqn (5.11). The equilibrium is constrained since the bilayer is forced into a curved, rather than a planar, geometry which was shown to be the global equilibrium geometry. The resulting interfacial tensions are displayed by the symbols in figure 5.2a for both a spherical and cylindrical geometry as a function of the curvature taking $\chi_{OW} = -0.5$. A direct fit to the interfacial tension with a second order polynomial, shown by the solid lines, yields according to eqn (5.14) the Helfrich constants. However, according to eqn (5.14), the Helfrich constants can also be found from a linear fit to

$$\frac{\Omega + p^{\beta}V}{JA} = \frac{\gamma_G}{J} = \begin{cases} \frac{1}{2}k_c\frac{1}{R_s} & \text{cylinders} \\ \left(k_c + \frac{1}{2}\overline{k}\right)\frac{1}{R_s} & \text{spheres} \end{cases} \tag{5.18}$$

The fit to eqn (5.18) is shown in figure 5.2b for the same data. Using both the fit to γ_G and $(\Omega + p^{\beta}V)/JA$ gives information about the accuracy of the fits. Deviations may occur for two reasons. First, the calculated interfacial tensions are subject to lattice artefacts. As can be seen from the magnifications in figure 5.2, the deviations from the fits are relatively small as expected for the given set of parameters. Second, the Helfrich equation is strictly only valid for $J \to 0$. However, as can most easily be seen from figure 5.2b, the description remains appropriate for relatively large curvatures. Consequently, the curvature energy, $(\partial^2\gamma_G/\partial J^2)_T$, is hardly dependent on the curvature. This explains why vesicles, although not the equilibrium structure of the bilayer membranes, are relatively stable; the system can hardly change its free energy by growing or shrinking the vesicles. The system can only lower its free energy by fusing vesicles, which is an activated process. The average Helfrich constants derived from figure 5.2, read $k_c = 1.645 \pm 0.002$ and $\overline{k} = -2.236 \pm 0.002$. Apparently, the errors are relatively small. Since they are of a total different origin, it is not likely that the two different types of errors cancel each other.

The Helfrich constants can also be determined mechanically, as given by eqn (5.15). The derivatives in eqn (5.15) are subsequently determined from a second order polynomial and linear fit to the zeroth and first bending moment respectively. Although the results are independent of the choice of the pressure profile, one may prefer a certain choice for favourable numerical accuracy. As can be seen from figure 5.3 for $\chi_{OW} = -0.5$ these fits are fairly accurate and are hardly subject to lattice artefacts. Moreover, $\mathbb{P}_0^{s,0} = \mathbb{P}_0^{c,0} = 0$ recovers the fact that the planar interface is tensionless by

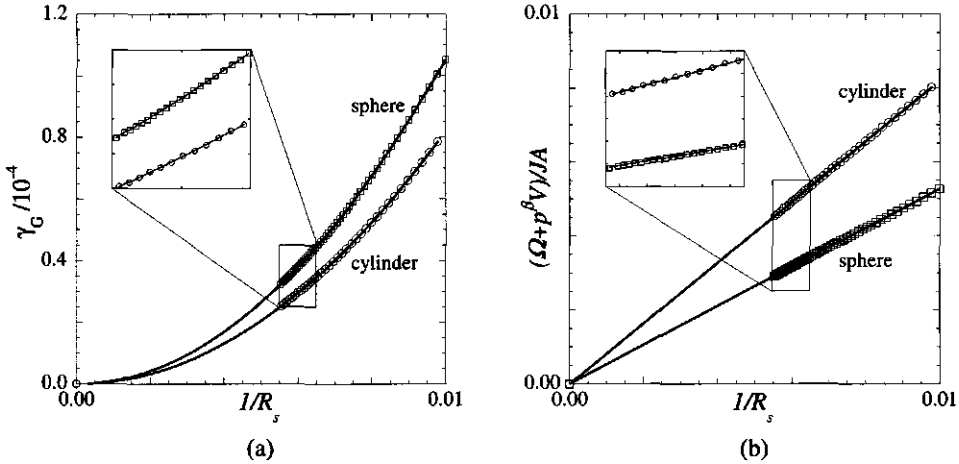

FIGURE 5.2. (a) The interfacial tension of $C_{12}E_5$ bilayer membranes in water as a function of the curvature, with $\lambda_0 = 1/3$, $\chi_{CW} = \chi_{CO} = 1.6$, and $\chi_{OW} = -0.5$. The position of the dividing plane is given by eqn (5.17). The squares apply to a spherical vesicle, whereas the circles give the calculated values for a cylindrical geometry. The solid lines are a second order polynomial fit to the points. (b) The linearized interfacial tension as given by eqn (5.18) as a function of the curvature. The solid lines are linear fits to the calculated points. The magnifications show that the calculated values are subject to a relatively small lattice artefact.

neglecting the translational entropy (*cf.* eqn (2.49)). Since the planar bilayer is completely symmetrical with respect to its centre (*cf.* eqn (5.17)), it is found indeed that $\mathbb{P}_1^{s,0} = \mathbb{P}_1^{c,0} = 0$. Furthermore, it is found that for the system as shown in figure 5.3 $\mathbb{P}_2^{s,0} = \mathbb{P}_2^{c,0} = -21.536$.

From the fits to the bending moments in figure 5.2, using eqn (5.15), it is found that $J_0 = 0.00$, $k_c = 1.61$, and $\overline{k} = -2.11$. The exact error in these values is unknown; the accuracy of the fits is hard to determine and the sum of the respective derivatives typically yields a number that is one order of magnitude smaller than the individual values. Otherwise stated, the discrepancies between the values for the Helfrich constants determined from the direct fit to the interfacial tension and those determined from the bending moments are due to numerical errors.

The above procedure has been repeated for several values of χ_{OW}. The results for the bending modulus and saddle-splay modulus are shown in figure 5.4. The solid lines connect the symbols calculated from the direct fits to the interfacial tension. The error bars are smaller than the symbols. The dotted lines connect the symbols

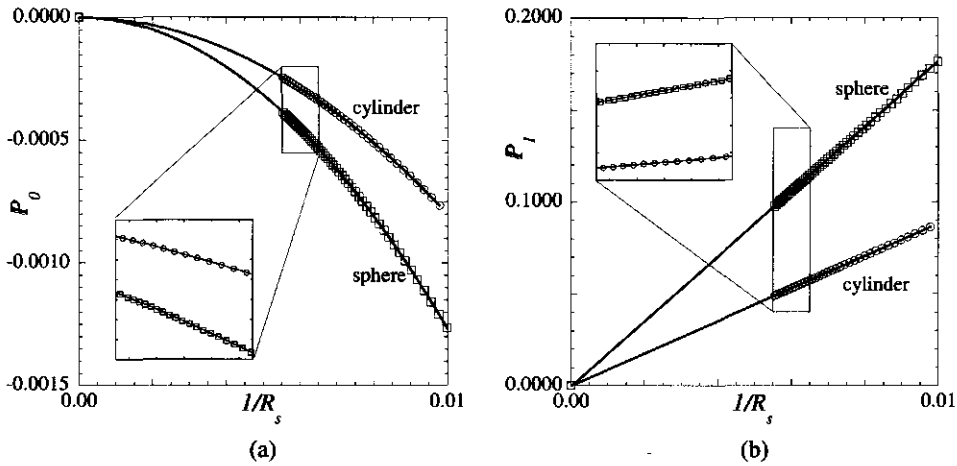

FIGURE 5.3. (a) The zeroth bending moment of $C_{12}E_5$ bilayer membranes in water as a function of the curvature, with $\lambda_0 = 1/3$, $\chi_{CW} = \chi_{CO} = 1.6$, and $\chi_{OW} = -0.5$. The position of the dividing plane is given by eqn (5.17). The squares refer to a spherical vesicle, whereas the circles give the calculated values for a cylindrical geometry. The solid lines are a second order polynomial fit to the points. The graph recovers the analytical result that the planar membrane is tensionless; $\gamma^0 = \mathbb{P}_0^0 = 0$. (b) The first bending moment as a function of the curvature. The solid lines are linear fits to the calculated points. As expected from symmetry considerations, $\mathbb{P}_1^0 = 0$. The magnifications show that the calculated values are subject to a relatively small lattice artefact.

determined mechanically from the bending moments. There appears to be a constant, minor deviations between the mechanically determined Helfrich constants and those determined from the fit to γ_G. This is due to the fact that the error in the fits to the bending moments is systematic. This apparently leads to the conclusion that the value for the mechanically determined bending modulus is always too low. Consequently, since the sum must yield the same interfacial tensions as those from the direct fit to γ_G, the saddle-splay modulus from the bending moments is always overestimated.

5.4. DISCUSSION

Consistent Helfrich constants have been determined from both a thermodynamic and mechanical route as a function of the hydrophilicity of the headgroup. Different regions may be distinguished in figure 5.4. For $\chi_{OW} \lesssim -0.8$ the value of k_c is almost constant and relatively high. Owing to the relatively good solubility of the O groups, the headgroups are well hydrated. Consequently, the hydrophobic tails of the surfactants

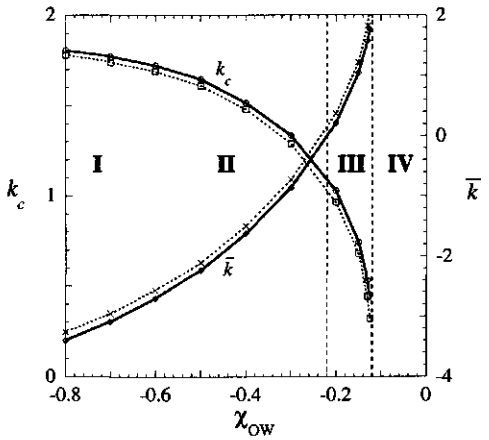

FIGURE 5.4. The bending modulus and saddle-splay modulus for a $C_{12}E_5$ bilayer membrane as a function of the hydrophilicity of the headgroup with $\chi_{CO} = \chi_{CW} = 1.6$, $\lambda_0 = 1/3$. The dividing plane is chosen to be in the middle of the membrane, using eqn (5.17). The roman numbers indicate different phase regions.

are forced more inwards into the bilayer, as outlined in section 5.1. As a result, the membrane remains relatively rigid.

Going through the range $-0.8 \lesssim \chi_{OW} \leq -0.22$, the hydrophilicity decreases such that the headgroups can dissolve easier in the hydrophobic core of the membrane, making the membrane less rigid. Consequently, the values of the bending modulus decreases. Hence, the undulations increase with increasing χ_{OW}. As can be seen from eqn (5.1), the repulsive forces in the system increase, which makes the spacing r between bilayer sheets larger. The correlates well with the experimental finding that the so-called L_α phase swell with increasing T [9, 10].

For $-0.22 < \chi_{OW} < -0.12$ the saddle-splay modulus becomes positive, which favours the formation of saddle planes. Consequently, although the low value of the bending modulus gives rise to a large repulsive force between the membrane sheets, connecting handles are formed between the bilayers. This may explain the experimentally observed L_3 or sponge phase at relatively high temperature [9].

If $\chi_{OW} \geq -0.12$, the bending modulus tends to become negative and, like the saddle-splay modulus, even seems to diverge. This implies that the bilayer membranes are no longer stable. Moreover, the solubility of the headgroup has become that low, that the system will phase-separate into an aqueous and a surfactant rich phase. Since the O and C groups still repel each other, the surfactant molecules tend to form inverted

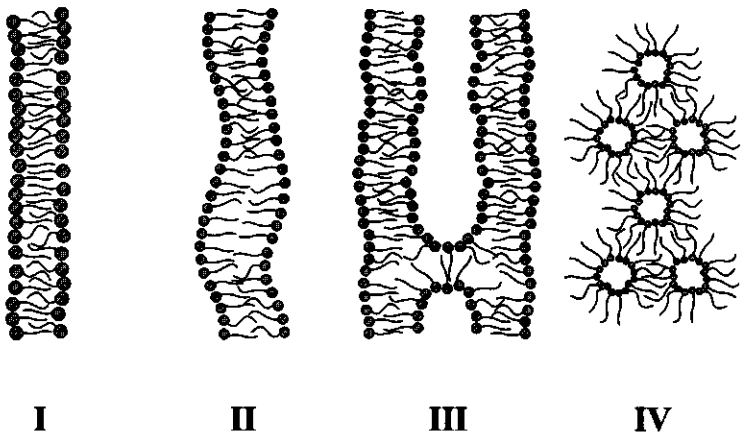

FIGURE 5.5. Different phases can be obeserved from the calculations for $C_{12}E_5$ vesicles. I. For $\chi_{OW} \lesssim -0.8$ the $C_{12}E_5$ membranes are relatively rigid. II. For $-0.8 \lesssim \chi_{OW} \leq -0.22$ k_c decreases, causing the bilayer to be less stiff and yields an increasing spacing between the membranes. III. For $-0.22 < \chi_{OW} < -0.12$ $\overline{k}$ becomes positive which favours the formation of connecting handles between the bilayers. IV. If $\chi_{OW} \geq -0.12$ the headgroups are not hydrophilic enough, such that the bilayers are instable and the surfactants phase separates into a phase of inverted micelles.

micelles in which small amounts of water are dissolved. Such phases have indeed been observed experimentally at high temperatures [9].

The described phase behaviour is summarized and illustrated schematically in figure 5.5 for the regions indicated in figure 5.4. Since all these phases have been observed experimentally for the $C_{12}E_5$ surfactant system in water [9, 10], it is concluded that the lattice model is suitable for studying the phase behaviour of surfactant systems. Already with a restricted set of parameters, the basic experimental features of the phase diagram can be recovered. In order to do so, vesicles were forced into a cylindrical and spherical geometry, thus neglecting the end-cap energy and translation entropy of the actual bilayer membranes. From these vesicles two independent fits to the interfacial tension yield consistent values for the Helfrich constants of the surfactant bilayer membrane as a function of the hydrophilicity of the headgroup. The values are recovered with less numerical accuracy from the mechanical expressions for the Helfrich constants. Consequently, a direct fit to the interfacial tension suffices for future studies.

From the sign and magnitude of the bending and saddle-splay modulus one can determine in what phase the surfactant layer prefers to be when the geometry restrictions are

relaxed. Hence, minimal surfaces may be studied from cylindrical and spherical interfaces only. Nevertheless, the balance between attractive and repulsive forces accounting for the translational entropy of the bilayers upon actual inclusion of multiple membrane sheets in the calculations remains of interest. Incorporation of the influence of charges in ionic surfactant systems [26] and the role of, e.g., a co-surfactant or co-solvent on the phase behaviour of surfactant layers are also challenges for future study. Moreover, the phase behaviour of surfactant monolayers, like e.g. in microemulsions [27], as a function of the aforementioned parameters deserves profound attention.

It has been argued that the bending route to the Helfrich constants, as elaborated here, may lead to different Helfrich constants and, by that, different phase behaviour as compared to the fluctuation route [28]. This may be due to the fact that the undulations on the interface of the vesicle are subject to boundary conditions which makes the number of waves quantized (*cf.* the 'particle in a box' from quantum mechanics). This restriction introduces another entropic term that is not accounted for in the above route to the Helfrich constants [29, 30]. It is also of interest to study the influence of this kind of entropy on the differences in Helfrich constants.

In the model for surfactant bilayers presented in this chapter, contributions of lattice artefact have shown to be negligible. However, in the previously recommended systems, this artefact may need attention. In the case of microemulsions, the amount of oil may be adjusted until the pressure difference due to the artefact is eliminated, like it has been done for the liquid-vapour interface (*cf.* appendix 4.A). Since the enclosed phase equals the outer phase, this method is not applicable to vesicle systems. In a previous study [18], the number of surfactants of a vesicle system had been adjusted until $\mathbb{P}_0 = 0$. As it can be seen from eqn (5.15), this implies that $\overline{k} = \mathbb{P}_2^0$, as had been found indeed. However, the condition $\gamma_G = \mathbb{P}_0 = 0$ only holds for the planar equilibrium membrane. This method eliminated thus the artefact by introducing one. Consequently, at present there is no longer a condition available to warrant artefact-free vesicles. Since the sign and the order of magnitude rather than the exact value of the Helfrich constants determines the phase behaviour, the lattice model may prove to be a very valuable tool for the study of surfactant systems.

REFERENCES

[1] D.F. Evans and H. Wennerström. *The Colloidal Domain: where physics, chemistry, biology and technology meet.* VCH Publishers, 1994.

[2] J. Israelachvili. *Intermolecular and Surface Forces.* Academic Press, 2nd edition, 1991.

[3] S.A. Safran. Statistical thermodynamics of surfaces, interfaces, and membranes. In D. Pines, editor, *Frontiers in Physics*, volume 90. Addison-Wesley, 1994.

[4] W. Helfrich. *Z. Naturforsch.*, 33a:305, 1978.

[5] D. Sornette and N. Ostrowsky. Lamellar phases: Effect of fluctuations (theory). In W.M. Gelbart, A. Ben-Shaul, and D. Roux, editors, *Micelles, Membranes, Microemulsions and Monolayers.* Springer-Verlag, 1994.

[6] W. Helfrich. Elasticity and thermal undulations of fluid films of amphiphiles. In J. Charvolin, J.F. Joanny, and J. Zinn-Justin, editors, *Liquids at Interfaces*, volume XLVIII. Les Houches, Elsevier, 1990.

[7] S. Hyde, S. Andersson, K. Larsson, Z. Blum, T. Landh, S. Lidin, and B.W. Ninham. *The Language of Shape: the role of curvature in condensed matter physics, chemistry and biology.* Elsevier, 1997.

[8] D.C. Morse. *Curr. Opin. Colloid Interface Sci.*, 2:365, 1997.

[9] R. Strey, R. Schomäcker, D. Roux, F. Nallet, and U. Olsson. *J. Chem. Soc. Faraday Trans.*, 86:2253, 1990.

[10] D.J. Mitchell, G.J.T. Tiddy, L. Waring, T. Bostock, and M.P. McDonald. *J. Chem. Soc. Faraday Trans. 1*, 79:975, 1983.

[11] H. Risken. *The Fokker-Planck Equation: Methods of Solution and Applications.* Springer, 2nd edition, 1989.

[12] J. Lyklema. *Fundamentals of Interface and Colloid Science*, volume I. Academic Press, 1991.

[13] P.M. Chaikin and T.C. Lubensky. *Principles of Condensed Matter Physics.* Cambridge University Press, 1995.

[14] J.K.G. Dhont. An introduction to dynamics of colloids. In D. Möbius and R. Miller, editors, *Studies in Interface Science*, volume 2. Elsevier Science, 1996.

[15] I. Szleifer and M.A. Carignano. In I. Prigogine and S.A. Rice, editors, *Advances in Chemical Physics*, volume XCIV, page 165. John Wiley and Sons, 1996.

[16] A.D. Mackie, A.Z. Panagiotopoulos, and I. Szleifer. *Langmuir*, 13:5022, 1997.

[17] O.A. Evers, J.M.H.M. Scheutjens, and G.J. Fleer. *Macromolecules*, 23:5221, 1990.

[18] P.A. Barneveld, J.M.H.M. Scheutjens, and J. Lyklema. *Langmuir*, 8:3122, 1992.

[19] W. Helfrich. *Z. Naturforsch*, 28c:693, 1973.

[20] D. Roux, C.R. Safinya, and F. Nallet. Lyotropic lamellar L_α phases. In W.M. Gelbart, A. Ben-Shaul, and D. Roux, editors, *Micelles, Membranes, Microemulsions and Monolayers.* Springer-Verlag, 1994.

[21] N.A.M. Besseling and J. Lyklema. *J. Phys. Chem.*, 98:610, 1994.

[22] P.L. Privalov and J.G. Stanley. *Pure Appl. Chem.*, 61:1097, 1989.

[23] C. Tanford. *The Hydrophobic Effect: Formation of Micelles and Biological Membranes.* Wiley, 1980.

[24] N.A.M. Besseling and J. Lyklema. *J. Phys. Chem. B*, 101:7604, 1997.

[25] F.A.M. Leermakers and J.M.H.M. Scheutjens. *J. Colloid Interface Sci.*, 136:231, 1990.

[26] P.A. Barneveld, D.E. Hesseling, F.A.M. Leermakers, J. Lyklema, and J.M.H.M. Scheutjens. *Langmuir*, 10:1084, 1994.

[27] F.A.M. Leermakers, J. van Noort, S.M. Oversteegen, P.A. Barneveld, and J. Lyklema. *Faraday Discuss.*, 104:317, 1996.

[28] E.M. Blokhuis, J. Groenewold, and D. Bedeaux. *Mol. Phys.*, 96:397, 1999.

[29] W.K. Kegel and H. Reiss. *Ber. Bunsenges. Phys. Chem.*, 100:300, 1996.

[30] W.K. Kegel and H. Reiss. *Ber. Bunsenges. Phys. Chem.*, 101:1963, 1997.

APPENDIX A

List of Symbols

TABLE A.1. Latin symbols

A	interfacial area
a	effective headgroup area of surfactant
a_0	unit area of a lattice site
$\mathbb{C}_1$	bending stress
$\mathbb{C}_2$	torsion stress
$\mathbb{C}_x$, $\mathbb{C}_y$	curvature coefficients
c_1, c_2	principal curvature
F	Helmholtz energy
f	Helmholtz energy per unit volume
$\vec{f}_i$	net force acting on particle i
$\vec{f}_{ij}$	force interacting between particles i and j
G	Gibbs energy
$h(x,y)$	height profile of interface
h	length of cylindrical lattice
J	total curvature
$\mathcal{J}$	extensive total curvature
J_0	spontaneous curvature
K	Gaussian curvature
$\mathcal{K}$	extensive Gaussian curvature
$\overline{k}$	saddle-splay modulus
k_B	Boltzmann's constant
k_c	bending modulus
$L(z)$	number of sites in lattice layer z
ℓ	characteristic size in a lattice
M	number of lattice layers
m_i	mass of particle i
N	total number of particles

N_i	chain length of molecules of type i
$\mathcal{N}$	number of small systems
$\hat{n}$	normal vector at interface
n_i	number of particles of component i
P	van der Waals pressure
$\mathbf{P}$	pressure tensor
$\mathbb{P}_0$	zeroth bending moment
$\mathbb{P}_1$	first bending moment
$\mathbb{P}_2$	second bending moment
p	bulk pressure
p	reduced van der Waals pressure
$p_N(\vec{r})$	normal pressure at position $\vec{r}$
$p_T(\vec{r})$	tangential pressure at position $\vec{r}$
Δp	Laplace pressure difference
q	heat
R_s	position of the interface
$\vec{r}_i$	position of particle i
$\vec{r}_{ij}$	path between particle i and j
S	entropy
s	entropy per unit area
T	temperature
t	reduced temperature
U	internal energy
u_A	energy encountered by a segment of type A
V	volume
V_m	molar volume
v	effective length of surfactant
v	reduced molar volume
v_0	unit volume of a lattice site
w	work done on the system
$\vec{v}_i$	velocity of particle i
Z	coordination number

z	lattice layer index
z	radial distance from the interface
z_{Gibbs}	position of Gibbs dividing plane in a planar interface
z_s	position of surface of tension in a planar interface

Table A.2. Greek symbols

Γ_i	adsorbed amount of type i
γ_{BN}	interfacial tension according to Boruvka and Neumann
γ_G	interfacial tension according to Gibbs
Δ	degeneracy
δ	Tolman length
$\delta(R)$	Dirac delta function
$\delta_{i,j}$	Kronecker delta function
ε	subdivision potential
$\theta(R)$	Heaviside step function
$\lambda_i(z)$	transition probability to go to layer $z+i$
μ_i	chemical potential of component i
ν_{ij}	interaction energy between species i and j
ξ	bulk correlation length
ρ	bulk density
$\rho(\vec{r})$	continuous density at position $\vec{r}$
ϕ	volume fraction in bulk
$\phi_i(z)$	volume fraction of i in layer z
$\varphi^0(z)$	density profile of the planar interface
φ_m	volume fraction of small systems
χ_{ij}	exchange interaction energy between species i and j
Ω	grand potential

TABLE A.3. Notations

$\bar{\mathrm{d}}$	inexact differential
^{0}	evaluated at the planar interface
$_c$	value in critical point
^{int}	contribution of interactions
^{k}	kinetic contribution
^{s}	with respect to the interface
$_s$	with respect to the surface of tension
$_t$	total over all small systems
$^{b,\alpha,\beta}$	with respect to the mentioned bulk phases
$^\nu$	based on interaction energies
$^\chi$	based on exchange energies
$\hat{}$	unit vector
$[\ldots]$	virtual displacement
$\langle\ldots\rangle$	ensemble average
$\langle\ldots\rangle$	contact fraction

Summary

Although relatively much is known about the physics of curved interfaces, several models for these kind of systems seem conflicting or internally inconsistent. It is the aim of this thesis to derive a rigorous framework of thermodynamic and mechanical expressions and study their relation to previous models.

In chapter 2 interfaces are described mathematically. It turns out that their curvatures can generally be determined by two independent coefficients, *viz.* the total curvature J and the Gaussian curvature K. These degrees of freedom of a system must be accounted for in the thermodynamic expression for the internal energy and are conjugated to the bending stress $\mathbb{C}_1$ and torsion stress $\mathbb{C}_2$, respectively. The curvatures can then be taken as intensive variables, as has been done by Gibbs, or as extensive variables, as proposed by Boruvka and Neumann. The two ways of accounting for curvature leads to different definitions of the interfacial tension, which are referred to as γ_G and γ_{BN}, respectively. In the former way the curvatures can be fixed when changing the interfacial area A, whereas in the latter the area times the curvature must be constant upon variation of the interfacial area. Consequently, the interfacial tension according to Boruvka and Neumann incorporates bending as well as stretching work. Hence, for homogeneously curved interfaces, the difference between γ_G and γ_{BN} is the bending work.

It follows from a quasi-thermodynamic description that the interfacial work according to Gibbs, $\gamma_G A$, can be described mechanically as the volume integral of the excess pressure profile. Writing the volume element in terms of the curvatures, γ_G can be expressed in terms of the zeroth, first, and second bending moments $\mathbb{P}_0$, $\mathbb{P}_1$, and $\mathbb{P}_2$, respectively. Using their thermodynamic definitions, the bending and torsion stress can also be given mechanically, i.e., in terms of the excess pressure profile. Subsequently, using the relation between γ_G and γ_{BN}, the interfacial tension according to Boruvka and Neumann is expressed in terms of the bending moments. The newly derived equations differ significantly from those known in the literature. However, it is shown that the Laplace equations of capillarity derived from either the thermodynamic or the mechanical route are consistent.

The mechanical and thermodynamic notion of 'pressure' are scrutinized in chapter 3. The mechanical or virial route to the pressure is reviewed as a result of the forces exerted

by the momenta and interactions of the particles per unit area. The mechanical pressure turns out to be a tensor quantity and is used to recover results known in the literature. Since the interactions cannot be assigned unambiguously to one position in space, the local pressure is found to be equivocal.

A lattice model allowing spatial gradients is elaborated. The grand potential density of a system, which is the work of changing the volume of the system reversibly, is identified as the scalar thermodynamic pressure. For a bulk system, the grand potential density recovers the Kamerlingh-Onnes virial expansion of the pressure and has the same features as the reduced van der Waals pressure. Moreover, it has been shown that in the continuous limit the Helmholtz energy of the lattice gas can be written as the Landau expression for the free energy. For an inhomogeneous system of monomers, pressure profiles are found from the grand potential density that have similar features as those found from the virial route. That is, in the vicinity of an interface both tensile and compressive regions are observed. In the model by Szleifer *et al.* the tensile, i.e., negative region of the locale pressure is omitted. Since that region may be necessary to obtain low interfacial tensions for some systems, an important feature of their 'pressure' has been ignored. Since the reference state of the energy of the lattice model can be chosen freely, it is concluded that the thermodynamic pressure can neither be given unambiguously.

The bending and torsion stress of a monomer liquid-vapour interface are determined from their mechanical expressions using two definitions of the local pressure. The expressions as derived in chapter 2 turn out to give unique consistent results, whereas the expressions known in the literature give ambiguous outcomes for the thermodynamically well-defined parameters. The latter is physically unacceptable. Since, unlike the virial route to the pressure, the thermodynamic pressure of the lattice model yields by definition a unique expression for the grand potential, it is concluded that this lattice model is a useful tool to model curved interfaces.

A phenomenological description of the curvature dependence of the interfacial tension is given in chapter 4. Up to first order in the curvature, the change of the interfacial tension is determined by the Tolman length. A second order description is given by the Helfrich equation, which, in turn, is determined by the bending modulus, k_c, and the saddle-splay modulus $\overline{k}$. These Helfrich constants turn out to be the (derivatives of the) bending and torsion stresses of the planar interface, respectively. As a consequence of the different mechanical expressions for $\mathbb{C}_1$ and $\mathbb{C}_2$, the Helfrich constants cannot be obtained from the properties of the planar interface only but also require the curvature dependence of the bending moments. This difference with the equations known in the

literature can be traced back to the difference of the definition of the pressure from either a virial or thermodynamic route. It is shown that for a simple liquid-vapour interface the extra terms are needed when the pressure is found from the grand potential density. Only then are the Tolman length and the mechanically obtained Helfrich constants consistent with a parabolic fit to the interfacial tension.

The Helfrich constants of the simple liquid-vapour interface can be determined as a function of the intermolecular interactions. It is shown that a van der Waals density functional theory and its asymptotic expressions reproduce the Helfrich constants found from the lattice model in the vicinity of the critical point. Away from the critical point the square gradient of the van der Waals theory is not sufficient to account for the changes in the density profile across the interfacial region.

The phase behaviour of a bilayer membrane is considered in chapter 5. In order to model surfactants, the lattice gas model is extended to chain molecules. It is thought that each segment of the chain emerges from its predecessor such that the end of the chain can be considered as a diffusing particle obeying the Fokker-Planck equation. The grand potential density is again identified as an (ambiguous) local pressure. By choosing proper interactions, the formation of surfactant vesicles can be modelled.

For this study, the non-ionic surfactant $C_{12}E_5$ is modelled. The interfacial tension of the vesicle is determined as a function of its radius. The resulting Helfrich constants determined both mechanically and from a parabolic fit to the interfacial tension are consistent. Keeping the hydrophobicity of the tail group constant, the Helfrich constants of the vesicle are obtained as a function of the hydrophilicity of the head group. It is found that for very hydrophilic head groups the bending modulus has an almost constant positive value, whereas the saddle-splay modulus is negative. This is thus interpreted that the membranes are relatively rigid. When the hydrophilicity decreases, the bending modulus becomes less positive and the saddle-splay modulus less negative. This renders less rigid bilayers, allowing large collective fluctuations, i.e. undulations, of the membranes. Hence, owing to steric hindrance, the spacing between a set of bilayers increases with decreasing hydrophilicity. For moderate hydrophilicity, the bending modulus is decreasingly positive. However, the saddle-splay modulus becomes positive which favours the formation of handles between the undulating bilayers. When the hydrophilicity is relatively low, the Helfrich constants seem to diverge because the head groups do not longer hydrated and the system phase-separates into surfactant and solvent rich phases. Since all these phases have been observed experimentally, it is concluded that the lattice model is a potentially valuable tool to study surfactant systems.

Samenvatting

Gekromde oppervlakken zijn fascinerend. Niet voor niets trekken vele Nederlanders tijdens hun vakanties de bergen in, of komen veel buitenlanders naar het 'vlakke land' voor onze duinen (om daar kuilen te graven). Ook op kleinere lengteschaal beheersen gekromde oppervlakken het dagelijks leven; een rimpelloze watervlakte of anders dan ronde regendruppels of hagelstenen zullen erg verrassend zijn. Op een nog kleinere lengteschaal, niet of nauwelijks met het blote oog waarneembaar, zijn gekromde oppervlakken eveneens overal aanwezig. Zo is in melk het vet als minuscule druppeltjes aanwezig, kunnen wasmiddelen vuil insluiten en zijn lichaamscellen vaak nagenoeg gesloten, ronde eenheden. Het zijn met name deze 'toepassingen' die een studie naar gekromde oppervlakken interessant maken. Hoe kan het dat gesmolten melkvet niet zomaar als druppeltjes in water kan oplossen? Aan welke eisen moet een wasmiddel voldoen om verschillende soorten vuil goed in te sluiten? Waarom zijn lichaamscellen gesloten, zodat er leven kon ontstaan?

Inmiddels is er redelijk veel inzicht verkregen in de vorming van gekromde oppervlakken. Langer houdbare melk en betere wasmiddelen zijn hier bijvoorbeeld het gevolg van. Deze, vaak empirische, kennis geeft echter geen antwoord op de overkoepelende vraag; waarom worden er in zijn algemeenheid gekromde oppervlakken gevormd? Om het antwoord op deze vraag inzichtelijk te maken, zijn er diverse theorieën ontwikkeld die gekromde systemen beschrijven of modelleren. Echter, sommige modellen geven (inwendig) tegenstrijdige voorspellingen. Het doel van dit proefschrift is om een eenduidige beschrijving te geven van gekromde oppervlakken en die te vergelijken met andere modellen.

In hoofdstuk 2 wordt een thermodynamische beschrijving gegeven van gekromde grensvlakken. Thermodynamica, in eerste instantie ontwikkeld om stoommachines optimaal te laten functioneren, is het vakgebied dat beschrijft hoe warmte en arbeid in elkaar kunnen worden omgezet. In essentie kan de thermodynamica worden terug gebracht tot twee zogenaamde hoofdwetten. De eerste hoofdwet zegt dat energie niet uit niets kan ontstaan, zodat warmte slechts in arbeid kan worden omgezet en omgekeerd. De tweede hoofdwet zegt dat er bij een gegeven hoeveelheid energie in een systeem altijd gestreefd wordt naar een zo groot mogelijke wanorde, die direct aan de verandering van de warmte in een systeem gekoppeld kan worden. Als een grensvlak gekromd wordt,

zijn er twee soorten arbeid noodzakelijk; de grensvlakarbeid en de krommingsarbeid. De grensvlakarbeid is die hoeveelheid energie die nodig is om een oppervlak te vergroten en is gerelateerd aan de zogenaamde grensvlakspanning. Dankzij deze grensvlakspanning kunnen insecten op het water drijven of kunnen steentjes met keilen op het water ketsen. De krommingsarbeid is die hoeveelheid energie die nodig is om een grensvlak te krommen en is gerelateerd aan de zogenaamde buig- en torsiespanning. Om nu een grensvlak met een gegeven oppervlak en mate van kromming te vervormen, kunnen er twee dingen worden gedaan. Eerst kan het oppervlak worden vergroot tot de gewenste eindwaarde en vervolgens kan dat oppervlak worden gekromd. Het is ook mogelijk om beide tegelijkertijd te doen. Hoewel beide manieren om van een gegeven begintoestand tot de gewenste eindtoestand te komen evenveel energie zal kosten, is de verdeling van die energie over grensvlakarbeid en krommingsarbeid anders. Dit leidt tot twee afwijkende definities van de grensvlakspanning. De eerste manier om te krommen is voorgesteld door Gibbs, de tweede manier door Boruvka en Neumann. Als de kromming overal op het oppervlak gelijk is, dan is het verschil tussen de grensvlakspanning van Gibbs, γ_G, en die van Boruvka en Neumann, γ_{BN}, juist de krommingsarbeid per oppervlakte-eenheid.

Het bestaan van de grensvlakspanning komt voort uit het feit dat moleculen in het grensvlak anders omringd zijn dan elders in het systeem. Dat wil zeggen dat de druk die een molecuul in het grensvlak ondervindt van de omringende moleculen verschilt van de druk die eenzelfde molecuul ervaart ver weg van het grensvlak. Deze lokale extra druk, ofwel overschotsdruk, kan dus gerelateerd worden aan de grensvlakspanning. Dit leidt tot de zogenaamde mechanische uitdrukking voor de grensvlakspanning. Gebruik makende van de hierboven vermeldde thermodynamische definitie, kunnen er nu ook mechanische uitdrukkingen worden gegeven voor de buigspanning $\mathbb{C}_1$ en de torsiespanning $\mathbb{C}_2$. Het blijkt nu dat de aldus gevonden mechanische uitdrukkingen niet dezelfde zijn als die die bekend zijn in de vakliteratuur. Er wordt bewezen dat zowel de thermodynamische als de mechanische vergelijkingen dezelfde uitdrukking oplevert voor het zogenaamde Laplace drukverschil dat over een gekromd oppervlak heerst.

De betekenis van het begrip 'druk' wordt onderzocht in hoofdstuk 3. Allereerst wordt de mechanische betekenis van de druk bekeken; de krachten die de moleculen uitoefenen per eenheid van oppervlakte. Volgens het zogenaamde viriaaltheorema zijn deze krachten gelijkelijk verdeeld over die veroorzaakt door de bewegingen van de individuele moleculen enerzijds en de paarsgewijze wisselwerking tussen moleculen anderzijds. Omdat deze krachten niet in alle richtingen even groot hoeven te zijn, heeft de mechanische druk dus behalve een grootte, ook een richting. Wiskundig betekent dit dat de

druk in het algemeen een tensoriële, in plaats van een scalaire grootheid is. Alle verkregen resultaten voor de mechanische druk komen overeen met die die bekend zijn in de vakliteratuur. De bijdrage aan de druk door de bewegingen van de moleculen is uniek op een plaats vast te leggen, namelijk op de plaats van het deeltje. De bijdragen van de paarinteracties laat zich echter niet eenduidig localiseren. Immers, de wisselwerking kan bijvoorbeeld worden toegekend aan de plaats van een van beide moleculen, maar ook ergens tussen de moleculen in. Het gevolg is dat de lokale mechanische druk niet ondubbelzinnig gedefinieerd kan worden.

De druk wordt thermodynamisch geïnterpreteerd als een arbeid die nodig is om het volume te veranderen. Om de eigenschappen van deze thermodynamische druk te bekijken, wordt een roostermodel afgeleid. De ruimte wordt daarbij zodanig in hokjes gedeeld, dat er per hokje maximaal een molecuul past. De moleculen worden op het aldus gevormde rooster geplaatst, zodat uit de wisselwerking met de naburige roosterplekjes de energie van het systeem kan worden bepaald. Er zijn echter vele manieren om de deeltjes op het rooster te plaatsten. Niet al deze mogelijkheden leveren dezelfde energie op; elk mogelijke energie moet worden gewogen met de kans dat zij voorkomt. Het aantal mogelijkheden om de moleculen op het rooster te plaatsen is een maat voor de wanorde van het systeem, hetgeen op zijn beurt via de tweede hoofdwet van de thermodynamica gekoppeld is aan de verandering van de warmte. Door deze van de meest waarschijnlijke energie af te trekken, wordt de totale hoeveelheid arbeid gevonden die in evenwicht aanwezig is in het systeem. Door hier vervolgens weer de zogenaamde chemische arbeid van af te trekken, blijft alleen de mechanische arbeid over. Het totaal aan mechanische arbeid wordt de grootse potentiaal genoemd. De grootse potentiaaldichtheid, de mechanische arbeid per volume eenheid, wordt dan geïndentificeerd als de (lokale) druk. De op deze manier gedefinieerde statistisch thermodynamische druk, blijkt ver van het grensvlak vandaan dezelfde eigenschappen te vertonen als bekend voor andere modellen in de vakliteratuur. Het drukprofiel heeft veel overeenkomsten met dat gevonden voor de mechanisch gedefinieerde druk. Er worden zowel uitrekbare, negatieve, als samendrukbare, positieve gedeeltes gevonden in het drukprofiel. Omdat de drukoverschotten ten grondslag liggen aan de grensvlakspanning, kunnen de negatieve lokale drukken van belang zijn om de lage grensvlakspanning, die in sommige systemen te vinden zijn, te realiseren. Een model dat deze, tegen-intuïtieve, negatieve druk weghaalt, verwaarloost daarmee dus een belangrijke fysische eigenschap van de druk. Ook in het roostermodel kunnen de paarinteracties niet eenduidig worden toegekend, zodat ook daar lokale druk niet ondubbelzinnig bepaald kan worden.

Voor twee verschillende definities van de thermodynamisch gedefinieerde druk, leveren de in hoofdstuk 2 gevonden mechanische uitdrukkingen voor de buig- en torsiespanning een eenduidig antwoord op. Dit zou ook zo moeten zijn omdat ze ondubbelzinnig gemeten kunnen worden. De uitdrukkingen zoals die bekend zijn in de vakliteratuur geven echter twee verschillende waardes.

In plaats van een gedetailleerde thermodynamische beschouwing, kan een krommingsproces ook meer beschrijvend worden gegeven. Bij een dergelijke fenomenologische beschrijving worden alleen de belangrijkste bijdragen meegeteld. In hoofdstuk 4 wordt beschouwd hoe de grensvlakspanning over het algemeen afhangt van de kromming. Door een grensvlak te beschouwen als een rekbare veer, blijken termen kwadratisch in de kromming nodig te zijn. Een zogenaamde tweede orde Taylorreeks van de thermodynamische uitdrukking voor de grensvlakspanning rond het vlakke grensvlak levert dan vier coëfficiënten op die de krommingsarbeid van een grensvlak fenomenologisch kunnen beschrijven. Een benadering tot op nulde orde is de grensvlakspanning van het vlakke grensvlak. Tot op eerste orde kan de grensvlakspanning benaderd worden door de zogenaamde Tolmanlengte of voorkeurskromming, die de buigspanning blijkt te zijn van het vlakke grensvlak. De kwadratische, tweede orde bijdrage aan de krommingsarbeid wordt gegeven door twee 'veerconstanten': de buigingsmodulus k_c en de zadelvlakmodulus $\overline{k}$. Deze blijken respectievelijk de afgeleide van de buigspanning en de torsiespanning van het vlakke oppervlak te zijn. Omdat de mechanische uitdrukkingen van de buig- en torsiespanningen anders waren dan die bekend in de literatuur, verschillen ook de vergelijkingen voor de fenomenologische krommingscoëfficiënten.

Om de geldigheid van de uitdrukkingen voor de vier fenomenologische krommingscoëfficiënten te controleren, wordt het bovengenoemde roostermodel gebruikt. De grensvlakspanningen worden berekend voor vloeistofdruppels van verschillende groottes. Het blijkt dat de fenomenologische beschrijving met de hier gevonden mechanische uitdrukkingen voor de krommingscoëfficiënten de werkelijk berekende grensvlakspanningen zeer nauwkeurig beschrijft ongeacht hoe de paarinteracties werden geteld in de lokale druk. Het domweg gebruiken van de vergelijkingen uit de vakliteratuur levert onnauwkeurige beschrijvingen op, die afhangen van de manier waarop de paarinteracties worden geteld.

De met het roostermodel verkregen waardes voor de krommingscoëfficiënten worden vergeleken met die van een zogenaamd Van der Waals-model. In het gebied waar laatstgenoemde geldig is, leveren beide modellen dezelfde resultaten op. Het Van der Waals-model is echter ook in overeenstemming met andere modellen uit de vakliteratuur. Dat de mechanische uitdrukkingen voor de krommingscoëfficiënten in de vakliteratuur toch

verschillen van de hier afgeleide, kan alleen maar worden toegeschreven aan het feit dat niet alle energiedichtheden 'druk' genoemd mogen worden.

Zoals de naam al doet vermoeden, kunnen oppervlakte-actieve stoffen het gedrag van grensvlakken beïnvloeden. Een laagje zeep op water verlaagt de grensvlakspanning dusdanig, dat insecten niet langer op het oppervlak kunnen drijven. In hoofdstuk 1 is benaderend uiteengezet hoe oppervlakte-actieve stoffen ook eventueel kromming kunnen aanbrengen. Dit ligt ten grondslag aan, bijvoorbeeld, de werking van wasmiddelen. Oppervlakte-actieve stoffen kunnen dit bewerkstelligen door de tweeslachtige aard van hun moleculen. Deze bestaan uit een waterminnend (hydrofiel) en een watervrezend (hydrofoob) deel. Als ze in water worden gebracht, zullen de hydrofiele delen graag in water oplossen, maar de hydrofobe delen niet. De hydrofobe delen kunnen echter hun leed verzachten door bij elkaar te gaan zitten, waardoor de hydrofiele delen hen afschermen van het water. De aldus gevormde gekromde systemen worden micellen genoemd waarin vuil dat slecht in water oplost, kan worden opgenomen.

In hoofdstuk 5 wordt het gedrag van vlakke micellen, ofwel bilagen, bestudeerd die model staan voor biomembranen. Door de bilaag te krommen en de uiteinden van een bilaag aan elkaar te koppelen, worden er gesloten blaasjes gevormd. De oppervlakte-actieve stoffen worden als een kralenketting in het roostermodel gemodelleerd, waarbij elke kraal in de ketting óf hydrofiel óf hydrofoob gemaakt kan worden. Door het aantal oppervlakte-actieve moleculen per blaasje gunstig te kiezen, kunnen er zo op het rooster gesloten bilagen met verschillende kromming ontstaan waarvoor telkens de grensvlakspanning wordt bepaald. Zodoende kunnen opnieuw de krommingscoëfficiënten worden bepaald. Er wordt bekeken hoe de waarde en het teken van die krommingscoëfficiënten afhangen van de opgelegde temperatuur. Hoe hoger de buigingsmodulus k_c, hoe moeilijker het is om een bilaag te vervormen. Daarentegen geeft een lage waarde voor k_c aan dat een bilaag slap is. Als k_c negatief wordt, dan zijn de bilagen instabiel en willen de oppervlakte-actieve stoffen niet meer in water oplossen. Het teken van de zadelvlakmodulus $\overline{k}$ geeft de neiging aan om zadelvlakken te vormen, dat wil zeggen de drang om handvatten tussen bilagen te laten ontstaan. Voor realistisch gekozen mate van hydrofobiciteit en hydrofiliciteit, wordt inderdaad in grote lijnen het experimenteel waargenomen gedrag van bilagen met het roostermodel gevonden. Er wordt geconcludeerd dat het roostermodel met de onderling overeenkomstige thermodynamische en mechanische beschrijving veel inzicht kan verschaffen in het gedrag van oppervlakte-actieve stoffen.

Levensloop

Toen ik op 4 augustus 1971 in Amsterdam geboren werd, gaven mijn ouders mij de naam Simon Martinus Oversteegen. Op de leeftijd van vier jaar verhuisde ik met hen naar het Twentse Oldenzaal. Daar behaalde ik in 1989 het atheneumdiploma aan het Thijcollege. Direct daarna ben ik Chemische Technologie (Informatica-variant) gaan studeren aan de Universiteit Twente. Bij het chemieconcern Sandoz te Basel (Zwitserland) liep ik een informatiseringsstage waarbij ik de dataverwerking van HPLC-metingen heb geautomatiseerd. Na mijn afstudeeropdracht bij de vakgroep Chemische Fysica, waar ik met moleculaire dynamica het gedrag van harde ellipsoïden bestudeerde, behaalde ik in 1995 mijn doctoraaldiploma. Vanaf 1 september van datzelfde jaar was ik als Onderzoeker in Opleiding werkzaam in dienst van het NWO, met als werklocatie het laboratorium voor Fysische Chemie en Kolloïdkunde van Wageningen Universiteit. Resultaten van het daar verrichte onderzoek zijn in dit proefschrift vastgelegd. Het werk presenteerde ik onder meer op de 'Student Conferences' in Groenlo (Nederland), Hebden Bridge (Groot-Brittannië) en Nauvo (Finland), op het twaalfde 'Surfactants in Solution'-symposium in Stockholm (Zweden) en tijdens 'Thermodynamics 99' in Londen (Groot-Brittannië).

Mijn opleiding heb ik onder meer gevolgd tijdens de NATO ASI-cursus 'Theoretical Challenges in the Dynamics of Complex Fluids', de RPK-cursussen 'Polymer Physics' en 'Rheology' en de IRI-cursus 'Neutronenverstrooiing'.

Sinds 1 november 1999 ben ik als postdoctoraal medewerker in dienst van het Debye Instituut aan de Universiteit Utrecht.

List of Publications

- F.A.M. Leermakers, J. van Noort, S.M. Oversteegen, P.A. Barneveld, and J. Lyklema. *Faraday Discuss.*, 104:317, 1996
- J. Lyklema and S.M. Oversteegen. *Adv. Colloid Interface Sci.*, 75:255, 1998; *Colloids and Surfaces A*, 143:133, 1998
- S.M. Oversteegen, P.A. Barneveld, J. van Male, F.A.M. Leermakers, and J. Lyklema. *PCCP*, 1:4987, 1999
- S.M. Oversteegen, P.A. Barneveld, F.A.M. Leermakers, and J. Lyklema. accepted by *Langmuir*, 1999
- S.M. Oversteegen and E.M. Blokhuis. accepted by *J. Chem. Phys.*, 1999